Aus dem

Institut für Molekulare Immunologie

Kom. Direktor: Prof. Dr. Ralph Mocikat

Comprehensive Pneumology Center

Direktor: Prof. Dr. Oliver Eickelberg

des Helmholtz Zentrum München

microRNA-based identification of pulmonary signaling pathways in experimental asthma -

The role of the cAMP responsive element binding protein (Creb1)

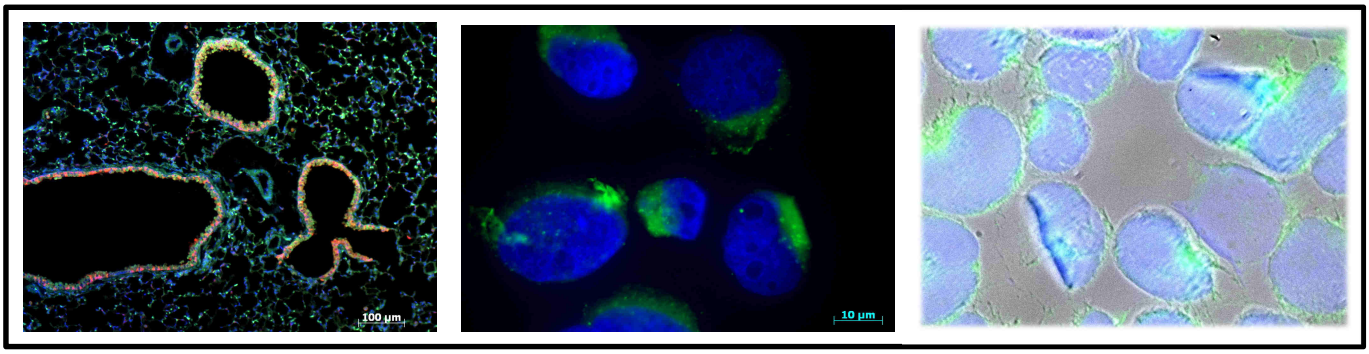

Dissertation

zum Erwerb des Doktorgrades der Naturwissenschaften

an der Medizinischen Fakultät

der Ludwig-Maximilians-Universität München

vorgelegt von

Sabine Bartel

aus Dachau

2015

Mit Genehmigung der Medizinischen Fakultät

der Ludwig-Maximilians-Universität München

Betreuerin:	Prof. Dr. rer. nat. Elfriede Nößner
Zweitgutachter:	Prof. Dr. rer. nat. Peter Jon Nelson
Dekan:	Prof. Dr. med. Dr. h.c. Maximilian Reiser, FACR, FRCR
Tag der mündlichen Prüfung:	30.04.2015

Nothing,

worth having in this world,

comes easily!

ZUSAMMENFASSUNG

Asthma ist die häufigste chronische Erkrankung bei Kindern und sie ist in ihrer Prävalenz und Inzidenz über die letzten Jahrzehnte stark angestiegen. Das Krankheitsbild an sich ist bis zum heutigen Zeitpunkt intensiv erforscht worden, wobei über die Entstehung von Asthma im Kindesalter noch wenig bekannt ist. Aus diesem Grund ist es wichtig, neue Signalwege zu identifizieren, die für die Asthmaentstehung relevant sind, auch um daraus eventuell neue therapeutische Ansätze oder präventive Strategien zu entwickeln.

Dafür haben wir microRNAs (miRNA) verwendet, die oft mehrere Schlüsselfaktoren in denselben Signalwegen regulieren. In vorrangegangener Arbeit hat unsere Gruppe gefunden, dass pulmonale miR-17 und miR-144 bei Ovalbumin (OVA) -induziertem experimentellen Asthma in Mäusen erhöht sind, und, dass sie den Transkriptionsfaktor „cAMP-responsive element binding protein“ (Creb) regulieren können. In dieser Arbeit haben wir nun weitere Bindestellen für miR-17 und -144, sowie auch für die neu miteinbezogene miR-21, in den 3’UTRs von Creb1 Co-Aktivatoren (Crtc1-3) gefunden und in *in vitro* Experimenten validiert. Sowohl Creb1 als auch die drei Crtcs waren in Lungengewebe von Tieren mit experimentell induziertem Asthma durch OVA und Hausstaubmilben (HDM) verringert. Weiterhin haben wir die Expression eines möglichen Creb1 Zielgenes, Sec14-like 3 (Sec14l3), untersucht, welches ebenfalls in beiden Asthma Mausmodellen im Lungengewebe herunterreguliert war. Außerdem war der Verlust an Sec14l3 Protein in der Lunge mit der Hyperplasie von Mucus-produzierenden Becherzellen assoziiert. In der Kultur von primären humanen Bronchialzellen (NHBE) führte eine Behandlung mit IL-13 zu einer transienten Herunterregulierung von Creb1, den Crtcs und Sec14l3. miR-17, -144 und -21 wurden nach IL-13 von diesen Primärzellen vermehrt in Exosomen sekretiert und diese konnten von Bronchialepithelzellen, und T Zellen aufgenommen werden. Die drei miRNAs konnten auch in Exosomen aus Nasenspülungen von Kindern mit allergischem Asthma und in bronchoalveolarer Lavage in Mäusen mit experimentellem Asthma gefunden werden. In nasalen Epithelzellen von Kindern mit allergischem Asthma waren miR-17, -144 und -21 stark erhöht und das Zielgen SEC14L3 herunter reguliert.

Alles in Allem, haben wir in dieser Arbeit eine neue molekulare Achse (miRNA-Creb/Crtc-Sec14l3) gefunden, die relevant sein könnte für die Asthmaentstehung bei der Maus aber auch bei Kindern. Die Sekretion der miRNAs in Exosomen könnte die Reaktion der Zellen auf asthmatische Stimuli auf mehrere, verschiedene Zelltypen verteilen.

SUMMARY

Asthma is characterized by chronic airway inflammation; mucus hypersecretion and episodes of airway obstruction. It is the most common chronic disease in children and its incidence and prevalence have been markedly increasing over the last few decades. While the pathophysiology has been intensively studied, the underlying causes for asthma development remain largely unknown. Hence there is an unmet, clinical need to identify novel, so far non-characterized pathways, relevant for this disease, to establish new therapies or preventive approaches.

We used miRNAs to do so as they are critical regulators of key molecules within signalling pathways. Our group previously identified a pulmonary increase of miR-17 and -144 in ovalbumin-induced allergic airway inflammation in mice and they were shown to target the transcription factor cAMP-responsive element binding protein 1 (Creb1). In this work, we found and validated additional binding sites for the two miRNAs and the newly included miR-21 in the 3'UTR of Creb1 co-activators CRTC1, -2 and -3. Creb1 and the three Crtcs were further shown to be down-regulated in two models of murine experimental asthma (ovalbumin and house dust mite). We postulated that a joint down-regulation of Creb plus its co-activators by the miRNAs might have detrimental, additive effects on the expression of target genes. In this respect, we identified the putative Creb1 target gene Sec14-like 3 (Sec14l3) which was down-regulated in both models for murine experimental asthma and its loss seemed to be associated with goblet cell metaplasia.

Furthermore, we found that IL-13 treatment of primary normal human epithelial (NHBE) cells led to a decrease of CREB1/CRTCs and SEC14L3, while the latter correlated with forkheadbox protein J1 (FOXJ1), a marker for ciliated cells. miR-17, -144 and -21 were actively secreted into exosomes by the primary NHBE cells upon IL-13 stimuli, which could be uptaken by a bronchial epithelial cell line and a T cell line . We could also detect miRNA-containing exosomes in nasal washes from children with allergic asthma and broncho-alveolar lavage fluid of mice with OVA-induced allergic airway inflammation.

In nasal epithelial cells of children with allergic asthma, the three miRNAs were highly increased compared to healthy controls, while SEC14l3 expression was reduced.

In conclusion, this work identified a novel molecular axis (miRNA-Creb/Crtc/Sec14l3) relevant for murine and paediatric asthma and gives first hints that miR-17, -144 and -21 in exosomes might be able to perpetuate the asthmatic response between different cell types.

TABLE OF CONTENTS

1. INTRODUCTION

1.1. Asthma

1.1.1. The increasing burden of asthma

Asthma is a chronic inflammatory lung disease affecting approximately 30 million people of different ages in Europe (1). It is the most common chronic disease in children that usually persists into adulthood.

According to the European Lung White Book the prevalence in Europe in adults is highest in the UK (10-13%) and lowest in Georgia (0.28%) (1). In Germany, the number of people suffering from asthma is estimated at 4 million. Of note, the prevalence of asthma, and also allergy, has markedly increased over the last few decades in westernized countries (2). In Western Europe, it has doubled in the last ten years (1) and according to the Global Initiative for Asthma (GINA), the number of people suffering from asthma worldwide will further increase over the next two decades (3).

The main symptoms are recurring episodes of breathlessness, chest tightening, wheezing and coughing. Of note, until puberty boys are more likely to develop asthma-like symptoms, which changes in adulthood, where women are more affected than men (4). Severe asthma can lead to irreversible airway remodeling and, thus, persistent respiratory dysfunction, which may already occur in very young children (5).

Thus, the disease asthma represents a huge burden for the healthcare systems due to medications, hospitalizations and also absence from work. The total cost of asthma in Europe was estimated to amount to € 17.7 billion per year (1) with the majority caused by severe uncontrolled asthma. Thus, there is an urgent need for improved therapies, both from the perspective of patients and the health care system.

1.1.2. Environmental influences on asthma development

The lung, and especially the bronchial epithelium, represent the first barrier to the outside world and therewith beyond others allergens, pollutants, toxins, microorganisms. While the pathogenesis of asthma is in part well understood, the underlying causes for asthma development remain unknown. Asthma and allergy are generally associated with a

westernized lifestyle and are more prevalent in developed countries, an effect that cannot be explained by genetic predisposition alone. Therefore, it is intriguing to speculate that the environment does influence the development of these diseases.

Proposed explanations are that modern housing and more time spent indoors has increased the exposure to house dust mite. Second, due to increased hygiene and the use of widespread antibiotics, we are exposed to a smaller variety of microorganisms – the so called hygiene hypothesis (reviewed in (2)). Third, the western diet has changed over the last few decades and the prevalence of obesity, especially in children, has increased (reviewed in (2)). Besides, various other factors like mode of delivery at birth (6), race or ethnicity (7), sex (8) and birth order (9), breastfeeding (10), keeping pets (11,12), viral (13,14) and bacterial infections (15), environmental tobacco smoke (16,17), and air pollution (18), have been shown to influence asthma risk. On the other hand, the environment can also protect from asthma, especially observed for (also *in utero*) exposures to a farming environment (19,20).

Several studies have also shown that not only the post-natal environment can influence the asthma risk, but also the fetal development represents a fragile, susceptible period for early programming. Hence, an *in utero* exposure to, e.g. allergens (21,22), maternal and grand-maternal smoking (23,24), but also the presence of maternal asthma (25), have been discussed to be important risk factors for the development of allergies and asthma later in life.

In summary, the underlying causes for the development of asthma need to be further investigated to identify early developmental windows for interventions to prevent the disease development.

1.1.3. Current therapy for asthma

Despite intensive research, the therapeutic options for asthma have remained limited and cannot prevent airway remodeling, which may already occur in wheezing preschool children (5). The majority of asthma cases can be controlled by inhaled anti-inflammatory gluco-corticosteroids and β2-receptor agonists. However, about 10% of all patients suffer from severe asthma with recurring exacerbations and the need for hospital and emergency room visits (1). So far, treatment is based on disease severity and control, rather than on the underlying mechanisms. To overcome this, several animal studies have been performed, showing promising results in using biological agents like monoclonal antibodies against IgE (26) or Th2 cytokines contributing to the asthma pathogenesis, like IL-5, IL-4 and IL-13 (27–

29). However, clinical studies with anti-IgE (30), anti-IL-5 (31,32), anti-IL-4 receptor (33) and anti-IL-13 (34) have overall shown limited efficacy in humans, hence being effective only in a small subgroup of patients, which is most likely due to the heterogeneity of human asthma.

Thus, there is a high and unmet clinical need to identify novel molecular pathways involved in the pathogenesis of asthma that can be used for therapeutic approaches.

1.1.4. Pathogenesis of asthma –current concepts

Asthma is not a single disease but rather a syndrome consisting of several different endotypes and phenotypes. General disease hallmarks are a chronic inflammation of the conducting airways, episodes of airflow obstruction associated with airway hyper-responsiveness (AHR), and mucus hyper-secretion. Along disease progression, the release of potent inflammatory mediators and also, in part, remodeling of the airway wall with smooth muscle cell hyper-proliferation, sub-epithelial fibrosis and goblet cell metaplasia can lead to chronic respiratory dysfunction (reviewed in (35)).

The most intensively studied phenotype, the so called allergic asthma, is characterized by a T-helper (Th) 2-mediated eosinophilic inflammation (reviewed in (36)). However, there are many different endotypes for asthma with different pathogenesis. For example, some subforms of severe, steroid-resistant asthma have been associated with Th17 cells and neutrophilic inflammation (37).

In general, asthma results from an allergic hypersensitivity, namely atopy, occurring mainly in childhood, against a normally harmless environmental substance such as house dust mite (HDM), animal dander, pollen or fungal spores (reviewed in (38)). In the lung, inhaled allergens, microorganisms and pollutants will first encounter the airway epithelium. Current concepts propose that this physical barrier to the outside can be damaged by infections, e.g. viruses enabling allergens to penetrate (reviewed in (39)), or can be attacked by proteases present in allergens themselves (reviewed in (38)). Upon first perturbation of this barrier, the epithelial cells secrete ‘danger signals’ like granulocyte-macrophage colony-stimulating factor (GM-CSF), thymic stromal lymphopoetin (TSLP), IL-25 and IL-33 (reviewed in (38)). The additional secretion of chemokines will attract immature antigen presenting cells (APC), namely dendritic cells (DC), towards the epithelium and the underlying mucosa (reviewed in (35)). The DCs will then take up and present the allergens to CD4 and CD8 T cells after

migrating to the draining mediastinal lymph nodes (Fig. 1.1) (reviewed in (40)). In allergic individuals, this process is enhanced as allergen can directly bind to its specific immunoglobulin E (IgE) molecules – derived from antigen specific B cells or plasma cells - that are attached to high affinity IgE receptors (Fcε-receptor I) on the DC surface (reviewed in (41)). This process can occur after penetration of the epithelium or even outside, as DCs can reach through the epithelial barrier with their dendrites to catch allergens via the IgE receptors (Fig. 1.1) (42). Presentation of the antigen to naïve and memory T cells in the lymph nodes leads to their polarization and maturation towards Th2 or also Th17 cells, depending on the cytokine environment. IL-4 from basophils for example skews naïve T cells towards a Th2 phenotype (reviewed in (38)). Those T cells can then migrate to the epithelium and modulate the allergic response via secreting pro-inflammatory cytokines such as IL-4, IL-5 and IL-13 for Th2 cells or IL-17 for Th17 cells. IL-4 and IL-13 for example can induce a class-switch towards IgE in B cells and a metaplasia of mucus-producing goblet cells in the airway epithelium (reviewed in (43)). IL-5 is involved in the recruitment of eosinophils to the airways (44). A relatively new cell type, the so called innate lymphoid cells (ILCs), which are lineage negative, can also contribute to asthma by secreting IL-5 and IL-13 after TSLP stimulus (reviewed in (38)).

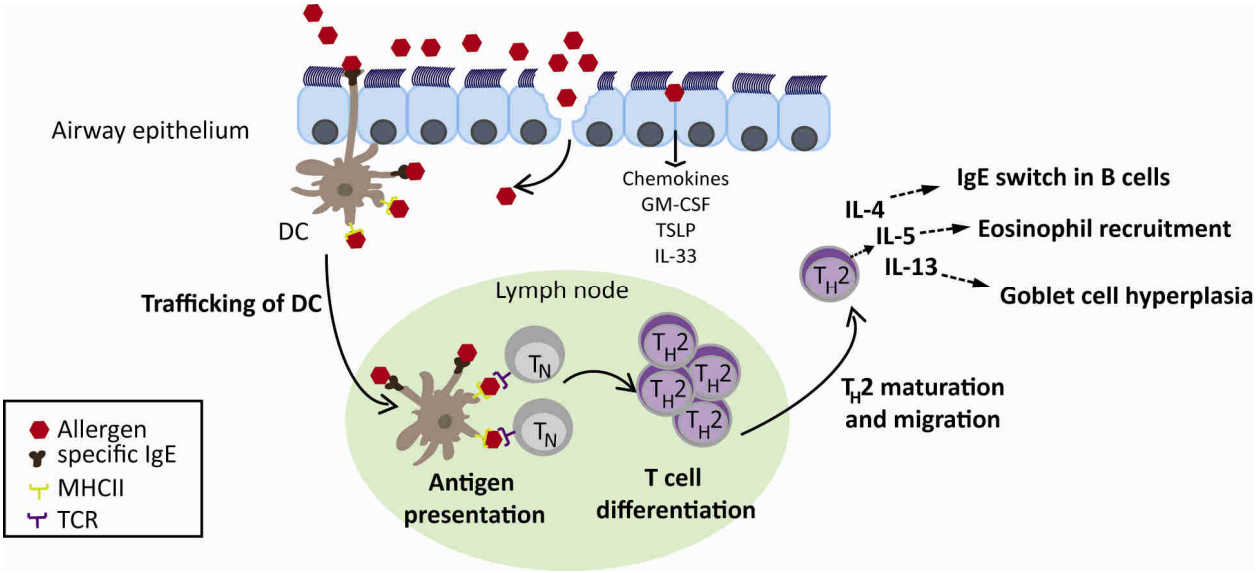

Figure 1.1: Simplified scheme of the interaction between the epithelium and the immune cells in allergic asthma. Upon exposure to allergen, the airway epithelium will secrete pro-inflammatory factors, such as granulocyte-macrophage colony-stimulating factor (GM-CSF), thymic stromal lymphopoetin (TSLP) and IL-33, beyond others. Dendritic cells can uptake allergens and present them to naïve T cells in the local lymph node, which induces a context-dependent differentiation. In asthma, this is mostly skewed towards a Th2 phenotype. The Th2 cells then expand and migrate towards the epithelium, while secreting cytokines such as IL-4, IL-5 and IL-13, leading to IgE production by B cells, recruitment of eosinophils and a hyperplasia of mucus-producing goblet cells in the epithelium. Adapted from (35,45).

The role of the airway epithelium in the perpetuation of allergic airway disease comes more and more into the focus of asthma research. It has been shown that its physical barrier function is intrinsically impaired due to an opening of the tight junctions that keep bronchial epithelial cells together, allowing allergens to penetrate (Fig.1.1) (39). This effect can be induced by Th-2 cytokines, especially IL-4 and IL-13 (46,47). The normal airway epithelium consists of ciliated cells, club cells, goblet cells and basal cells. Upon exposure to Th2 cytokines, ciliated cells and club cells can transdifferentiate into goblet cells – the so called goblet cell metaplasia - resulting in mucus hypersecretion and, in severe cases, to airway obstruction by mucus plugging (reviewed in (45)). Additionally, airway epithelial cells express pattern recognition receptors (PRR) such as toll-like receptors (TLR) and nucleotide oligomerization domain (NOD) receptors (48). A binding of allergen to those receptors initiates a secretion of pro-inflammatory stimuli, like TSLP, IL-33 and GM-CSF by the epithelial cells, propagating cascades in the asthma pathogenesis like Th2 differentiation (reviewed in (45)).

In summary, there is a complex interplay between the airway epithelium and the immune system in asthma that has not been fully elucidated at the moment and needs to be further investigated to understand underlying causes for asthma development.

1.2. miRNAs

1.2.1. Biogenesis and function

Environmental stimuli might influence the pathogenesis and development of asthma for example via microRNAs. These short, ~22nt long, non-coding single stranded RNAs can regulate gene expression by binding to the 3'UTR in the mRNA of their target genes with their so called seed sequence. They have been already shown to be essential for the development of the immune system (reviewed in (49)) and the lung (reviewed in (50)).

miRNAs have been discovered in the nematode *Caenorhabditis elegans* (*C. elegans*) 21 years ago (51) and to this day around 1,872 human miRNAs have been identified (www.mirbase.org).

Their biogenesis starts in the nucleus when the miRNA encoding genes are transcribed by the RNA polymerase II or III intro primary miRNA transcripts (pri-miRNA) (52–54). Both polymerases are differentially regulated and transcribe different miRNA families, enabling a huge variety of regulation already at this early stage (reviewed in (55)). Some miRNA families are located in genomic clusters and often transcribed simultaneously; however, they can also be independently regulated (43). The capped and poly-adenylated pri-miRNA forms a hairpin stem of 33 basepairs, two single-stranded flanking regions and a terminal loop (Fig. 1.2) (reviewed in (55)). The two 5' and 3' arms of the pri-miRNA hairpin are then subsequently cleaved 11bp away from the single stranded RNA/double stranded RNA junction by the RNase III enzyme Drosha, after interaction with DiGeorge critical region 8 protein (DGCR8) that determines the exact cleavage site (57). The resulting precursor miRNA (pre-miRNA) is exported to the cytoplasm where it is cleaved by a complex of the TAR RNA-binding protein (TRBP) and the RNase Dicer to its mature length of around 22nt (58). After dissociation of Dicer and TRBP, the duplex is separated by helicases into the functional guide strand, complementary to its target, and the passenger strand. The latter is degraded, while the two strands are distinguished by the thermodynamic stability of the base pairs at the two ends of the duplex: the strand with more stable base pairs will be discarded (59). The mature miRNAs then form the RNA-induced silencing complex (RISC) together with Argonaute proteins (Ago). A complimentary base-pairing of the miRNA with a respective target messenger RNA (mRNA), mostly in the 3'UTR, guides the RISC to either degrade, destabilize by deadenylation, or translationally inhibit the bound mRNA (60).

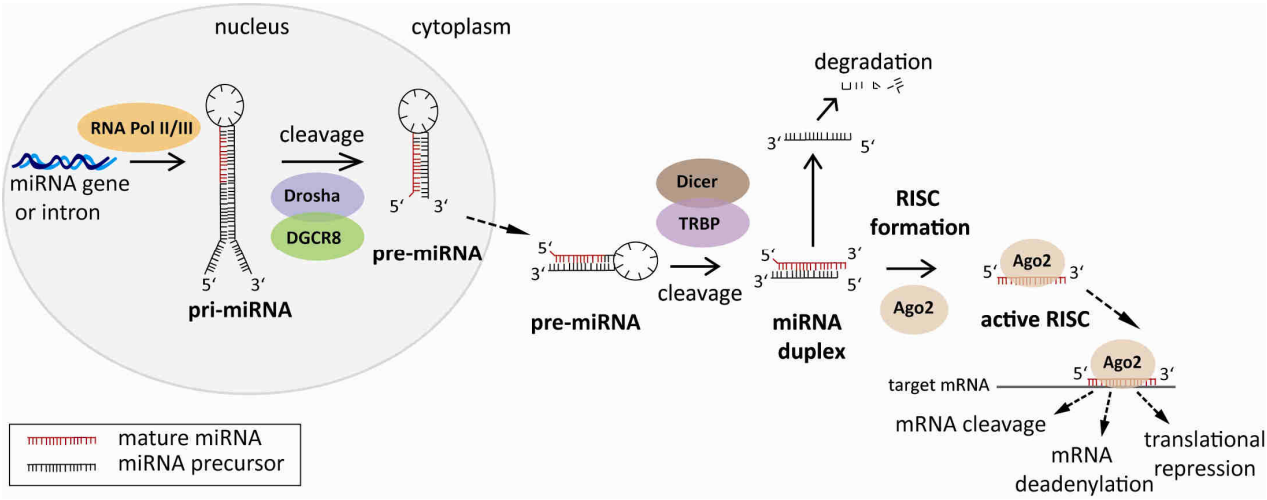

Figure 1.2: miRNA biogenesis and function. After transcription by RNA Polymerase II/III, the pri-miRNA is cleaved by a complex of Drosha and DiGeorge critical region 8 (DGCR8). The resulting precursor miRNA (pre-miRNA) is exported to the cytoplasm and further cleaved by Dicer and TAR RNA binding protein (TRBP) to a miRNA duplex. While the functional miRNA strand is incorporated into the RNA-induced silencing complex (RISC) with Argonaute 2 (Ago2), the passenger strand is degraded. The binding (perfect or imperfect) of an active RISC complex to its mRNA target leads to mRNA cleavage, deadenylation, or translational repression. Adapted from (55).

In contrast to small interfering RNAs (siRNAs), miRNAs can bind their targets also with imperfect base pairing as long as this does not occur in the 2-8nt long so-called "seed region" (61). This also explains the wide variety of genes that can be targeted by one single miRNA. However, they tend to address several key regulatory molecules in cellular pathways, such as transcription factors (62–64). This simultaneous regulatory fine tuning of several pathway components can then lead to pronounced downstream effects.

1.2.2. Extracellular miRNA transport in exosomes

The detection of miRNAs in serum and plasma gave rise to the idea that they might exert a biological function outside their cell of origin and can also be exploited as biomarker for diseases (reviewed in (65)). While a grand proportion of extracellular miRNAs is bound to Ago proteins and most likely is released from dying cells, some miRNAs are present in so called exosomes. Exosomes are small (30-90nm), very stable membrane vesicles of endosomal origin that are actively secreted from both immune cells and also structural cells in the lung (66–69). The biogenesis of exosomes starts with endocytic vesicles that form at the plasma membrane and then fuse to form early endosomes. After maturation to late endosomes, intraluminal vesicles budd off into the lumen resulting in multivesicular bodies (MVB) (reviewed in (70)). After fusion of MVBs with the cell membrane, exosomes are

released into the extracellular environment. Up to now, the mechanism of miRNA packaging into exosomes is not fully understood but seems to depend on the association of RISC complexes with the MVBs (reviewed in (65)). As the composition of miRNAs differs between exosomes and the originating cells, they seem to be specifically packaged (71). Besides miRNAs, exosomes also carry mRNA, enzymes or proteins such as major-histocompability complex (MHC) proteins (71), and their composition corresponds to their cellular origin. Exosomes can be characterized by specific surface molecules, especially tetraspanins such as CD9, CD81 and CD63 or MHCII (71).

Fusion of the exosomes with target cells or internalization by endocytosis is often guided by target cell-specific receptor molecules and allows for directed transfer of internal components and, in particular, functional transfer of miRNAs. Thus, they can be considered as a means of inter-cell-communication (reviewed in (72)).

miRNA-containing exosomes have already been found in a variety of body fluids, such as saliva, plasma, breast milk (73) and broncho-alveolar lavage fluid (BALF) (74). The distribution of miRNA through exosomes to multiple cell types throughout the body increases the complexity of how cells communicate in health and disease.

1.2.3. A role for miRNAs in asthma

To this day, miRNAs have been shown to be of utmost importance in normal physiological processes like development, growth, differentiation and programmed cell death (49,75–78). A dysregulation of miRNAs has been observed and proven to be important in complex diseases like cancer (79). Regarding asthma, the miRNA expression in airways of patients with asthma has been shown to be altered compared to healthy controls (80,81). Several distinct miRNAs, namely miR-145 (82), miR-126 (83), miR-106 (84), let7 (85) and miR-21 (86,87) that target asthma-relevant molecules, like IL-13 (let-7) or IL-12p35 (miR-21), have been identified to be dysregulated in murine experimental asthma models and were targeted in a preventive setting. Thereby, the miRNAs were inhibited during or before the induction of the allergic airway inflammation but not therapeutically in established disease. This questions the relevance for treatment of human asthma where the patients already suffer from advanced disease at the time of diagnosis and preventive treatments are hardly possible.

1.3. The transcription factor cAMP-response element binding protein (Creb)

1.3.1. Gene and protein structure

The cAMP-response element binding protein (*Creb*) is a central transcription factor involved in many biological processes such as metabolism, neurotransmission, cell cycle, immune regulation and development (reviewed in (88)). *Creb*-/- mice seem fully developed but die at birth from respiratory failure due to pulmonary atelectasis and show impaired fetal T cell development (89), making this gene an interesting target to study in inflammatory lung disorders such as asthma.

*CREB*1 is encoded on chromosome 2 of the human genome and has 17 splice variants, 10 of which are protein coding. The most prominent transcript variant is 7650 bp of length and consists of nine exons. In mice, *Creb1* is located on chromosome 1, features 11 splice variants, six being protein coding and the main transcript has 8364 bp and eight exons.

In mammalian systems, the *Creb* family of cAMP-responsive activators consists of *Creb*, the activating transcription factor 1 (*Atf1*) and the cAMP response element modulator (*Crem*). *Creb* and *Atf1* are ubiquitously expressed throughout the body, *Crem* expression is highest in neuro-endocrine tissues (reviewed in (88)). The family members have a similar modular protein structure: it includes a basic leucine zipper (bZIP) domain at the carboxy-terminus that is required for DNA-binding and dimerization, and an amino-terminal transactivation domain (TAD) (Figure 1.3) (reviewed in (90)). The latter is required for the response to cAMP and consists of a central 60 amino-acid kinase-inducible domain (KID) and a glutamine-rich (Q2) constitutive activation domain, which can enhance transcription by binding the TBP-associated factor 4 (TAF4) (reviewed in (90)). Outside of the TAD domain towards the N-terminus there is another glutamine-rich domain (Q1) functioning, together with Q2, as constitutive activators *in vitro* (reviewed in (88)). In contrast, the KID domain is activated only after phosphorylation in response to cAMP and calcium (91).

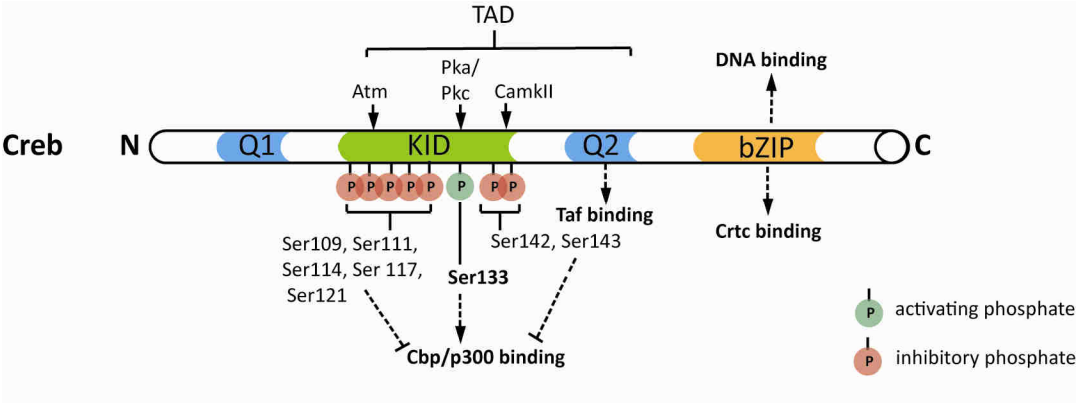

Figure 1.3: Schematic protein structure of Creb. Creb and family members have a similar modular organization, containing two Gln-rich domains (Q1+Q2) that function as constitutive activators, a kinase-inducible domain (KID) with inhibitory phosphorylation sites for Atm at Ser109, Ser111, Ser114, Ser117, Ser121 and for CamkII at Ser142 and Ser143 that hinder Cbp/p300 binding. Phosphorylation at Ser133 by Pka/Pkc favors Cbp/p300 binding hence activates transcription. KID plus Q2 domain that can bind TAF represents the transactivation domain (TAD). The bZIP domain at the C-terminus is required for DNA binding, nuclear localization and binding to Creb-regulated co-activators (Crtcs). Adapted from (90).

1.3.2. Transcriptional regulation of Creb1 target genes

Creb and its family members Atf1 and Crem were the first transcription factors shown to be activated by phosphorylation (reviewed in (88)). This was discovered roughly 25 years ago through the binding to the CRE element in the promoter of somatostatin, a neuropeptide gene (92–94).

As indicated in the name, Creb is activated by phosphorylation upon cAMP stimulus. This prominent second messenger accumulates after activation of guanine-nucleotide-binding (G)-protein coupled receptors, the synthesis being catalyzed by adenylyl cyclase (Ac) (95). cAMP then liberates the C subunit of protein kinase A (Pka), which under basal conditions resides in the cytoplasm as an inactive hetero-tetramer of paired regulatory (R) and catalytic (C) subunits. The free C subunit then diffuses into the nucleus and phosphorylates Creb at serine residue 133 in the KID domain (96). This recruits the Creb-binding protein (Cbp) and its paralogue p300, and Creb proteins bind as dimers to the DNA to initiate transcription (reviewed in 75). Cbp/p300 binding is required as it acetylates histones and also recruits the RNA polymerase II complexes (reviewed in (90)). This process usually takes about 30 min and lasts for two to four hours until Ser133 is dephosphorylated by the serine/threonine phosphatases Pp-1 and Pp-2A (reviewed in (88)). Of note, there are also other regulatory phosphorylation sites within the Creb KID domain that act inhibitory, such as Ser111 and Ser121, phosphorylated by ataxia-telangiectasia mutated (Atm) (97), and Ser142, targeted by calcium- and calmodulin-dependent kinase II (CamkII) (98).

Creb and family members initiate the target gene transcription by binding to cAMP response elements (CRE) at promoters. These can appear as palindromic (TGACGTCA) or half-site motifs (TGACG or CGTCA) (94). There are about 750,000 palindromic and half-site CREs present in the human genome, whereby the majority of them are unoccupied due to an inhibitory cytosine methylation of the CREB binding site (reviewed in (99)). The functional, non-methylated, sites are mostly localized to promoter proximal regions within 250 bp of the transcription start site and occur in about 5,000 genes (reviewed in (99)). However, even upon binding of phosphorylated Creb after cAMP stimulation, only a small number (~100) of genes are induced and this also strongly depends on the cell type (reviewed in (99)). This might be in part explained by the absence of canonical TATA boxes in two-thirds of Creb-occupied promoters that are required for transcriptional induction by cAMP (100). Additionally, some Creb binding sites might be epigenetically modified to limit accessibility. Finally, the transcription of Creb target genes in a cell-type or stimulus-specific manner is dependent on further activators.

1.3.3. Creb Co-activators

Indeed, recently a class of proteins, termed cAMP-regulated transcriptional co-activators (Crtc), has been identified that plays a role in modulating Creb target gene expression (101,102). This family consists of three members (Crtc-1, -2, and -3) with a similar modular structure: a C-terminal TAD domain, a splicing domain (SD), a central regulatory domain (REG), and a N-terminal Creb-binding domain that interacts with the bZIP domain of Creb (Fig. 1.4) (reviewed in (90)).

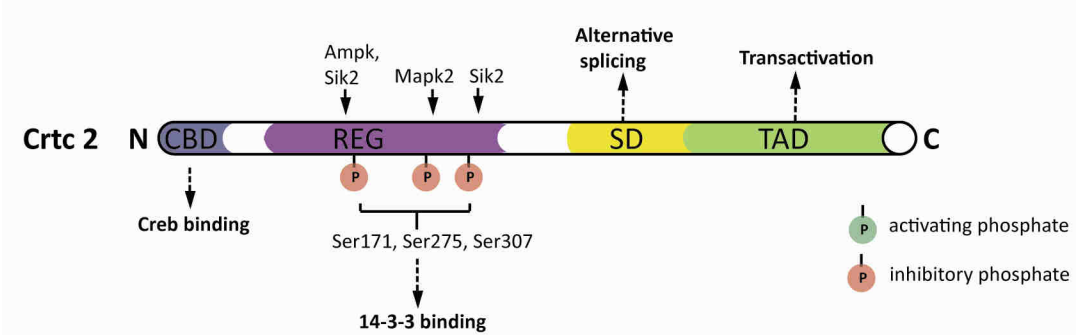

Figure 1.4: Schematic protein structure of the Crtcs - exemplarily for Crtc2. Crtc1, -2 and -3 share a similar modular organization: an N-terminal Creb-binding domain (CBD), followed by the regulatory domain (REG) which entails three inhibitory phosphorylation sites at Ser171 (Ampk, Sik2), Ser275 (Mapk2) and Ser307 (Sik2) enabling binding to 14-3-3 protein in the cytoplasm; an alternative splicing domain (SD) and an C-terminal transactivation domain (TAD). Adapted from (90).

In contrast to Creb, the Crtcs are under basal conditions sequestered in the cytoplasm, associated to 14-3-3 proteins via three phosphorylation sites, phosphorylated by either AMP-activated kinase (Ampk), mitogen-activated protein kinase 2 (Mapk2) or salt-inducible kinase 2 (Sik2) (reviewed in (90)). Dephosphorylation by calcineurin (Cn) is triggered by cAMP and calcium and leads to nuclear translocation of the Crtcs, which then bind together with Creb over relevant promoters (Fig. 1.5). This binding increases Creb occupancy on CRE sites (103) and thereby enhances transcription of target genes. Hence, the regulation of Creb target gene transcription can be seen as a two-hit model with first requiring phosphorylation of Creb itself and, second, the dephosphorylation and nuclear translocation of its co-activators (reviewed in (90)).

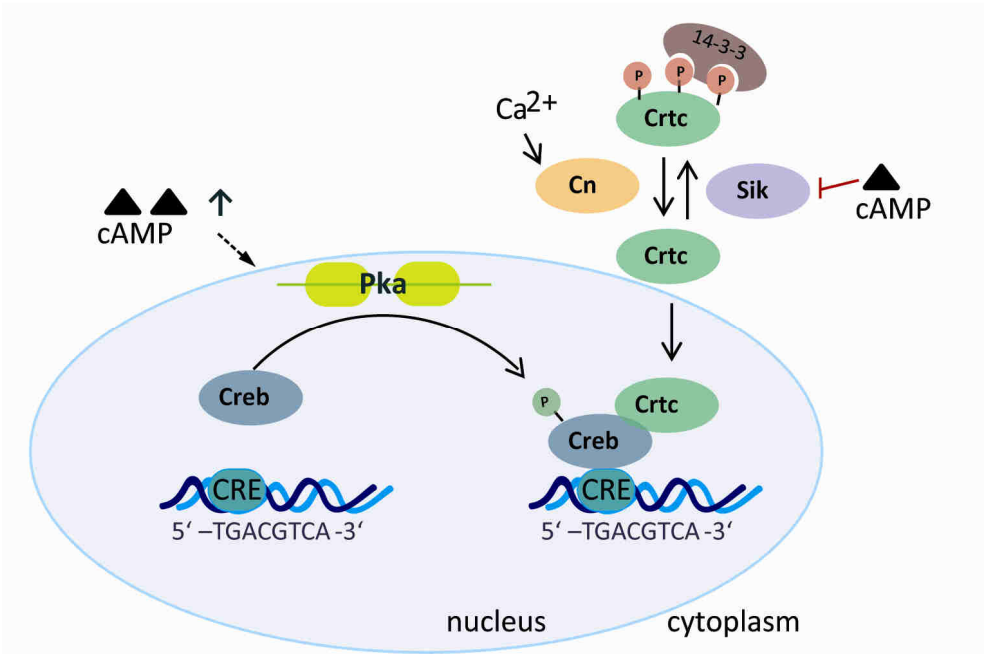

Figure 1.5: The two-hit model for Creb/Crtc mediated regulation of transcription. Creb binds to CRE sites in promoter regions upon phosphorylation at Ser133 by protein kinase A (Pka) after cAMP stimulus and initiates target gene transcription. The Crtc proteins are sequestered in the cytoplasm. Upon cAMP accumulation, they are dephosphorylated by calcineurin (Cn) and translocate to the nucleus where they bind together with Creb over relevant promoters and further enhance gene transcription. Adapted from (90).

Of note, there are numerous other factors that can interact with Creb to activate target gene transcription such as CBP or to repress it such as CREM. Alone 28 different factors are reviewed in (95). To investigate all of those would be out of the scope for this study, and hence they are not described in more detail.

2. AIMS AND OBJECTIVES

In previous work of the group, dysregulated pulmonary miRNAs were identified in a murine model of ovalbumin-induced allergic airway inflammation. miR-17 and miR-144 were prioritized for further investigation and shown to target the transcription factor Creb1 (104). However, single miRNAs tend to target several critical regulators within a given pathway (62–64).

Therefore, we hypothesized in the present work that miR-17 and miR-144 might also target other signaling components of the Creb1 pathway such as the co-activators Crtc1-3. We further postulated that a joint down-regulation of both Creb1 and Crtcs by miRNAs could lead to an additive, detrimental effect on the transcription of target genes and this could be relevant for the pathogenesis of asthma.

In particular, we aimed to:

- Identify and validate a possible binding of the dysregulated miRNAs to the Crtcs.
- Evaluate the expression of the Creb1/Crtc pathway in murine experimental asthma.
- Identify putative Creb1 target genes relevant for murine experimental asthma.
- Study Creb/Crtc-mediated signaling during early asthmatic responses.
- Investigate the relevance of the identified pathway for human paediatric asthma.

3. MATERIAL

3.1. Chemicals and reagents

Table 3.1: Chemicals and reagents

Substance	Manufacturer	Country
4′,6-Diamidin-2-phenylindol (DAPI)	Sigma-Aldrich	St. Louis (USA)
Acetic Acid	Carl Roth	Karlsruhe (GER)
Adenosine triphosphate (ATP)	pjk	Kleinblittersdorf (GER)
Agarose	Life Technologies	Darmstadt (GER)
Albumin from chicken egg white, grade V (OVA)	Sigma-Aldrich	St. Louis (USA)
Ammoniumpersulfate (APS)	Sigma-Aldrich	St. Louis (USA)
Antibody diluent	Zytomed Systems	Berlin (GER)
BEGM Medium	Lonza	Wokingham (UK)
Bovine serum albumin (BSA)	Sigma-Aldrich	St. Louis (USA)
Bromphenolblue	Merck	Darmstadt (GER)
Citric Acid Monohydrate	Carl Roth	Karlsruhe (GER)
CML Latex 4% w/v 4 µm	Life Technologies	Darmstadt (GER)
Coelenterizine	SynChem	Illinois (USA)
Coenzym A	pjk	Kleinblittersdorf (GER)
cOmplete mini protease inhibitor cocktail	Roche	Mannheim (GER)
Dermatophagoides pteronyssinus extract (Nr. 218234)	Greer	Lenoir, USA
Dimethyl sulfoxide (DMSO)	Sigma-Aldrich	St. Louis (USA)
Dithiothreitol (DTT)	pjk	Kleinblittersdorf (GER)
D-Luciferin	SynChem	Illinois (USA)
ECL, ECL dura, ECL femto	Thermo Fisher Scientific	Waltham (USA)
Entellan	Merck	Darmstadt (GER)
Ethanol	Merck	Darmstadt (GER)
Ethylenediaminetetraacetic acid (EDTA)	Sigma-Aldrich	St. Louis (USA)
Exoquick-TC, Exosome precipitation solution for culture media, spinal fluid and urine	System Biosciences	San Francisco (USA)
Exosome-depleted FBS Media Supplement	System Biosciences	San Francisco (USA)
Fetal calf serum (FCS)	Life Technologies	Darmstadt (GER)
Fluorescence Mounting Medium	Dako	Hamburg (GER)
Formaldehyde solution 32 %	Carl Roth	Karlsruhe (GER)
Formamide	Carl Roth	Karlsruhe (GER)
Glycin	PanReac Applichem	Darmstadt (GER)
HBSS, 10x, Calcium, Magnesium, no Phenol Red	Life Technologies	Darmstadt (GER)
human placental collagen type IV	Sigma-Aldrich	St. Louis (USA)
Hydrochloric acid (HCl), 2 M	Merck	Darmstadt (GER)
Hydrogen peroxide (H_2O_2)	Merck	Darmstadt (GER)
Imject® Alum	Thermo Fisher Scientific	Waltham (USA)
Ketamin	CD-pharma	Québec (CAN)
Light Cycler 480 SYBR Green I Master Mix	Roche	Mannheim (GER)
Lipofectamine™ 2000	Life Technologies	Darmstadt (GER)
Lyophilized exosomes from colon cancer cell line (COLO1)	Hansa Biomed	Tallin (EE)

Substance	Manufacturer	Country
Magnesium carbonate (pentahydrate) $(MgCO_3)_4Mg(OH)_2 *5H_20$	Carl Roth	Karlsruhe (GER)
Magnesium sulfate (heptahydrate) $MgSO_4*7H_2O$	Carl Roth	Karlsruhe (GER)
Mayers Haematoxylin (hemalum solution)	Merck	Darmstadt (GER)
MEM (Minimal Essential medium)	Life Technologies	Darmstadt (GER)
Methanol	Carl Roth	Karlsruhe (GER)
N,N,N′,N′-Tetramethylethylenediamine (TEMED)	Sigma-Aldrich	St. Louis (USA)
Na_3VO_4	Sigma-Aldrich	St. Louis (USA)
NaF	Sigma-Aldrich	St. Louis (USA)
Paraffin 53-54°	Carl Roth	Karlsruhe (GER)
peqFECT DNA	peqLab Biotechnolgies	Erlangen (GER)
peqFECT siRNA	peqLab Biotechnolgies	Erlangen (GER)
periodic acid cristals	Merck	Darmstadt (GER)
Phosphate buffered saline (PBS)	Life Technologies	Darmstadt (GER)
PKH67 green fluorescent cell linker kit	Sigma-Aldrich	St. Louis (USA)
PneumaCult™-ALI medium	StemCell technologies	Köln (GER)
Prestained protein page ruler	Thermo Fisher Scientific	Waltham (USA)
psiCHECK™-2 Vector	Promega	Wisconsin (USA)
Qiazol lysis reagent	Qiagen	Hilden (GER)
recombinant murine Interleukin 13	R&D systems	Wiesbaden (GER)
RestorePlus® Stripping buffer	Thermo Fisher Scientific	Waltham (USA)
RNAlater®	Life Technologies	Darmstadt (GER)
Rotiphorese® Gel 30	Carl Roth	Karlsruhe (GER)
Schiff's reagent	Merck	Darmstadt (GER)
Sodium bicarbonate ($NaHCO_3$)	Merck	Darmstadt (GER)
Sodium carbonate (Na_2CO_3)	Sigma-Aldrich	St. Louis (USA)
Sodium chloride (NaCl)	Merck	Darmstadt (GER)
Sodium dodecyl sulfate (SDS)	GE Healthcare	Chalfont St Giles (UK)
sodiumhydrogensulfite 39%	Merck	Darmstadt (GER)
Sulfuric acid (H_2SO_4)	Carl Roth	Karlsruhe (GER)
TaqMan® Universal PCR Mastermix, no AmpErase® UNG	Life Technologies	Darmstadt (GER)
Tricine	Carl Roth	Karlsruhe (GER)
Tris	Carl Roth	Karlsruhe (GER)
Triton X-100	Sigma-Aldrich	St. Louis (USA)
Trypan blue	Sigma-Aldrich	St. Louis (USA)
Trypsin-EDTA	Life Technologies	Darmstadt (GER)
Tween 20	Sigma-Aldrich	St. Louis (USA)
Xylazin	aniMedica	Senden-Bösensell (DE)
Xylene	Merck	Darmstadt (GER)
Xylol	PanReac Applichem	Darmstadt (GER)

3.2. Buffers and solutions

Table 3.2: Buffers and solutions

Name		Substance	Volume
0.5M Tris-Cl, pH 6.8		Tris	15.41 g
	add	H_2O bidest	250 ml
		adjust pH to 6.8 with HCl	
1.5M Tris-Cl, pH 8.8		Tris	45.43 g
	add	H_2O bidest	250 ml
		adjust pH to 8.8 with HCl	
Flow cytometry wash buffer (exosomes)		FBS (exosome depleted)	3%
	add	PBS	500 ml
6x Laemmli loading dye		Tris	375 mM
		DTT	600 mM
		SDS	12%
		Dissolve and adjust pH to 6.8	
		Glycerol	60%
		Bromphenolblue	0.06%
Citrate buffer (pH 6)		Citric acid	2.1 g
	add	H_2O bidest	1 l
		adjust pH to 6	
Na-Tris (10x)		Tris	60.5 g
		Aqua dest.	700 ml
		adjust pH to 7.6 with 2M HCl	
	add	Aqua dest.	1000 ml
		NaCl	90 g
MES buffer		Glycine	0.10%
		sodium azide	0.10%
	add	PBS	500 ml
Lysis buffer (pH 7.4)		Tris	15.14 g
		Triton X-100	5 g
	add	H_2O	500 ml
Periodic acid		periodic acid cristals	0.5g
	add	H_20 bidest	100ml
		adjust pH to 7.2 with 2M HCl	
RIPA buffer		Tris (pH 7.4-8)	50 mM
		NaCl	150 mM
		Triton X-100	1%
		Sodiumdeoxycholate	0.5-1 %
		NaF	5-10 mM
	add prior to use	Na3VO4	1 mM
		DTT	1 mM
		Protease Inhibitor	1x

Name		Substance	Volume
Running Gel SDS Page (for 2 gels)		H_2O bidest	3.08 ml
		Rotiphorese® Gel 30 Acrylamid	3.3 ml
		1.5 M Tris-Cl, pH 8.8	4.18 ml
		10 % SDS in H_2O	110 µl
	add directly before usage	10 % APS in H_2O	220 µl
		TEMED	5.5 µl
		pour between two glass plates and cover surface with H_2O till dry	
Stacking Gel SDS Page (for 2 gels)		H_2O bidest	3 ml
		Rotiphorese® Gel 30 Acrylamid	650 µl
		0.5 M Tris-Cl, pH 6.8	1.25 ml
		10 % SDS in H_2O	50 µl
	add directly before usage	10 % APS in H_2O	50 µl
		TEMED	5 µl
		pour on top of running gel and insert comb	
Sulfite water		sodiumhydrogensulfite 39%	100ml
	add	H_20 bidest	300ml
TAE buffer (pH 8.5)		Tris	242 g
		Acetic acid	57.1 ml
		EDTA, 0.5 M	100 ml
	add	H_2O	1000 ml
TBE buffer (5x)		Tris	54.51 g
		Boric acid	27.51 g
		EDTA-Na_2	4.65 g
	add	H_2O	1000 ml
	prior to use	Dilute to 1x with H_2O bidest	

Name		Substance	Volume
Western Blot 10x running buffer		Tris	30 g
		Glycin	144 g
		SDS	10 g
	add	H_2O	1l
	prior to use	Dilute to 1x with H_2O bidest	
Western Blot 10x transfer buffer		Tris	30 g
		Glycin	141 g
	add	H_2O	1l
	prior to use	Dilute to 800 ml 1x with H_2O bidest	
	add	MeOH	200 ml
Western Blot 10x TBS		Tris	12.1 ml
		NaCl	40 g
	add	H_2O	500 ml
Western Blot 1x TBST	for 1 l	10x TBS	100 ml
		H_20 bidest	900 ml
	add	Tween 20	1 ml

3.3. Antibodies

Table 3.3: Antibodies

	Antibody	Molecular Weight	Application	Manufacturer	Country
Primary	CREB rabbit mAB (#9197)	43 kDa	Western Blot	Cell Signaling Technology	Danvers (USA)
	CRTC1 rabbit mAB (#2587)	80 kDa	Western Blot	Cell Signaling Technology	Danvers (USA)
	CRTC3 rabbit mAB (#2720)	78 kDa	Western Blot	Cell Signaling Technology	Danvers (USA)
	GAPDH rabbit mAB (#2118)	37 kDa	Western Blot	Cell Signaling Technology	Danvers (USA)
	FOXJ1 mouse mAB (#365216)	55 kDa	Western Blot, Immunofluorescence	Santa Cruz Biotech	Dallas (USA)
	SEC14l3 rabbit pAB (ab113799)	46 kDa	Western Blot, Immunofluorescence (mouse)	Abcam	Cambridge (USA)
Secondary	Immun-Star Goat anti-rabbit HRP-conjugate IgG	-	Western Blot	Biorad	Hercules (USA)
	Alexa-Fluor 568 goat anti-rabbit IgG (H+L)	-	Immunofluorescence	Life Technologies	Darmstadt (GER)
	Purified mouse anti-human CD63 (#556019)	25kDa	flow cytometry	BD Biosciences	Franclin Lakes (USA)
	Purified anti-mouse CD63 (#143901)	25kDa	flow cytometry	Biolegend	San Diego (USA)

3.4. Oligonucleotides

All oligonucleotides were synthesized by Metabion International AG (Martinsried, Germany). Prior to use, they were validated for specificity by melting curve analysis and gel electrophoresis and tested for efficiency.

Table 3.4: Primer sequences used for qRT-PCR

Gene name	Species	fwd 5'->3'	rev 5'->3'
CRTC1	hsa	GAATCCTTTAGCAGTGGGTCC	TTTGTCTGCCTCTGATGTGG
CRTC2	hsa	GACAAGCTCTGACTCTGCCC	CCATCCAGAATACCCCCAC
CRTC3	hsa	AGATGTGGGTTTTGACCAGC	TGTTGAGGTCTTTGAACAGGC
SEC14l3	hsa	CAAGGGGTTGCTCTTCTCAG	TCCCTAGCCTCTCTGTCTGC
MUC5AC	hsa	GCCTTCACTGTACTGGCTGAG	AGGGTCTGAAGATGGTGACG
FOXJ1	hsa	TCGTATGCCACGCTCATCTG	CTTGTAGATGGCCGACAGGG
HPRT	hsa	TTGTTGTAGGATATGCCCTTGAC	TCTCATCTTAGGCTTTGTATTTTGC
CREB1	mmu/hsa	CCCAGCAACCAAGTTGTTGTT	CTG CCT CCC TGT TCT TCA TTA GAC
Crtc1	mmu	CGGGCTCCACACTCAACTA	TGCTCAGTTCCTTAGAGAGGCT
Crtc2	mmu	GTACAACGAGATGCCCGC	CTAAACAACTGCCCCTTCTCAG
Crtc3	mmu	GCATGAGTGTGGGGAACAG	TGGATGGAAGGGTTACTTCG
Sec14l3	mmu	CATGTGTCAGCGAAATCCC	TCTATGTCAATGCAGCGAGTG
Hprt	mmu	CAGGCCAGACTTTGTTGGAT	ACGTGATTCAAATCCCTGAAGT

Table 3.5: miRNA mimics

TaqMan® miRNA-Assays	miRNA Sequence	Provider
hsa/mmu-miR-17	CAAAGUGCUUACAGUGCAGGUAG	Life technologies, Darmstadt (GER)
hsa/mmu-miR-144	UACAGUAUAGAUGAUGUACU	Life technologies, Darmstadt (GER)
hsa/mmu-miR-21	UAGCUUAUCAGACUGAUGUUGA	Life technologies, Darmstadt (GER)
miRNA mimics		
negative control (scrambled miRNA)	Ambion® Pre-miR™ Precursors	Life technologies, Darmstadt (GER)
hsa/mmu-miR-17	Ambion® Pre-miR™ Precursors	Life technologies, Darmstadt (GER)
hsa/mmu-miR-144	Ambion® Pre-miR™ Precursors	Life technologies, Darmstadt (GER)
hsa/mmu-miR-21	*mir* Vana® miRNA mimics	Life technologies, Darmstadt (GER)

3.5. Commercial kits

Table 3.6: Commercial kits

Kit	Provider	Country
BCA protein assay kit	Thermo Fischer Scientific	Waltham (USA)
Clonetics™ ReagentPack™	Lonza	Wokingham (UK)
Diff-Quick kit	Medion Diagnostics	Düdingen (CH)
Exosome CD63 ELISA	Systems Biosciences	San Francisco (USA)
miRNeasy micro kit	Qiagen	Hilden (GER)
miRNeasy mini kit	Qiagen	Hilden (GER)
Quantitect Reverse Transcription kit	Qiagen	Hilden (GER)
TaqMan® miRNA reverse transcription kit	Life Technologies	Darmstadt (GER)

3.6. Cell lines and mouse strains

Table 3.7: Cell lines

cell line	origin	Provider
16HBE14o$^-$	Isolated from human bronchial epithelium. Transformed with SV-40 virus	Dieter C. Gruenert
MLE-12	murine transgenic lung epithelial cells, transformed with SV-40 virus	ATCC; LGC Standards, Wesel (GER)
NHBE	primary normal human bronchial epithelial cells from cadavers	Lonza, Wokingham (UK)

Table 3.8: Mouse strains

Strain	Provider	Country
Balb/c	Charles River	Sulzfeld (GER)

3.7. Miscellaneous consumables

Table 3.9: Miscellaneous consumables

Consumables	Provider	Country
6 & 12 well plates Nunc™	Thermo Fischer Scientific	Waltham (USA)
12-well transwell inserts (clear, 0.4µm)	Corning	New York (USA)
12-well transwell inserts (transparent, 0.4 µm)	Greiner Bio-One	Frickenhausen (GER)
Cell culture flasks 75cm^2, 175cm^2	Greiner Bio-One	Frickenhausen (GER)
Cell scraper 240m, blade width 13mm	TPP	Trasadingen (CH)
Cryotubes	Sarstedt	Nürnbrecht (GER)
Glass slides	Gerhard Menzel	Braunschweig (GER)
Histology cassettes	Thermo Fischer Scientific	Waltham (USA)
LumiNunc, F96	Thermo Fischer Scientific	Waltham (USA)
Microplate 96 well	Greiner Bio-One	Frickenhausen (GER)
Mini-PROTEAN® Tetra Cell 1D electophoresis system	Biorad	Hercules (USA)
qPCR plate	Biozym	Hessisch-Oldendorf (GER)
Shandon cytofunnels	Thermo Fischer Scientific	Waltham (USA)

3.8. Software and websites

Table 3.10: Software and websites

Software	Source
Axio Vision	Zeiss, Oberkochen (GER)
GraphPad Prism v5.0	GraphPad Prism Software, San Diego (USA)
LightCycler® 480 Software v1.5	Roche, Mannheim (GER)
Target Scan	www.targetscan.org
miRbase	www.mirbase.org
MatInspector Release professional 8.0.5, March 2011	(Database version: ElDorado 08-2011; MatInspector library: Matrix Family Library Version 8.4 (June 2011))
ImageLab™ v5.1	Biorad, Hercules (USA)
Flow Jo v10	FlowJo, Ashland (USA)

3.9. Equipment and devices

Table 3.11: Equipment and devices

Equipment/ device	Name	Provider	Country
Centrifuges	Mikro 200	Hettich Zentrifugen	Tuttlingen (GER)
	Mikro 200R	Hettich Zentrifugen	Tuttlingen (GER)
	Rotina 420R	Hettich Zentrifugen	Tuttlingen (GER)
Cytospin centrifuge	Cytospin 4	Thermo Fischer Scientific	Waltham (USA)
Embedding Machine	Microm EC350	Zeiss	Oberkochen (GER)
Flow cytometer	BD LSRII	Becton Dickinson	Franclin Lakes (USA)
Fluorescence plate reader	Sunrise®	Tecan	Männedorf (CH)
Fridge/Freezer	4°C	Liebherr	Biberrach an der Riss (GER)
	-20°C	Liebherr	Biberrach an der Riss (GER)
	-80°C	Eppendorf	Hamburg (GER)
Fume Hood	Airflow Control	Vinitex	Sint Oedenroede (NL)
Gel Imager	ChemiDoc™ Imaging System	Biorad	Hercules (USA)
Hemocytometer	Neubauer cell chamber	GLW	Würzburg (GER)
Homogenizer	MagnaLyser	Roche	Mannheim (GER)
Homogenizer	Polytron TP2100	Thermo Fischer Scientific	Waltham (USA)
Incubator	Heraeus Function Line Incubator BDG220	Thermo Fischer Scientific	Waltham (USA)
Liquid nitrogen tank	Apollo	Cryotherm	Kirchen/Sieg (GER)
Mastercycler	Mastercycler Gradient	Eppendorf	Hamburg (GER)
Microscopes	Axiovert 40c	Zeiss	Oberkochen (GER)
	Axio Imager	Zeiss	Oberkochen (GER)
Microtom	Hyrax M55	Zeiss	Oberkochen (GER)
Nebulizer	pari Boy	Pari	Starnberg (GER)
Platform shaker	Duomax 1030	Heidolph	Schwabach (GER)
Real-time Thermocycler	Light Cycler 480	Roche	Mannheim (GER)
Spectrophotometer	Nanodrop ND-1000	PeqLab Biotechnology	Erlangen (GER)
Sterile hood	Herasafe KS	Thermo Fischer Scientific	Waltham (USA)
Tissue processor	Microm STP420D	Thermo Fischer Scientific	Waltham (USA)
Water bath	Aqualine AL12	Lauda	Lauda-Königshofen (GER)
Western blot developer	ChemiDoc™ Imaging System	Biorad	Hercules (USA)
Xray developer	Curix60	Siemens Healthcare	Sankt Wolfgang (GER)

4. METHODS

4.1. Mouse models

4.1.1. Animal maintenance

Female Balb/c mice were obtained from Charles River (Sulzfeld, Germany) and housed in individually ventilated cages. A standard pellet diet and water were provided *ad libitum*. The study was conducted under the federal guidelines for the use and care of laboratory animals and was approved by the Government of the District of Upper Bavaria.

4.1.2. Induction of allergic airway inflammation

Female 6 to 8 weeks old Balb/c mice were sensitized by six consecutive intra-peritoneally (i.p.) injections of ovalbumin (OVA) in alum (1µg in 200 µl PBS) or PBS in alum for controls on days 0, 7, 14, 28, 42, and 56. Allergic airway inflammation was triggered by two ovalbumin aerosol challenges (20min, 1% OVA in PBS) at day 70 and 71. Mice were sacrificed on day 29 or 72 (Fig. 4.1) Treatments were performed by Dr. Francesca Alessandrini (ZAUM, Munich) and the model is described in (105).

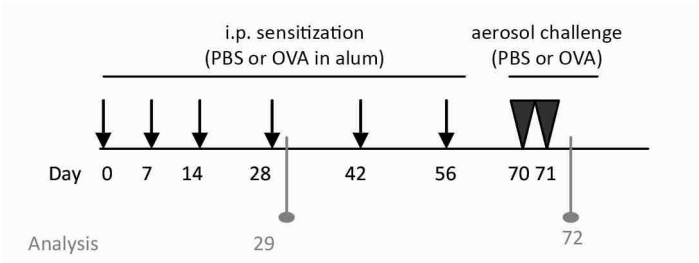

Figure 4.1: Treatment scheme for OVA-induced allergic airway inflammation. 6-8 week old female Balb/c mice were sensitized intra-peritoneally (i.p.) six times with ovalbumin (OVA) in alum or PBS for control groups and then subjected to two consecutive OVA aerosol-challenges (1% OVA in PBS) on day 70 and 71. Animals were sacrificed either on day 29 or day 72.

For house dust mite (HDM) induced asthma, mice were treated intra-nasally three times per week over five weeks with 20 µg Dermatophagoides pteronyssinus in 30 µl PBS or PBS only

for controls. Treatments were performed together with Petra Nathan, Katrin Milger and Jeremias Götschke (CPC Munich).

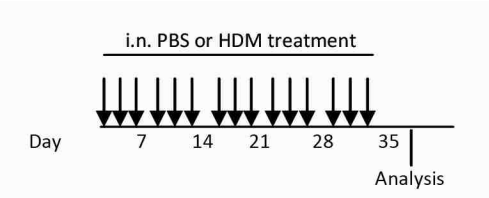

Figure 4.2: Treatment scheme for HDM-induced allergic airway inflammation. 6-8 week old female Balb/c mice were treated three times per week over five weeks intra-nasally (i.n.) with either house dust mite extract (HDM) or PBS for controls. Animals were sacrificed 24 h after the last allergen challenge.

4.1.3. Lung function

Animals were injected i.p. with ketamine (140 mg/kg) and xylazine (7 mg/kg). When the anaesthesia was deep enough, the mice were tracheotomised and intubated with an 18G tube, placed on a warming plate and ventilated with a tidal volume of 10 ml/kg at a frequency of 150 breaths/minute and a positive end-expiratory pressure of 2 cm H_2O on a Buxco system (R/C system). To assess airway hyperreactivity (AHR), the mice were challenged with the broncho-constrictor metacholine in physiological saline generated with an in-line nebulizer and administered directly with increasing concentrations (0, 6.25, 12.5 mg/ml) by the ventilator for 20 seconds. Resistance (R) and Compliance (C) were measured continuously for 2 min and the average was calculated and plotted against the concentration. Measurement was performed by Petra Nathan, Katrin Milger and Jeremias Götschke (CPC Munich).

4.1.4. BAL analysis

Broncho-alveolar lavage (BAL) was performed by three times intra-tracheal instillation and retrieval of 0.8 ml PBS. The cellular fraction was separated from the fluid by centrifugation for 10 min at 4 °C and 1200 rpm. The BAL fluid (BALF) was stored at -80 °C until further use while BAL cells were immediately further processed.

4.1.4.1. Total cell counts

After resuspension of the BAL cell pellet in 160 µl of cold PBS (with 5% FCS), the cells were counted by using a hematocytometer, diluted1:1 with trypan blue. The total cell number was calculated with the following formula: total cell number = (counted cells in 4 squares / 4) * 2 (* dilution) * 10^4/ml.

4.1.4.2. Differential cell counts

10^4 to 10^5 cells in 150 µl PBS (with 5% FCS) were transferred to a glass slide by 10 min cyto-centrifugation at 400 rpm. The cytospins were dried over night at room temperature and subsequently stained with the May-Giemsa-Grünwald staining (Diff-Quick kit) according to the manufacture's recommendations. The DNA-rich nuclei are stained dark blue or violet by the alkaline components methylene blue and azur B. The cytoplasm appears in light blue with dark blue granula for basophils and acidophilic pink eosin-stained granula in eosinophils. The granula in neutrophils are only week acidophilic and therefore are not visible in the stain. Furthermore, macrophages were distinguished from lymphocytes by their larger size and bigger cytoplasm. Differential cell counts were performed with a light microscope at a 40x magnification and at least 500 cells per slide were counted.

4.2. Histopathology – Periodic Acid Schiff stain

To analyze inflammation and lung structures, the left lung lobe was fixed by instillation of 4% paraformaldehyde (PFA) and immersion over 24 h at 4 °C. Afterwards, the tissue was incubated with 70% ethanol for up to three days in histology cassettes. In a tissue processor, washing steps with increasing concentrations of ethanol (ethanol 70%, 80%, two times 95%, two times 100%) were applied to dehydrate the tissue and it was washed two further times for 5min with xylene. The transwell membranes of the NHBE primary cell cultures were first embedded in 2% agarose in HBSS to protect them during the dehydration process. Afterwards, the tissue was embedded in paraffin while the NHBE membranes were put in a vertical position to enable cross-sectioning. 3 µm thick sections were cut with a microtome, put on glass slides, air-dried and stored until further processing. For staining with either dyes or fluorescent antibodies, the paraffin was removed from lung slices by brief incubation in

xylol and a decreasing EtOH row (two times 2 min in 100%, 1 min in 90%, 1 min in 80%, 1 min in 70% and 30 sec in H_2O).

A periodic acid Schiff stain was used to evaluate goblet cell metaplasia and mucus production in the murine lungs and the cross-section cut NHBE membranes. The stain is used to detect glycol groups that are oxidized by the periodic acid to aldehyde groups. These aldehyde groups can then bind the fuchsin sulfurous acid in the Schiff's reagent, which results in a switch from colorless to bright pink. Hence, neutral muco-substances will be demonstrated in pink, while the nuclei are stained blue by hematoxylin.

Briefly, the de-paraffinized sections were first incubated for 10 min in periodic acid, then washed 10 min with ddH_20 and stained with Schiff's reagent for another 10 min. Afterwards the sections were incubated three times for 5 min each in three different cuvettes with sulfite water and washed again for 10 min with ddH_20. For staining of the nuclei, the sections were kept for 2.5 min in Mayer's Hematoxylin, washed shortly first with ddH_20 and then 0.3% HCl in 70% EtOH. After another 10 min wash with ddH_20, the samples were dehydrated by an increasing alcohol row (3 times quickly dipping into 70% and 80% EtOH, then 1 min each in 90%, 96% and 100% EtOH followed by 2 min in 100% EtOH and two times 5 min in xylol. Afterwards, the sections were covered with a coverslip and entellan and analyzed by light microscopy. The stainings were performed by Rabea Imker (CPC Munich).

4.3. Cell culture

4.3.1. Culture of different cell lines

The transformed cell lines of murine lung epithelial cells (MLE-12) and human bronchial epithelial cells (16-HBE14o$^-$) (106) were cultured in MEM medium supplemented with 10% FCS at 37°C and 5% CO_2 without antibiotics under standard conditions. To detach the cells, they were incubated with 2 ml of trypsin for 5 min at 37°C or until the detachment was visible per microscopy. The reaction was stopped by addition of fresh media and the cells were transferred to new flasks or well plates. To determine the cell number, the cells were counted as described in 4.1.4.1.

4.3.2. Air-liquid interface culture of primary human bronchial epithelial cells

Primary normal human bronchial epithelial cells were cultured in T25 cm^2 flasks in BEGM medium at 37°C, 95% CO_2 and 5% O_2 in a humidified incubator. When the density reached 80%, cells were passaged using the Clonetics™ ReagentPack™ for subculturing. The cells were washed with 5 ml of pre-warmed HBSS and detached with 2 ml pre-warmed trypsin/EDTA for 3 - 5 minutes on 37°C followed by gentle tapping the side of the flask. Trypsin was inactivated by addition of 4 ml pre-warmed TNS and the entire mixture was transferred to a tube. Residual cells were collected by rinsing the flasks with 2 ml of pre-warmed HBSS. After pelleting the cells for 5 min at 220x g at room temperature, they were resuspended in 1 ml BEGM medium. Cell numbers were determined as described in 4.1.4.1 and subsequently either frozen for cryopreservation or seeded for experiments.

4.3.2.1. Differentiation of NHBE cells at the air-liquid interface

For air-liquid interface experiments the NHBE cells were cultured on 12-well transwell inserts that were pre-coated with human-placental collagen type IV. Collagen type IV pre-coating was performed with 8.9 µg/cm^2. Collagen type IV, supplied as cotton ball, was dissolved in ddH_20 / 0.2% acetic acid at 37 °C for 15 - 30 min to a concentration of 500 µg/ml, aliquoted and stored at -20 °C. It was diluted with HBSS and 200 µl were added to each transwell insert and incubated for 3 hours at room temperature. Pre-coated inserts were either used immediately, or stored at 4°C. Prior to cell seeding, the remaining lid was aspirated and each well was washed with 500 µl HBSS and the membranes were exposed to UV light in the laminar flow hood for 30 minutes to ensure sterility.

80,000 - 90,000 cells at passage 2 were seeded onto the pre-warmed human placental collagen type IV-coated 12-well transwell inserts in pre-warmed BEGM medium and expanded to confluency for approximately two days. Then, the apical medium was aspirated and the basal medium was changed to PneumaCult™-ALI medium containing 1% penicillin/streptomycin to start the air-liquid interface culture (d0). For differentiation into a pseudo-stratified epithelium, the NHBE cells were left for 28 days (Fig. 4.3) with regular changes of the basal medium every two days. The apical mucus was removed by weekly washes with 500 µl of HBSS.

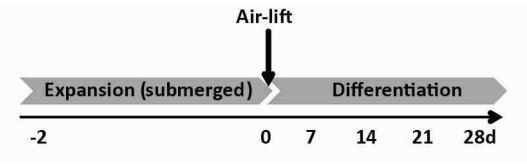

Figure 4.3: Differentiation of NHBE cells at the air liquid interface. Primary normal human bronchial epithelial cells were plated into 12-well transwell inserts (pre-coated with human collagen type IV) and expanded under submerged conditions. When the cells were fully confluent (typically after two days) the apical medium was aspirated (air-lift) and the cells were left to differentiate for 28 days with regular changes of the basal medium (every two days).

4.3.2.2. Treatment of NHBE cells with IL-13

In order to induce "asthma-like" changes to the bronchial epithelial cells including goblet cell, metaplasia and mucus hypersecretion, the cells were treated with interleukin-13 (IL-13). Therefore, 10 ng/ml of IL-13 (diluted in PBS) was added to the basal PneumaCult^{TM}-ALI medium at d0 of airlift and at every consecutive medium change. After 24 hours, four days and seven days cells were sampled for RNA and protein expression analysis and histology (Fig. 4.4). Additionally, the apical side was washed with 500 µl of HBSS to collect secreted exosomes. This supernatant, as well as the basal medium, was frozen at –80°C until analysis. The NHBE cultures and IL-13 treatments were performed together with Andrea C. Schamberger (RG Oliver Eickelberg, CPC Munich).

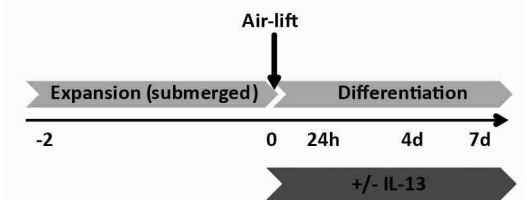

Figure 4.4: Induction of goblet cell metaplasia by IL-13 in NHBE cells. Primary normal human bronchial epithelial cells were plated into 12-well transwell inserts (pre-coated with human collagen type IV) and cultured under submerged conditions. When they reached confluency, the apical medium was aspirated (air-lift) and 10 ng/ml IL-13 was added to the basal medium, which was renewed every 2 days. Samples were taken at 24 hours, four days and seven days post air-lift.

4.3.3. Cryopreservation

In order to maintain low passage numbers, cells were frozen and stored in liquid nitrogen until further use. Therefore, cells were harvested by trypsination and 1-5 x 10^6 cells/ml were aliquoted into cryotubes in 1 ml of medium containing 20% FCS and 10% DMSO. The vials were slowly cooled down to -80°C by using a Mr. Frosty® freezing device filled with isopropanol. After two days, the cell vials were transferred to liquid nitrogen for long term

storage. To thaw cells, the frozen vials were warmed up to 37°C in a waterbath, pelleted by centrifugation and then seeded in appropriate fresh cell culture medium into a 75cm^{2}flask.

4.3.4. Transfection

Transfection experiments were conducted with Lipofectamine 2000™ in 12-well plates following manufacturer´s instructions. PremiRs for miR-17, -144 and -21 were transfected in duplicates to a final miRNA concentration of 20 nM per well. Briefly, premiRs were mixed with Lipofectamine 2000™ in a 1.5 ml tube and incubated for 20 min. Afterwards, the mixture was added to the cells and further incubated for 72 h. The medium was changed after 24 h to remove the lipid complexes and increase cell viability.

4.4. Paediatric asthma samples

4.4.1. Study population

The expression of miRNAs and target genes was investigated in nasal epithelial cells and nasal washes from children diagnosed with allergic asthma, or healthy controls. The patients were participants in the Asthma Severity Modifying Polymorphisms (AsthMaP) Project, a study of asthma in urban children and adolescents based at the Children's National Medical Center (Washington, DC, USA). The AsthMaP Project is described in detail elsewhere (107–111). The collection and storage of study samples was done and provided by the laboratory of Prof. Dr. Robert J. Freishtat (Washington DC, USA).

We included in this study 7 children with allergic asthma and compared those to 10 healthy children without history of asthma or wheezing as controls (Table 4.1). Inclusion criteria were a physician-diagnosed asthma, present at least for one year, elevated blood eosinophil counts (>4%) and serum IgE levels (>398 U/ml). Age-matched, non-atopic healthy control samples were collected at the Princess Margaret Hospital in Subiaco (Australia).

Table 4.1: Patient demographics

Phenotype	number	ethnicity	sex (m/f)	age (years)	FEV1 (% predicted)	serum IgE (U/ml)	blood eosinophils (%)
Allergic asthma	n=7	black	(4/3)	**9.43** ± 1.51	**83.14** ± 15.46	**1095.14** ± 543.28	**9.91** ± 4.20
Healthy controls	n=10	caucasian	(5/5)	**9.11** ± 2.89			

4.4.2. Isolation of nasal epithelial cells

A cytology brush was used to obtain epithelial cells by brushing the medial aspect of the inferior turbinate of each nare. The samples were pooled in one container prior to isolation. The epithelial cells were isolated from the nasal brushings as follows. Briefly, the cytology brush was centrifuged in a 15 ml falcon tube containing 5 ml medium. The cells were then incubated in MEM medium containing 10% FCS and 1% P/S over night in 6-well plates. The next day, the epithelial cells were attached to the surface of the cell culture plate and other cell types could be removed by washing the plates with PBS. This was done and provided by the laboratory of Prof. Dr. Robert J. Freishtat (Washington DC, USA).

4.4.3. Collection of nasal washes

Nasal washes were performed by instilling 3 ml of sterile isotonic saline into each nare, holding for 10 s and then collecting in a specimen collection container. The withdrawal was centrifuged to remove the mucus and cellular debris. The remaining nasal wash supernatant was stored at -80°C until further use. The washes were performed and provided by the laboratory of Prof. Dr. Robert J. Freishtat (Washington DC, USA).

4.5. RNA expression analysis

4.5.1. Isolation of total RNAs including small RNA

Prior to RNA isolation from murine lung tissue, the lungs were depleted from blood by trans-cardial transfusion. Therefore, approximately 5 ml of PBS were injected in the right ventricle and blood loss was monitored via the color change in the tissue. The lung tissue was then

dissociated in Qiazol reagent by a bead-based tissue homogenization using a MagnaLyser (Roche).

For isolation of RNA from cell culture or exosomes, the Qiazol was directly added to the pellet and the samples were incubated for 5 min at room temperature and thoroughly vortexed. The isolation procedure was performed by using the miRNeasy Mini Kit (Qiagen) or the miRNeasy Micro Kit (Qiagen) for samples with low RNA amounts, like exosomes, according to the manufacture's protocol. The concentration of RNA was determined by absorbance measurements (Nanodrop).

4.5.2. Quality testing

RNA quality was checked via agarose gel electrophoresis. Therefore, 1 µg of RNA was incubated with 5 µl formamide in a 10 µl reaction and denatured at 65°C for 15 min. Afterwards, the samples mixed with loading buffer containing SYBR green and separated in a 1% agarose gel in TAE buffer at 65 V for 45 min. Afterwards, the gel was analyzed for the 28S and 18S peaks of intact RNA with a Chemidoc XRS+ Imaging system. Only samples with satisfactory RNA quality were used for further analysis.

4.5.3. Reverse-transcription quantitative real-time PCR

4.5.3.1. Expression analysis of mRNA

Expression levels of different genes were analyzed by qRT-PCR in a two-step procedure. First, the RNA was converted to cDNA with the Quantitect Reverse Transcription kit according to the manufacturer's instructions. The remove residual genomic DNA 500 ng to 1 µg of RNA per sample were incubated with gDNA wipe out buffer for 5 min at 42°C. Afterwards the master mix for the reverse transcription containing the enzyme, buffer and a random hexamer primer mix was added and incubated at 42°C for 30 min and 3 min at 95°C. The cDNA mix was diluted 1:10 prior to qPCR.

Therefore, 2.5 µl of the specific cDNA was incubated with Light Cycler 480 SYBR Green I Master Mix and 3 pmol each of custom-designed primers (forward and reverse) for the gene of interest in a total volume of 10 µl in 96 well plates (primer sequences are listed under

MATERIALS section 3.4.). The thermal cycling conditions applied by the ROCHE LIGHT CYCLER 480 II platform were as follows:

Step		Temperature	Time	
Pre-incubation		95°C	10:00	
Amplification		95°C	0:10	
	repeated for 50 cycles	60°C	0:15	
		72°C	0:10	
		78°C	0:01	Quantification, single
Melting Curve		95°C	0:05	continuous 5/°C
		60°C	1:00	
		99°C	-	
Cooling		40°C	0:10	

4.5.3.2. Expression analysis of miRNA

For reverse transcription of miRNAs the TaqMan® reverse transcription kit was used according to the manufacturer's instructions. Based on this technology, first a miRNA-specific RT stem-loop primer (TaqMan® assay) is attached to the miRNAs and then they are converted to cDNA (112). Due to the high specificity of the miRNA primers, only 10 ng of total RNA were reversely transcribed for each sample and for each miRNA in separately. Thermal cycling conditions were 30 min at 16°C, 30 min at 42°C followed by 5 min at 85°C. Afterwards, the cDNA was diluted 1:1 prior to qPCR.

For quantification, 2 µl of the specific cDNA was incubated with the miRNA-specific PCR primer (TaqMan® assay) and the TaqMan® Universal PCR master mix, NO AmpErase® UNG in a total volume of 10 µl in white 96 well plates. The reaction was performed using a ROCHE LIGHT CYCLER 480 II platform with the following thermal cycling conditions.

	Temperature	Time	
Initial Denaturation	95°C	10 min	
Denaturation	95°C	15s	repeated for
Annealing/Extension	60°C	60s	50 cycles
Cool down	40°C	∞	

4.5.4. Normalization

After the qPCR run, the data was processed and analyzed by the ROCHE LIGHT CYCLER software. For normal mRNA runs, the melting curves were evaluated to ensure generation of specific PCR products. The resulting Cp values were exported and used to calculate differences in expressions with the ΔΔCp method with dCp=Cp(gene of interest)-Cp (reference gene). Hereby, HPRT was used as a stable reference gene for mRNA data normalization and the small nuclear RNAs RNU-6B (human) or sno-234 (mouse) for miRNA normalization. To normalize the expression of exosomal miRNAs, a defined amount (5.6 x 10^6 copies/sample) of a C. elegans derived miRNA, called Ce-miR-39, was added during the miRNA isolation process. qPCR results were then normalized to the expression of this spike-in control.

4.6. Protein expression analysis

4.6.1. Isolation of proteins

In order to isolate proteins from lung tissue, approximately 1/4th of a lung lobe was manually dissected into small pieces by using a scalpel and then further homogenized (Polytron TP2100) in 300 µl RIPA buffer. Cells grown in adherent cultures were detached from the surface in RIPA buffer with cell scrapers and vortexed thoroughly for homogenization. The samples were incubated on ice for 45 min, vortexed every 10 min, followed by 2 times sonification (10 s, 5 cycles, power 20%). Cell debris was removed by a 10 min centrifugation at 10,000g at 4°C and the proteins were stored at -20°C until further analysis or -80°C for long term storage.

4.6.2. Measurement of protein concentration

The protein samples were measured with a BCA protein assay kit according to the manufacturer's recommendations and analyzed with a fluorescence plate reader (Tecan Sunrise) at wavelength 595 nm. Concentrations were calculated by referring absorbance values to a linear BSA protein standard (concentrations 2 – 0.00097 mg/ml) on the same plate.

4.6.3. Western blot

For detection of specific proteins, they were firstly separated by size with an SDS gel electrophoresis. Therefore, 20 µg of each protein lysate was mixed with 6x Laemmli loading dye and RIPA buffer to an equal volume and applied into single lanes in a 20% polyacrylamide gel. Electrophoresis was performed in Tris-based running buffer with SDS for 120 min at 100 V. Afterwards, proteins were transferred to PVDF membranes for 90 min at 4°C by a standard wet blotting procedure in transfer buffer without SDS. The membranes were blocked in TBST containing 5% bovine serum albumin (BSA) for one hour at room temperature and then incubated under constant agitation over night at 4°C with antibodies against CREB1, CRTC1, CRTC3, SEC14L3 or GAPDH (all 1:1000 in 5% BSA in TBS-T). After washing, the membranes three times with TBST for 10 min at room temperature and constant agitation, they were incubated 1.5 h at room temperature with secondary HRP-conjugated goat anti-rabbit IgG antibody (1:40000, 5% BSA in TBS-T). The secondary antibody was removed by three 10 min washing steps in TBS-T. Prior to development the HRP substrates ECL, Dura-ECL or Femto-ECL were applied to the membrane, incubated for 5 min and the chemiluminescent signal was recorded with a Chemidoc XRS+ imaging system. For reprobing with new antibodies, membranes were incubated for 5 min at room temperature in RestorePlus® stripping buffer, washed three times with TBST and then blocked in 5% BSA for 1 h. Quantification of band intensities was performed with the Image Lab software v4.01 and normalized to the intensity of the loading control (GAPDH).

4.6.4. Immunofluorescence

Sec14l3 expression in murine lung tissues was determined by immunofluorescence using a specific Sec14l3 antibody. After removal of paraffin and rehydration of the tissue (see 4.2.) antigens were demasked by treatment of sections with citrate buffer (pH 6) at 125°C for 30 s and at 90°C for 10 s. After washing the sections three times in Na-Tris buffer, endogenous peroxidises were blocked for 15 min by an aqueous H_2O_2 solution. The sections were again washed three times with Na-Tris buffer, air-dried and then incubated with primary antibody (rabbit anti-Sec14l3; 1:200 in 100 µl antibody diluent) for 1 h at room temperature. After three washing steps with Na-Tris buffer, the secondary antibody Alexa Fluor 568 goat anti-rabbit IgG (H+L) (1:250 in 100 µl) was added onto the slides and left for 30 min at room temperature in the dark. Slides were washed three times with Na-Tris buffer and nuclei were co-stained with DAPI (1:2500, 0.5 µg DAPI/ml) for 1 min at room temperature. Finally, the

sections were washed again and then covered with fluorescence mounting medium and a cover slide. The slides were stored in the dark at 4°C.

If the identical sections were used for a subsequent PAS staining they were incubated overnight in Na-Tris buffer to remove the water soluble mounting medium and the cover slide. Afterwards, the slides were washed in ddH_2O to remove salt residues and stained as described in 4.2.

4.7. Isolation and analysis of exosomes

4.7.1. Isolation of exosomes

Exosomes were isolated from body fluids or cell culture medium by precipitation with ExoQuick-TC reagent according to the manufacturer's instructions. Briefly, cell debris was removed by a 10 min centrifugation at 3000 g, then $1/5^{th}$ volume of ExoQuick-TC was added to the supernatant and incubated over night at 4°C. The exosomes were spun down at 1500 g for 30 min and the exosome pellet was resuspended in either 200 µl exosome binding buffer for quantification by ELISA, 200 µl PBS for flow cytometry analysis or 700 µl of Qiazol reagent for miRNA isolation.

4.7.2. Quantification by CD63 ELISA

The exosomes collected from the supernatants of the primary NHBE culture were quantified by a specific CD63 ELISA kit according to the manufacturer's recommendation. Briefly, the exosome pellet after the precipitation with Exoquick-TC was resuspended in 200 µl exosome binding buffer, vortexed, incubated for 20 min at 37°C and centrifuged for 5 min at 1500 g. The supernatant containing the liberated exosome proteins was then added to a 96 well plate in duplicates, together with defined amounts of an exosomal standard (range from 1.35×10^{10} to 2.1×10^{8} exosomes) and then incubated overnight at 37°C to enable binding of the exosomes to the microplate. The next day, the plate content was emptied by inversion and hard tapping it on a paper towel and washed three times for 5 min with 100 µl of wash buffer per well under constant agitation. Next, the primary antibody against CD63 was diluted 1:100 in blocking buffer and 50 µl of the respective solution was added to each well and incubated for 1 h at room temperature with shaking. After three further 5 min washing steps, the HRP-

coupled secondary antibody (1:5000 in blocking buffer) was incubated in 50 µl per well for 1 h at room temperature and shaking. Residual antibody was washed away three times for 5 min and the plate was developed by addition of 50 µl TMB ELISA substrate per well and shaking for 15 min at room temperature. The substrate reaction was stopped with 50 µl of Stop buffer, which changed the color from blue to yellow. The plate was subsequently analyzed with a plate reader at 450 nm wavelength.

4.7.3. Quantification by flow cytometry

Exosomes are too small to be analyzed by regular flow cytometry techniques, thus the use of latex beads coated with an antibody against the common exosomal protein CD63 was necessary.

Therefore, 4µm latex beads were washed twice with MES buffer for 15-20 min at 1500 g and then coated with a CD63 antibody (1:20 in MES buffer) overnight under constant agitation at room temperature. The next day, the beads were washed three times for 20 min each at 1500 g with PBS and afterwards resuspended in 100 µl of MES buffer. Meanwhile, the exosomes were labeled with PKH-67, a green fluorescent membrane dye that binds to lipid regions of cells or vesicles due to its long aliphatic tail. The exosomes were resuspended in 500 µl of diluent C and 4 µl of the PKH dye were added to a separate tube with 500 µl of diluent C to obtain the PKH working solution. Both, the PKH working solution and the exosome solution were combined in one tube and incubated for 5 min at room temperature. The labeling was stopped by adding 1 ml of exosome-depleted FCS to the tube. After a 5 min incubation, the labeled exosomes were added to the antibody-coated beads and kept overnight at 4°C under constant agitation. The exosome-bead complexes were washed twice in PBS containing 1% exosome-depleted FCS at 800 g for 10 min and then resuspended in 500 µl of flow cytometry buffer. The fluorescence was analysed in the FITC channel on the LSRII flow cytometer. For quantification the sample fluorescence was compared to a standard curve of six defined amounts of purchased exosome standards (derived from a colon carcinoma cell line) in a concentration range from 12-0 µg/ml that were processed the same way as the samples.

4.7.4. Microscopy uptake studies of exosomes to target cells

For visual assessment of the exosome uptake to different cell lines by microscopy, the exosomes were labeled with PKH-67 as described in 4.7.3. The labeled exosomes were then incubated with different cell types in 48 well plates. After 24 h the cells were washed with PBS and spun on a glass slide with a cytospin centrifuge (10 min, 300 g). The slides were air-dried overnight and then the nuclei were stained with DAPI as in 4.6.4.

4.8. *In silico* research

4.8.1. miRNA target prediction

miRNA bind to the 3'UTR of their target genes with their 2-8 nucleotide long seed sequence. In this study, the 3'UTR of the *Creb1* co-activators *Crtc-1, -2* and *-3* were screened for binding sites of the candidate miRNAs miR-17, miR-144 and miR-21 by using the free available algorithm TargetScan (www.targetscan.org).

4.8.2. Identification of asthma-relevant putative Creb1 target genes

The transcription factor Creb and its co-activators bind to palindromic CRE sites in the promoter region of their target genes to initiate transcription. In order to identify Creb downstream targets relevant for the pathogenesis of experimental asthma, a dataset from a previously performed microarray (courtesy of Francesca Alessandrini, ZAUM Munich) of lung homogenate of OVA-treated animals vs. PBS-treated controls was used. As the transcription factor Creb1 was found to be down-regulated in experimental asthma, only genes down-regulated in experimental asthma were screened for CRE sites in their promoter region by using the MatInspector Release professional 8.0.5 software. The identification of CRE sites and analysis of the conservation throughout different species was performed by Andreas Kowarsch and Steffen Sass (MIPS, Munich).

4.9. Statistical analysis

The acquired data was analyzed with the GraphPad Prism (Version 5.04) software. The graphs represent mean ± SD. Statistical significance is assumed if $p \leq 0.05$. All experiments

were analyzed with the non-parametric Mann-Whitney U test, unless stated otherwise in the figure legends. Each experiment was performed at least three independent times and the exact number is stated in the figure legends.

5. RESULTS

5.1. Characterization of animal models for allergic airway inflammation

In order to investigate molecular pathways of relevance for asthma, we artificially induced allergic airway inflammation (AAI) in mice by several sensitization steps and challenges with two different allergens: ovalbumin and house-dust mite.

5.1.1. Ovalbumin model

5.1.1.1. Inflammatory cell counts in broncho-alveolar lavage (BAL)

For validating the induced allergic inflammation in the airways, we first assessed the inflammatory cell numbers in the BAL of the mice.

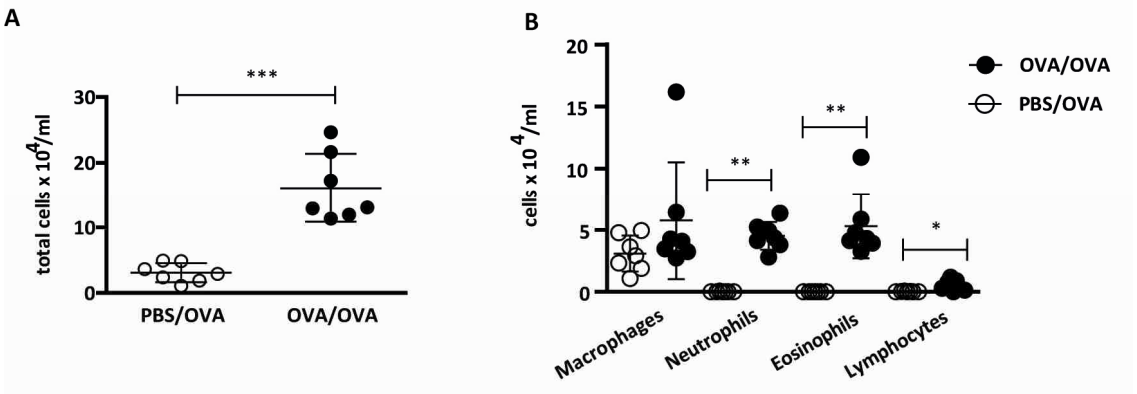

Figure 5.1: Increased inflammatory cell counts in BAL of OVA-induced allergic airway inflammation. A, Total cell count in BAL. **B,** Differential cell counts of cytospins of PBS/OVA, OVA/PBS and OVA/OVA treated mice, n = 7-15 per group. *p<0.05, ***p<0.001 vs. PBS/OVA. Courtesy of Dr. Nikola Schulz (104).

The total BAL cell number was significantly increased in OVA/OVA treated animals but not in animals that were only challenged (PBS/OVA) (Fig. 5.1A). The differential cell counts revealed a significant increase in neutrophils, eosinophils and lymphocytes in animals with OVA-induced allergic inflammation compared to the controls (Fig. 5.1B). This data was generated and provided by Dr. Nikola Schulz (104).

5.1.1.2. Histology

Histological analysis of lung sections showed some cellular infiltrates (Fig. 5.2) around the major airways and blood vessels, as well as a pink staining for mucus producing cells in the bronchi, suggesting goblet cell metaplasia in the OVA/OVA animals. This effect was not seen in PBS/OVA control animals.

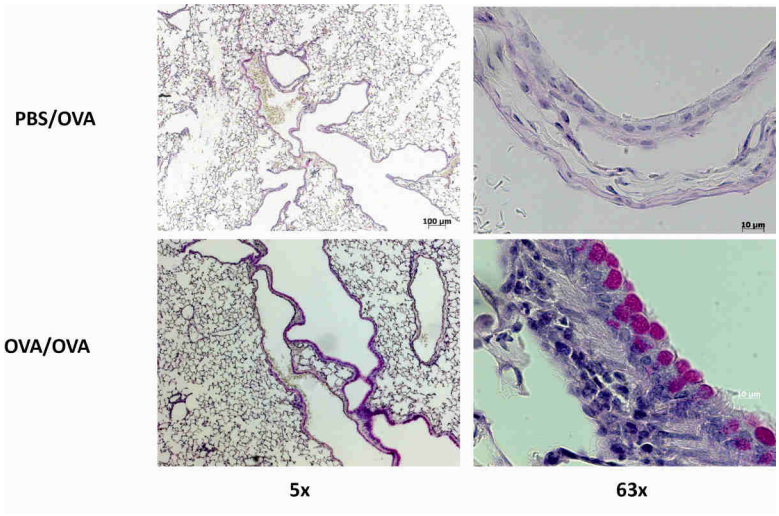

Figure 5.2: OVA/OVA treatment induces inflammatory cell infiltrates and goblet cell metaplasia. PAS staining of lung tissue of PBS/OVA (upper panel) and OVA/OVA (lower panel) treated mice. Representative images of n=4 mice per group are shown. Left panel 5x objective, right panel 63x objective.

Taken together, the data suggests that the applied ovalbumin treatment results in a moderate AAI in mice. This model has been performed by Francesca Alessandrini, ZAUM Munich, and is already described in the PhD thesis of Dr. Nikola Schulz (104).

5.1.2. House dust mite model

Next, we aimed to validate our findings in a second murine model that is more relevant to human asthma. Therefore, we used the model of house dust mite (HDM) induced allergic airway inflammation.

5.1.2.1. Inflammatory cell counts in broncho-alveolar lavage

HDM-treated mice showed significantly higher total cell counts in BAL (Fig. 5.3A) and also higher numbers of macrophages, eosinophils, neutrophils and lymphocytes (Fig. 5.3B) compared to PBS treated controls.

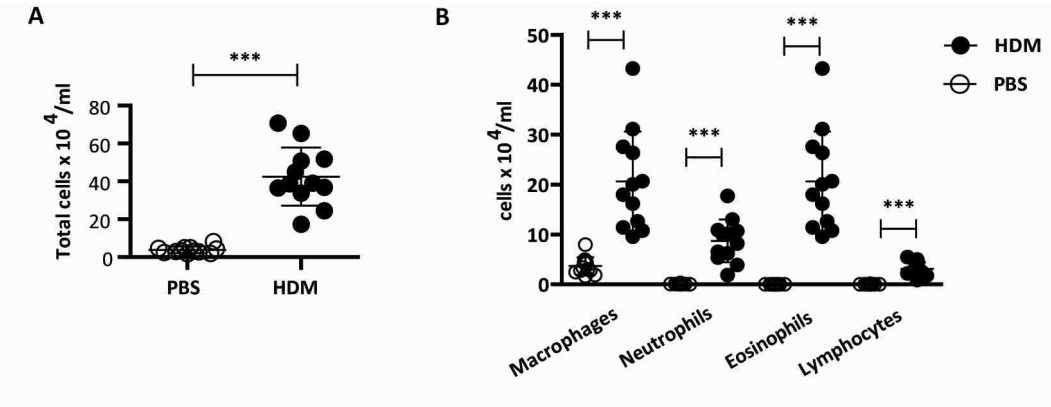

Figure 5.3: Increased inflammatory cell counts in BAL of HDM-treated mice. A, Total cell count in BAL. **B,** Differential cell counts of cytospins of PBS vs. HDM-treated mice, n = 12 per group. ***p<0.001 vs. PBS

5.1.2.2. Histology

PAS staining of lung sections demonstrated a moderate goblet cell metaplasia with pink staining for mucus-producing cells in major airways, as well as immune cell infiltrates around blood vessels and airways (Fig. 5.4).

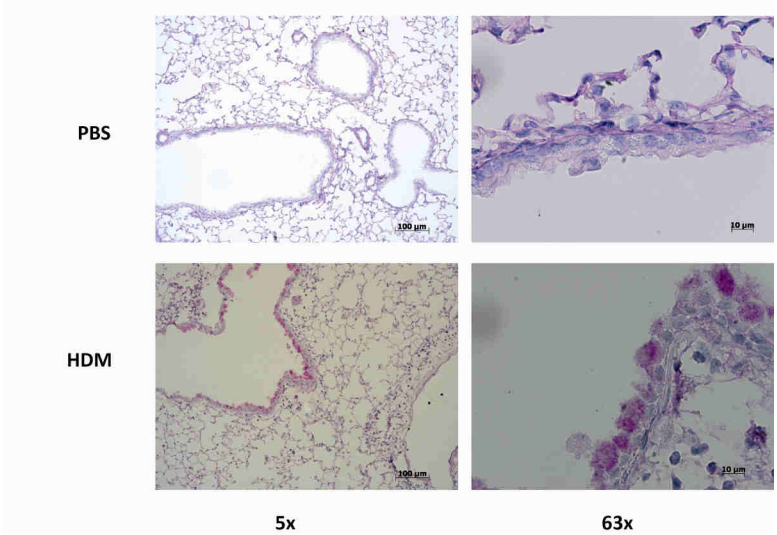

Figure 5.4: HDM-treatment induces airway inflammation and goblet cell metaplasia. PAS staining of PBS (upper panel) and HDM (lower panel) treated mice. Representative images of n=4 mice per group are shown. Left panel 5x objective, right panel 63x objective.

5.1.2.3. Airway hyperreactivity after metacholine challenge

In order to investigate if the animals display airway hyperreactivity (AHR), HDM or PBS-treated mice were tracheotomised and subjected to increasing doses of the broncho-constrictor metacholine. As shown in Figure 5.5, animals treated with HDM extract showed significantly higher airway resistance after metacholine challenge than PBS-treated control animals.

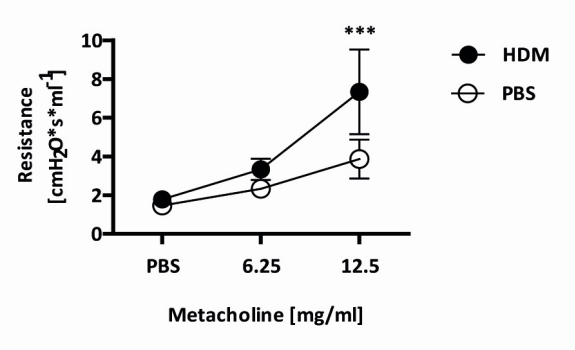

Figure 5.5: HDM-treated mice show increased airway hyperreactivity in response to metacholine. Airway resistance (RI av.) after metacholine challenge, n=12/group, ***p<0.001 vs. PBS.

In summary, HDM-treated mice displayed the expected symptoms of experimental allergic airway inflammation such as inflammatory cell infiltrates, goblet cell metaplasia and increased AHR in response to metacholine. The HDM-induced AAI was more severe with regards to airway inflammation than the phenotype observed in the ovalbumin model. Treatments and analysis were performed together with Petra Nathan, Katrin Milger and Jeremias Götschke (CPC Munich).

5.2. Identification of Creb1 co-activators as targets for candidate miRNAs

5.2.1. *In silico* research for miRNA binding sites in the Creb1 pathway

MiRNAs tend to address several molecules along single signaling pathways (62–64). Thus, a joint down-regulation of several factors along one pathway could lead to more profound downstream effects. Therefore, we screened the 3'UTRs of the Creb1 co-activators *Crtc-1*, *-2* and *-3* for binding sites of miR-17 and miR-144 that also target C*reb*1. *In silico* research identified miR-17 and -144 binding sites in the 3'-UTRs of *Crtc-1*, *-2* and *-3* in mice and human, whereas miR-17 binding sites were only present in the human *CRTCs* (Table 5.1). miR-21 was newly included as it was the second highest "hit" in the initial array used for the target prediction (adj. p-value 6.18 x 10^{-13}) and was predicted to target *CRTC-1*, *-3* and *CREB1*.

Table 5.1: predicted miRNA binding sites

miRNA	*Crtc1* mmu (hsa)	*Crtc2* mmu (hsa)	*Crtc3* mmu (hsa)	*Creb1* mmu (hsa)	*Sec14l3* mmu (hsa)
miR-17	- (+)	- (-)	- (+)	+ (+)	- (-)
miR-144	+ (+)	+ (-)	+ (+)	+ (+)	- (+)
miR-21	+ (+)	- (-)	- (+)	+ (+)	- (-)

5.2.2. Over-expression of miR-17/-144 and -21 in MLE-12 cells

In silico target predictions can produce false negative hits. Therefore, we aimed to validate the miRNA-dependent regulation of *Creb1* and the *Crtcs* by evaluating the effect of *in vitro* miRNA over-expressions on the endogeneous expression of the putative target genes.

In vitro, miR-144 and miR-21 over-expression reduced significantly the mRNA levels of all three Crtcs in a murine bronchial epithelial cell line (MLE-12) (Fig. 5.6A). PremiR-17 decreased *Crtc2* mRNA levels and Creb1 and trendwise Crtc1 and -3 protein levels (Figure 5.6A, B). The Creb1 protein levels were also significantly decreased after PremiR-144 treatment (Fig.5.6B).

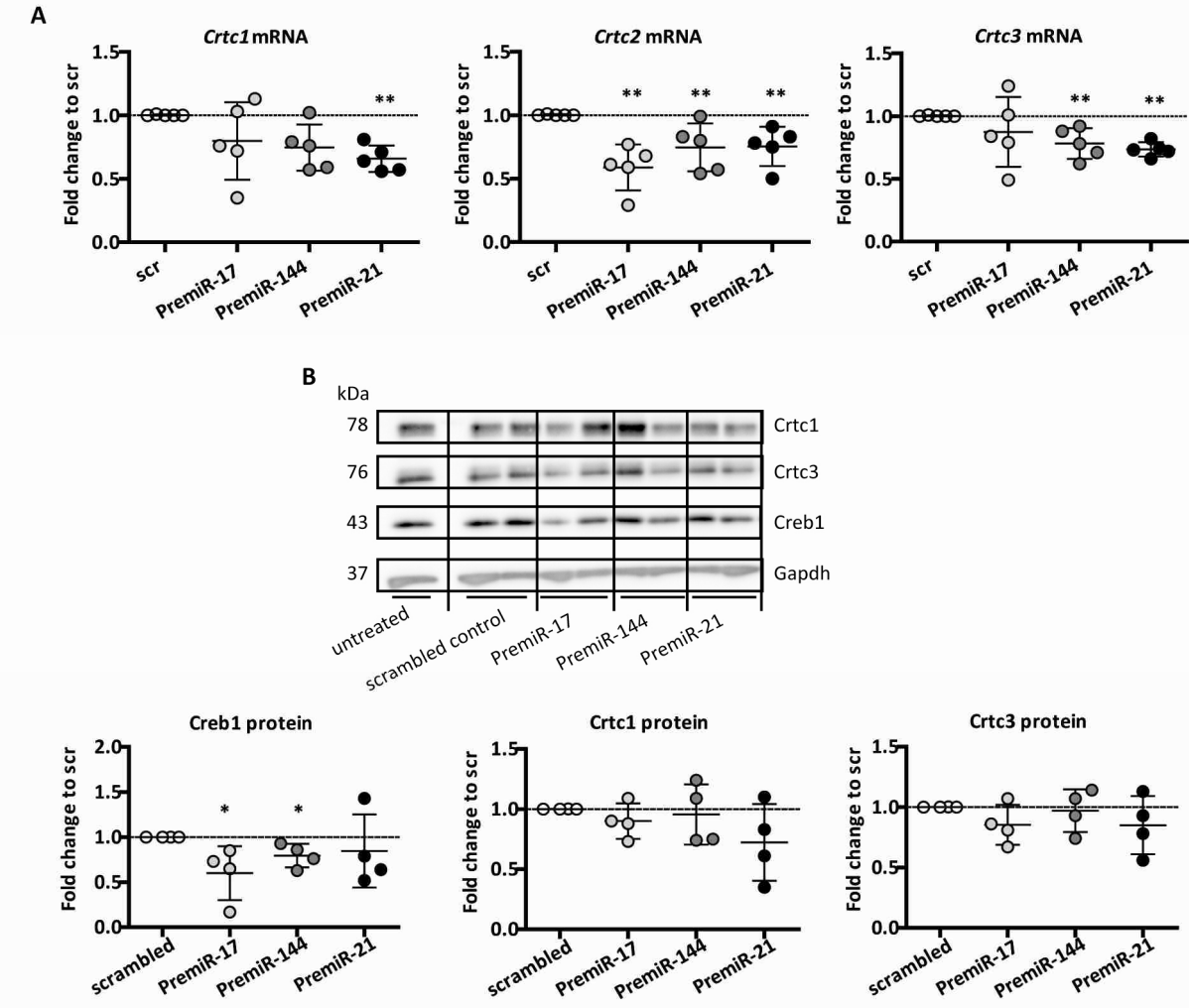

Figure 5.6: miRNA-mediated regulation of Crtcs *in vitro*. Transfection of MLE-12 cells with PremiRs vs. a scrambled miRNA control for 72 h. **A**, qRT-PCR for *Crtc1,-2 and -3* and **B**, representative western blot (different transfection conditions are depicted as duplicates) and densitometrical analysis, n=4-5 independent experiments. *p<0.05, **p<0.01 vs. scrambled control.

In summary the data suggests that miR-17, miR-144, and miR-21 might play a role in the regulation of Creb/Crtc-mediated signaling in murine cells.

5.3. Down-regulation of Creb1 and Crtcs in murine experimental asthma

5.3.1. Creb1 and Crtc mRNA and protein expression in OVA-induced AAI

In a next step, we wanted to investigate if Creb1 and its co-activators are involved in the pathogenesis of asthma. Therefore, we evaluated their expression in lung homogenates of animals with OVA-induced AAI.

There was a significant increase in miR-17, -144, and -21 (Fig. 5.7A) in lung homogenates of OVA-treated animals compared to PBS-treated controls after the allergen challenge at day 72, but not at day 29 within the sensitization period (104). At day 72, *Creb1* and trendwise *Crtc1* (p=0.095) were decreased on mRNA level compared to PBS-treated controls (Fig. 5.7B). The total transcript levels of *Creb1* and all three *Crtcs* decreased in lung homogenate of mice that developed AAI along the treatment protocol from day 29 to day 72 (Fig. 5.7B).

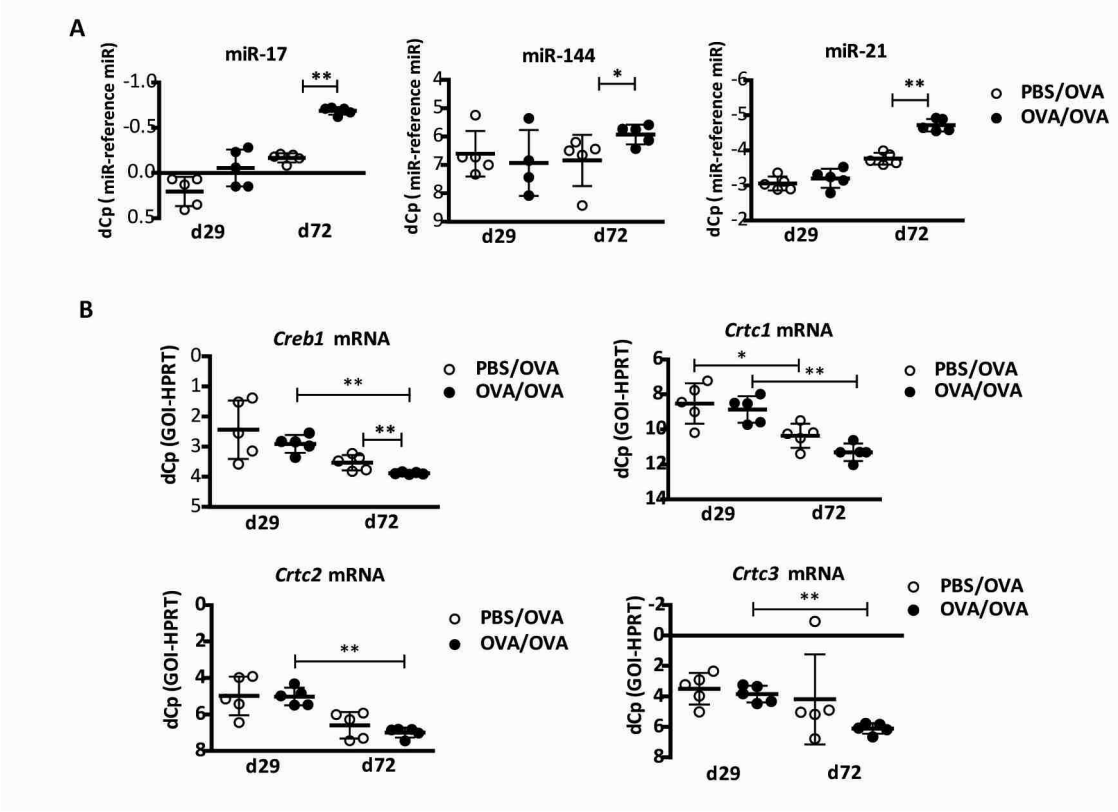

Figure 5.7: Inverse correlation between miRNA and *Creb1/Crtc* expression in OVA-induced allergic airway inflammation. A, qRT-PCR for miRNA on lung homogenates at d29 and d72. Already published in the PHD Thesis of Dr. Nikola Schulz (104) .**B,** qRT-PCR for *Creb1 and Crtcs* at d29 and d72. Graphs depict fold change to PBS/OVA controls, n=5 animals per group, dCp=Cp(gene of interest)-Cp (reference gene). *p<0.05, **p<0.01 vs. PBS.

On protein level, Crtc1 and Crtc3 increased from d29 to d72 in control mice. This increase was significantly attenuated for Crtc3 and trendwise for Crtc1 (p=0.095) in mice that developed allergic airway inflammation (Figure 5.8).

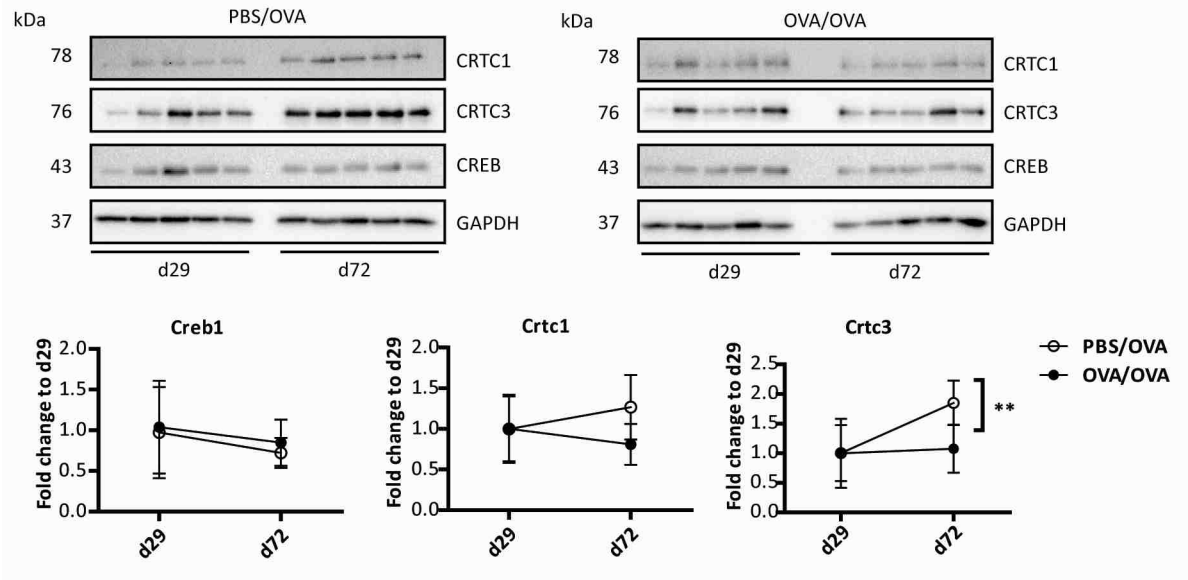

Figure 5.8: Crtc3 protein levels decrease in OVA/OVA-treated animals. Western blots of lung homogenates of n=5 mice from d29 to d72. Crtc2 cannot be assessed due to the lack of a specific antibody. **p<0.01 vs. d29.

Creb1 mRNA is decreased in OVA-induced AAI, its co-activators show only a small trend after the challenge but are decreased by a continuous OVA treatment along the treatment protocol.

5.3.2. Creb1 and Crtc mRNA and protein expression in HDM-induced AAI

As the ovalbumin-model has limited relevance for human asthma, we further wanted to validate our findings in HDM-induced experimental allergic airway inflammation. *Creb1* and all three *Crtc* mRNA levels were highly significantly decreased in HDM-treated animals (Fig. 5.9A). HDM-treatment also significantly reduced Crtc3 and trendwise Creb1 protein levels (Figure 5.9B). This regulation was more pronounced than in the OVA model.

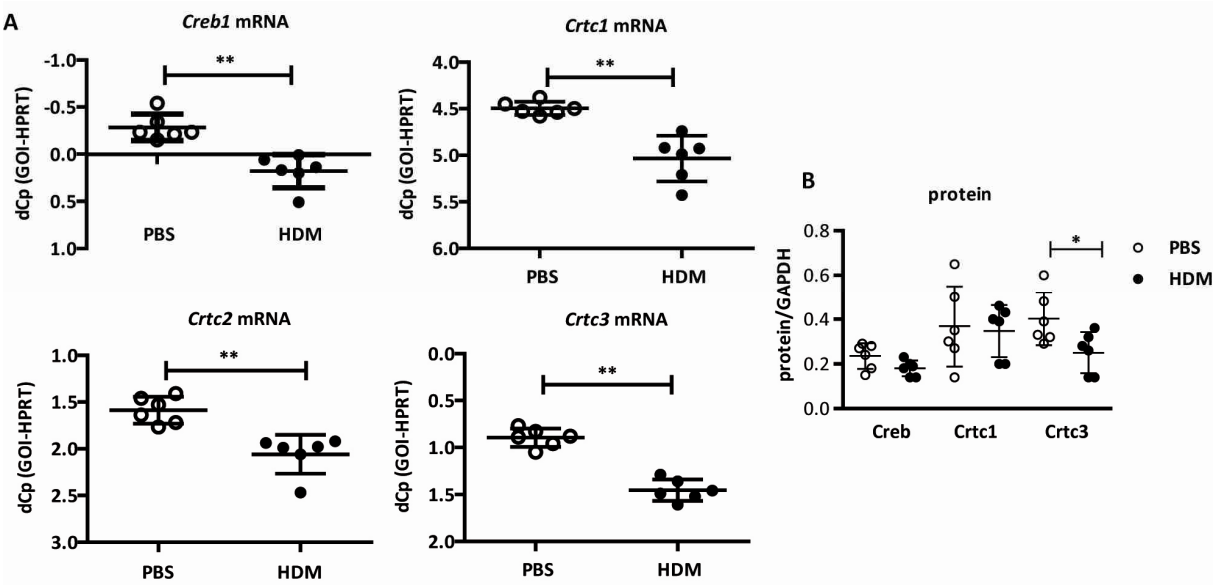

Figure 5.9: Creb1 and Crtcs are decreased in HDM-induced experimental asthma. Expression analysis of lung homogenates of HDM-treated mice vs. PBS-treated controls. **A**, qRT-PCR for *Creb1* and *Crtc1-3* **B**, Densitometrical analysis of Creb1 and Crtc-1 and -3 of a western blot (n=6 mice per group), dCp=Cp(gene of interest)-Cp (reference gene). *p<0.05, **p<0.01 vs. PBS.

In summary, we could observe a trend towards a decrease of the putative targets of miR-17, -144, and -21 Creb1 and Crtc1-3 in the OVA-model for AAI. This could be validated with more pronounced regulations in HDM-induced AAI.

5.4. Identification of relevant Creb1 target genes in experimental asthma

5.4.1. Prioritization strategy

As our data suggested Creb1 and Crtcs to be important for the development of experimental asthma, we asked whether their down-regulation also results in a decreased transcription of Creb1 target genes. To this end, we searched an earlier performed mRNA array (113) (GEO database, ID: GSE6496 (http://www.ncbi.nlm.nih.gov/geo) (Courtesy of Francesca Alessandrini, ZAUM Munich) for down-regulated genes containing CRE-sites in OVA/OVA versus PBS/OVA mice. Of 185 decreased genes, 35 contained CRE-elements (Table 5.2). In a pilot approach, we selected Sec14-like 3 (Sec14l3) for further investigation as it had already been found to be decreased in allergic airway inflammation in rats (114) and to be specifically expressed in murine airway ciliated cells (115).

Table 5.2: Dysregulated putative Creb1 target genes in OVA-induced asthma

Gene symbol	GeneID	logFC (OVA/OVA vs PBS/OVA)
Dcpp1	13184	**-2.69**
Tnnt3	21957	**-2.30**
Tnni2	21953	**-1.89**
Ddx5	13207	**-1.84**
Tnnc2	21925	**-1.80**
Car3	12350	**-1.77**
Lor	16939	**-1.71**
Ghitm	66092	**-1.69**
Calml3	70405	**-1.62**
Sec14l3	**380683**	**-1.34**
Gpd1	14555	**-1.29**
Tubb2c	227613	**-1.21**
Rbbp7	245688	**-1.20**
Caprin1	53872	**-1.17**
Son	20658	**-1.17**
Ddx17	67040	**-1.15**
Cap2	67252	**-1.13**
Mgll	23945	**-1.09**
Mapk3	26417	**-1.07**
Ltbp4	108075	**-1.05**
Ppp1cb	19046	**-1.05**
Rsrc2	208606	**-1.04**
Tap1	21354	**-1.02**
Akap3	11642	**-1.02**
Tcp1	21454	**-1.01**
Krt14	16664	**-1.00**
Nup155	170762	**-0.95**
Dnajb6	23950	**-0.94**
Mark3	17169	**-0.91**
Cask	12361	**-0.89**
Lypd3	72434	**-0.89**
Cidea	12683	**-0.86**
Sypl	19027	**-0.86**
Atp8a1	11980	**-0.84**
Fabp5	16592	**-0.83**

5.4.2. Expression Sec14l3 in OVA-induced AAI

The putative Creb1 target gene *Sec14l3* was significantly decreased at d72, but not at d29 within the sensitization period, at the mRNA level in lung homogenate of OVA/OVA animals compared to PBS/OVA controls (Fig. 5.10A). The Sec14l3 protein increased from d29 to d72, like observed for Crtc-1 and -3, and this was significantly attenuated in OVA-induced allergic airway inflammation (Fig. 5.10B).

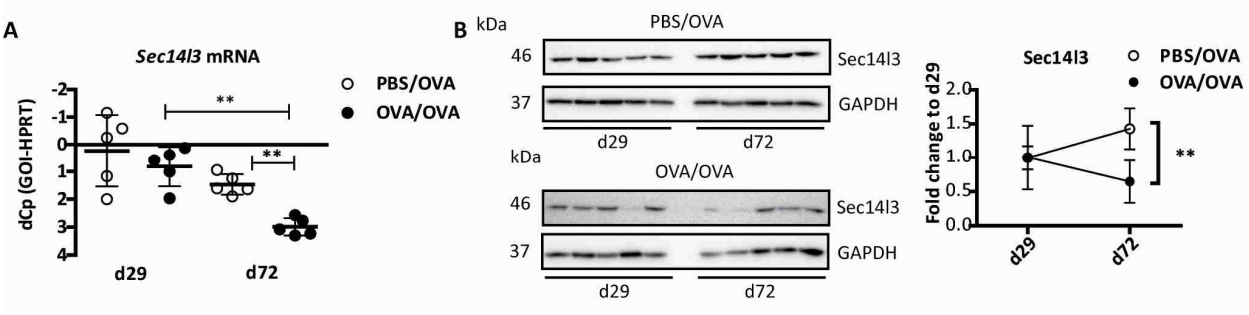

Figure 5.10: Sec14l3 is decreased in OVA-induced allergic airway inflammation. Lung homogenates of OVA/OVA-treated animals vs. PBS/OVA-treated controls. **A**, qRT-PCR for *Sec14l3*. **B**, Western blot of animals on d29 and d72 and respective densitometrical analysis (n=5 mice per group). dCp=Cp(gene of interest)-Cp (reference gene). **p<0.01 vs. PBS/OVA or d29.

According to published data, Sec14l3 is specifically expressed in airway ciliated cells in murine lungs (115). To further investigate its expression in OVA-induced allergic airway inflammation we performed specific immunofluorescent stainings on lung sections. Indeed, Sec14l3 was expressed in ciliated bronchial epithelial cells and this was decreased in allergic airway inflammation (Fig. 5.11). Where the Sec14l3^{+} cells were lost in OVA-treated animals (lower panel, arrows), a goblet cell could be identified by subsequent PAS staining of the identical sections (Fig. 5.11). Hence, the loss of Sec14l3 expression may be associated with goblet cell metaplasia, a common hallmark for allergic airway disease.

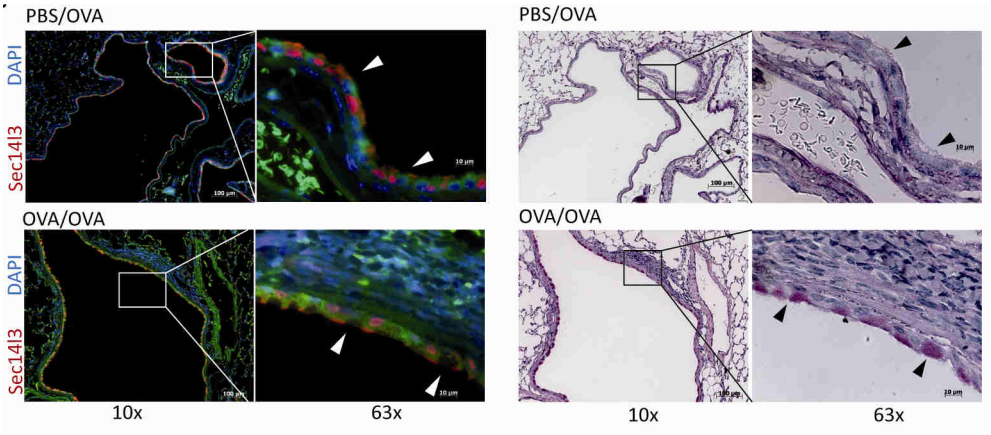

Figure 5.11: Sec14l3 is expressed in airway ciliated cells and decreased in OVA-induced allergic airway inflammation. Left panel: Immunofluorescent staining of paraffin lung sections of PBS/OVA (upper panel) and OVA/OVA mice (lower panel): Sec14l3 (red) vs. DAPI (blue) and lung autofluorescence (green). Right panel: PAS staining of the identical lung sections. Arrows indicate ciliated cells in the upper panel and goblet cells in the lower panel. Representative images for n=4 mice per group.

5.4.3. Expression of Sec14l3 in HDM-induced AAI

Sec14l3 was found to be decreased on mRNA (Fig. 5.15A) as well as protein level in lung homogenate of HDM treated mice compared to the healthy controls (Fig. 5.12B).

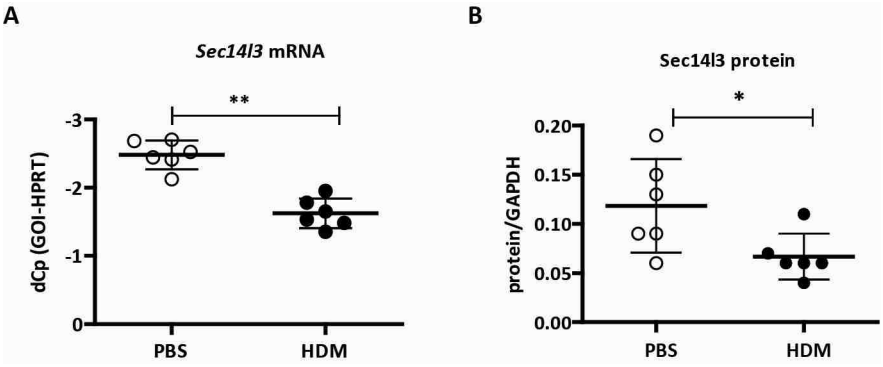

Figure 5.12: Sec14l3 is decreased in HDM-induced allergic airway inflammation. Lung homogenate of HDM-treated mice vs. PBS-treated mice. **A**, qRT-PCR for Sec14l3. **B**, Densitometrical analysis of western blot. (n=6 mice per group), *p<0.05, **p<0.01 vs. PBS.

Furthermore we observed the same association with goblet cell metaplasia than in the ovalbumin model (5.4.2) (Fig. 5.13).

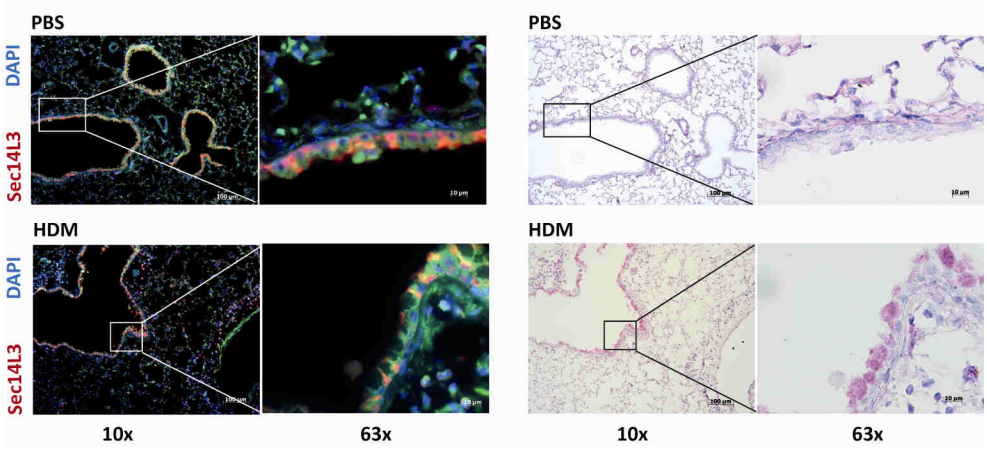

Figure 5.13: Sec14l3 is expressed in airway ciliated cells and decreased in HDM-induced allergic airway inflammation. Left panel: Immunofluorescent staining of paraffin lung sections of PBS (upper panel) and HDM mice (lower panel): Sec14l3 (red) vs. DAPI (blue) and lung autofluorescence (green). Right panel: PAS staining of the identical lung sections. Arrows indicate ciliated cells in the upper panel and goblet cells in the lower panel. Representative images for n=4 mice per group.

Thus, the putative Creb1 target gene Sec14l3 was, similar to Creb1 and co-activators, down-regulated in lung homogenates of both murine models for allergic airway inflammation, thus independent of the type of allergen. Additionally, the Sec14l3 loss seemed to be associated with goblet cell metaplasia.

5.5. Investigation of the miRNA/CREB1/SEC14L3 axis in air-liquid interface differentiation of primary NHBE

So far, we used murine lung homogenates to investigate the expression of miRNAs and the Creb1/Crtc pathway. However, current concepts propose that the bronchial epithelium may contribute actively to the pathogenesis of asthma. Therefore, we used primary normal human bronchial epithelial cells (NHBE) to investigate the role of *SEC14L3* in the development of experimental asthma and in normal lung homeostasis. Those cells, when cultured on transwell inserts at the air-liquid interface, differentiate into a pseudo-stratified epithelium containing ciliated cells, club cells, goblet cells and basal cells over a period of 21-28 days (116).

5.5.1. Timeline of normal differentiation

First we assessed the expression of Sec14l3 during the 28 days of differentiation of primary NHBE cells at the air-liquid interface.

On day 0, the day of air-lift, *SEC14L3* mRNA could not be detected, but it increased continuously until day 28 (Fig. 5.14A). We found a very close correlation of *SEC14L3* mRNA level with the expression of the transcription factor forkhead box protein J1 (*FOXJ1*) that is associated with the development and function of ciliated cells (117) (Fig. 5.14B).

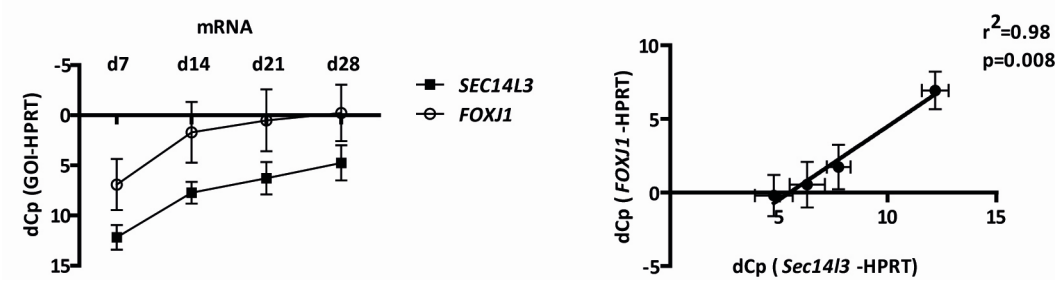

Figure 5.14: *SEC14l3* mRNA correlates with ciliated cells in NHBE cells. NHBE cells were differentiated at the air-liquid interface for 28 days. **Left panel:** qRT-PCR for *SEC14L3* and *FOXJ1*. **Right panel:** Linear correlation of *SEC14L3* and *FOXJ1* mRNA levels. n=4 independent experiments.

5.5.2. Treatment of primary NHBE cells with IL-13

5.5.2.1. Induction of goblet cell metaplasia

The NHBE cells were treated with IL-13 for seven days in basal medium to induce a goblet cell metaplasia (118) and to model the initial development of "asthma-like" changes in the bronchial epithelium.

Samples were taken at 24 hours, four days and seven days after air-lift (d0) to get an insight into the dynamic changes induced by the cytokine treatment. PAS stainings of the cross-section transwell membranes showed an increased mucus production of the IL-13-treated cells (displays as pink color) compared to the untreated controls. This was especially visible after 7 d of culture (Fig. 5.15A). A prominent marker for mucus-producing goblet cells, mucin 5AC (MUC5AC) (119), also significantly increased at mRNA level over the treatment period (Fig. E.15B).

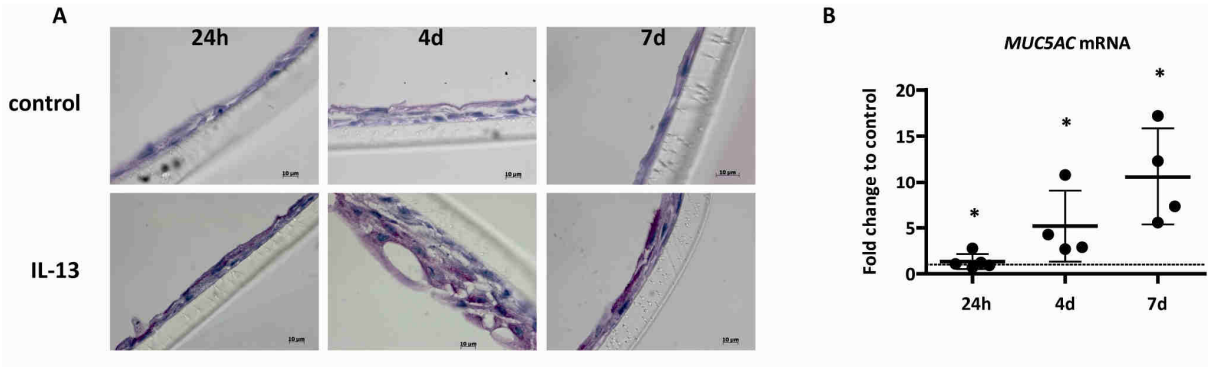

Figure 5.15: IL-13 induces goblet cell metaplasia and mucus production in NHBE cells. NHBE cells were treated with 10ng/ml IL-13 for 7d. **A**, Representative PAS-stainings of cross sections of the transwell membranes of untreated cells (upper panel) vs. IL-13 treated cells (lower panel) at 24 h, 4 d and 7 d post airlift. **B**, qRT-PCR of *MUC5AC*. n=4 independent experiments, *p<0.05 vs. untreated.

5.5.2.2. Expression of miRNAs

The expression of the three candidate miRNAs in the primary NHBE cells did not significantly change after treatment with IL-13. There might be a trendwise increase for miR-144 and miR-21 after 7 days of treatment (Fig. 5.16) although this did not reach statistical significance.

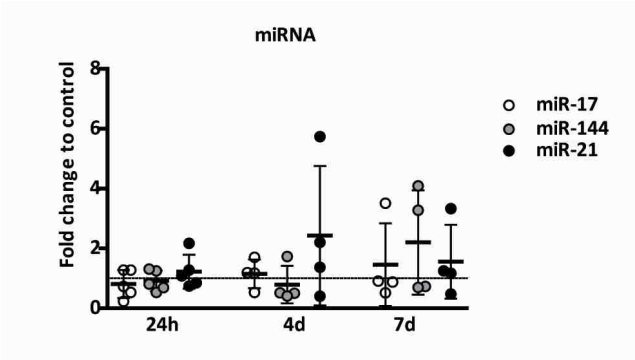

Figure 5.16: miRNA expression in NHBE cells after IL-13 treatment. qRT-PCR for miR-17, -144 and -21 in NHBE cells at 24 h, 4 d and 7 d post air-lift.

5.5.2.3. Secretion of miRNAs in exosomes

As we did not observe changes in miRNA levels in the total cell lysates, we asked if they might be secreted into exosomes upon IL-13 stimulus. We could detect CD63 positive exosomes by ELISA in the basal compartment of our culture model as well as in washes of the apical side (Fig. 5.17A). We could not observe an enhanced secretion of exosomes after IL-13 treatment to either apical or basal cell compartments but the basal compartment contained per se more exosomes than the apical at every time point (Fig. 5.17B).

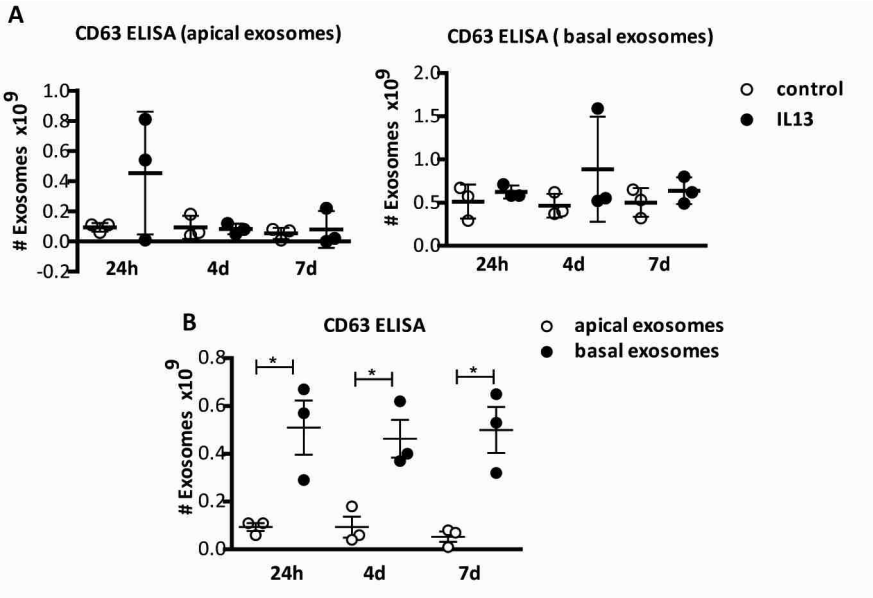

Figure 5.17: Exosomes are secreted apically and basally after IL-13 treatment in NHBEs. ELISA for exosome-specific CD63 from (**A**) apical and basal compartments of NHBE cells after IL-13 or control treatment**. B**, comparison of CD63-positive exosomes between apical and basal compartments in untreated cells. Amounts were calculated by an internal standard curve with defined amount of exosomes. n=3 independent exosome isolations. *p<0.05 vs. apical exosomes

In our culture model, we could isolate miRNAs from exosomes of the apical, as well as the basal side. In untreated cells, the total levels of miR-17 and trendwise miR-21 were higher in the basal compartment, especially after 7 days of culture (Fig. 5.18). This might relate to the higher amount of exosomes that are present in the basal compartment (Fig. 5.17B). However we could not observe this pattern for miR-144 (Fig. 5.18).

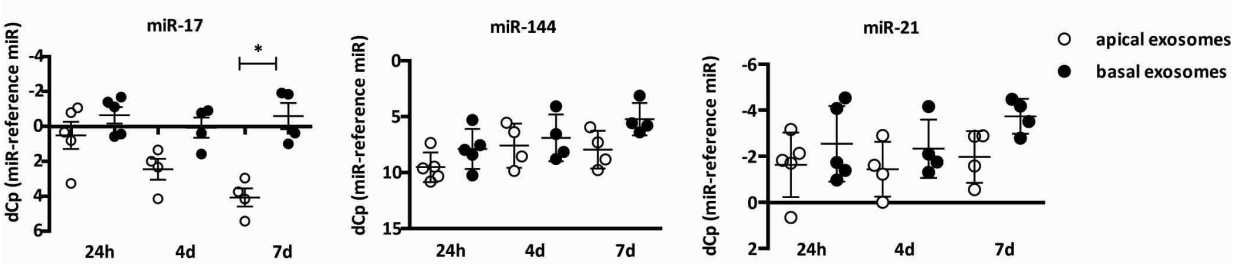

Figure 5.18: miRNAs are present in exosomes secreted by primary NHBE cells. qRT-PCR for miR-17, -144 & -21 in isolated exosomes from the apical and basal cell side after 24 h, four days and seven days of culture without treatment. *p<0.05 vs. apical exosomes.

Of note, there were significantly higher amounts of miR-17 and -21 in the basal compartment after 24 hours and 4 days of IL-13-treatment (Fig. 5.19A). After seven days this significant increase in the miRNAs was observed on the apical side, suggesting that IL-13 affects the direction of miRNA secretion in a temporal manner (Fig. 5.19B). This might indicate either an altered secretion mechansism upon continuous IL-13 treatment or a diffusion from basal exosomes to the apical side through openend tight junctions. MiR-144 only showed a trendwise increase in either apical or basal compartment (Fig. 5.19A, B) but it did not reach statistical significance. Eventhough the number of exosomes was always higher in the basal compartment than in the apical, the pattern of the miRNA levels was not so clear. This could indicate a specific packing of miRNAs into exosomes depending on the stimulus.

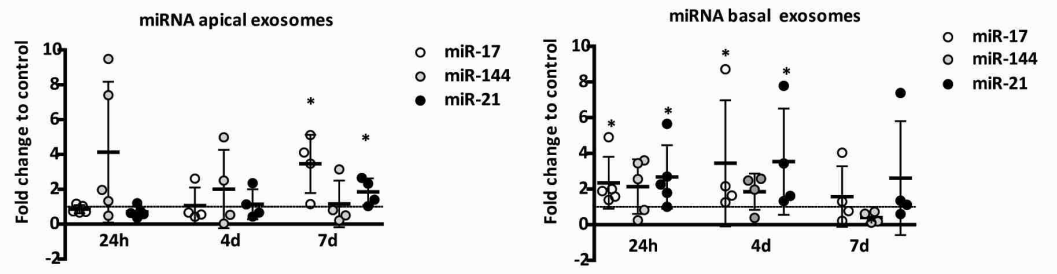

Figure 5.19: miRNAs are secreted into exosomes after IL-13 treatment by primary NHBE cells. qRT-PCR for miR-17, -144 & -21 in isolated exosomes from the apical (left panel) and basal (right panel) cell side. *p<0.05 vs. untreated.

5.5.2.4. CREB/CRTC-mediated transcription

Regarding CREB1 and its co-activators CRTC we could observe a significant decrease 24 h after the IL-13 treatment start on the transcriptional level, which then resolved over time (Fig. 5.20A). *SEC14l3* and *FOXJ1* transcripts could not be detected after 24 hours but where significantly lower in the IL-13 treated cells at four and seven days compared to the non-treated controls. The treatment abolished the increase we observed during the normal differentiation (Fig. 5.20B).

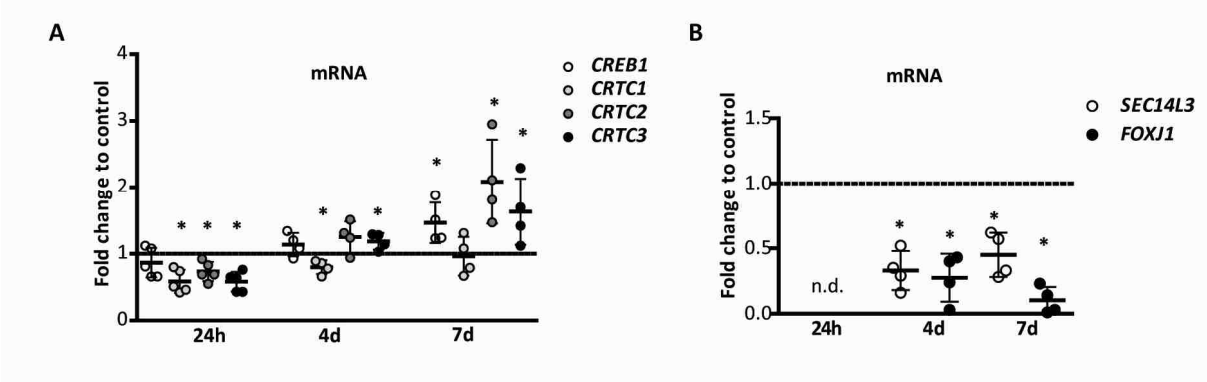

Figure 5.20: *CREB1/CRTCs* and *SEC14L3* are dysregulated by IL-13 treatment in primary NHBE cells. qRT-PCR for *CREB1*, *CRTC1-3* **(A)** and *SEC14L3* and *FOXJ1* **(B)** in IL-13 treated NHBE cells vs. untreated controls. n.d. = non detectable. *p<0.05 vs. untreated.

Our findings were largely mirrored on the protein levels, although the decrease of CREB1 and CRTCs was first visible after 4 days and 7 days (Fig. 5.21). FOXJ1 down-regulation was less profound than on mRNA level.

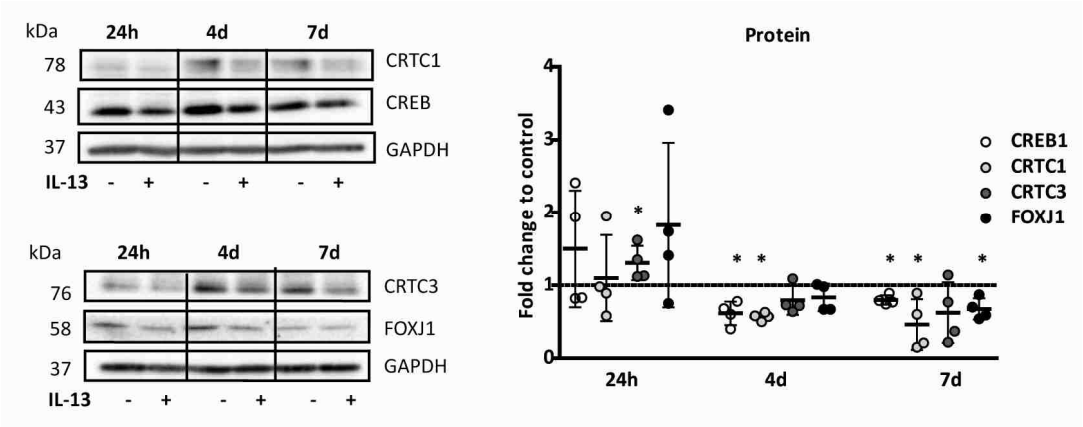

Figure 5.21: CREB1/CRTC and FOXJ1 protein levels are decreased by IL-13 treatment in primary NHBE cells. Left panel: Western blot of IL-13 treated cells vs. untreated control cells. Right panel: Densitometrical analysis of n=4 independent experiments. *p<0.05 vs. untreated.

In summary, a decreased CREB1/CRTC-mediated transcription of possibly SEC14L3 and others might be involved in early changes in the bronchial epithelium after "asthmatic stimuli".

5.6. Investigation of the miRNA/CREB1/SEC14L3 axis in human paediatric asthma

Next, we wanted to investigate to what extent the results obtained *in vitro* and in mouse models translate to human paediatric asthma. To this end, we analyzed the expression of the miRNA/CREB1/SEC14L3 axis in nasal epithelial cells from children with allergic asthma compared to healthy controls.

5.6.1. miRNA expression in nasal epithelial cells

We first compared the expression of miRNAs in the nasal epithelial cells of children with allergic asthma and healthy controls. miR-17, miR-144 and miR-21 were significantly up-regulated in children with allergic asthma: miR-144 in particular was expressed at very low baseline levels in healthy controls but increased to a high level in most children with allergic asthma (Fig. 5.22).

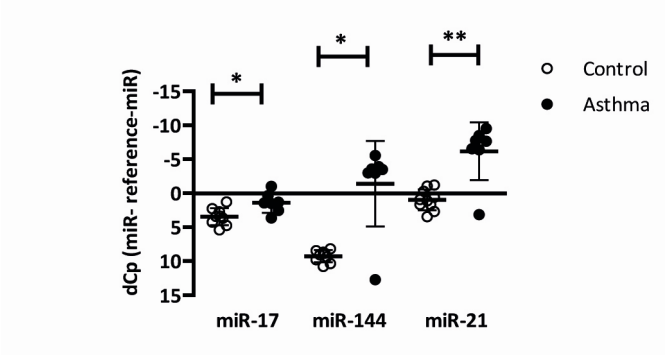

Figure 5.22: miR-17, -144 and -21 are increased in children with allergic asthma. qRT-PCR of nasal epithelial cells from children with allergic asthma (n=7) vs. age-matched healthy controls (n=10). dCp=Cp(gene of interest)-Cp (reference gene). *p<0.05, **p<0.001vs. control.

5.6.2. *CREB1/CRTC* and *SEC14L3* mRNA expression

The mRNA levels of *CREB1* and the three *CRTCs* were not changed between children with allergic asthma and healthy controls (Fig. 5.23).

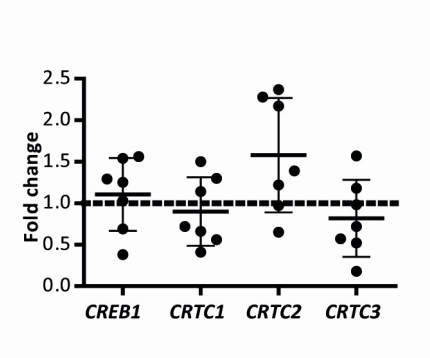

Figure 5.23: *CREB1* and *CRTCs* are unchanged in paediatric allergic asthma. qRT-PCR of nasal epithelial cells from children with allergic asthma (n=7) vs. age-matched healthy controls (n=10).

Nonetheless, *SEC14L3* was markedly and significantly decreased in children with allergic asthma (mean fold change to control: 0.13±0.05; p=0.0007) (Fig. 5.24A) and this dysregulation was more pronounced than what we had observed in the murine models. In experimental asthma, loss of SEC14L3 was associated with goblet cell metaplasia. Hence we investigated the expression *MUC5AC* as surrogate marker for goblet cells (119) and found it to be increased in nasal epithelial cells of asthmatic children (Fig. 5.24B).

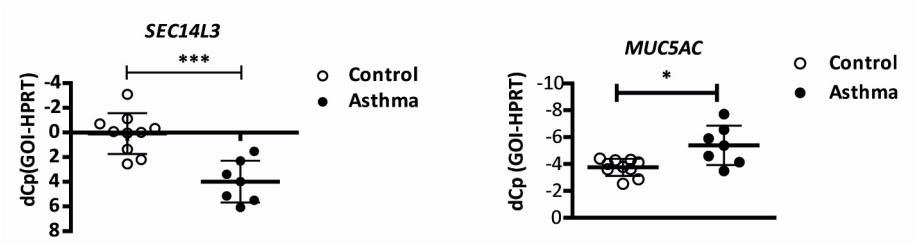

Figure 5.24: *SEC14L3* is decreased in children with allergic asthma. qRT-PCR of nasal epithelial cells from children with allergic asthma (n=7) vs. age-matched healthy controls (n=10). **Left panel**: *SEC14l3*. **Right panel**: *MUC5AC*. dCp=Cp(gene of interest)-Cp (reference gene) *p<0.05, ***p<0.001 vs. control.

5.6.3. Presence of miRNA containing exosomes in nasal washes and murine BAL fluid

As the primary NHBE cells secreted miRNAs into exosomes, we investigated biofluids of the OVA-mouse model and the asthmatic children for the presence of miRNA-containing exosomes. We did not observe a significant increase in $CD63^+$ exosomes in BALF of OVA-treated mice (Fig. 5.25A). Nonetheless, miR-17, and -21 were significantly increased compared to PBS/OVA treated controls, while miR-144 was not detectable (Fig. 5.25B).

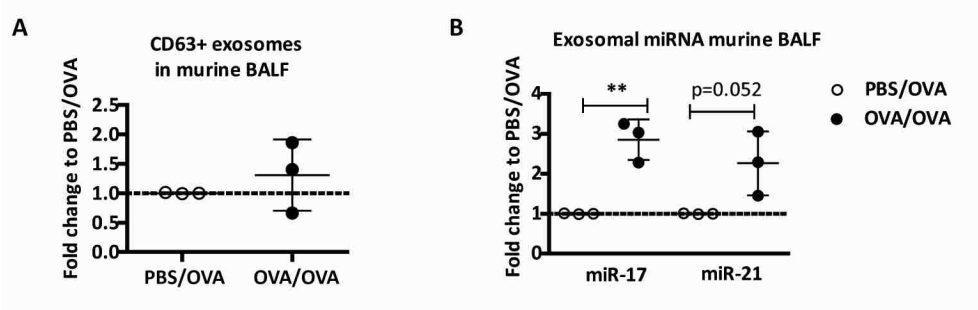

Figure 5.25: miRNAs are present in exosomes in murine BALF. A, quantification of CD63+ exosomes by flow cytometry, isolated of 200 µl of murine BALF. **B**, qRT-PCR on isolated exosomes of murine BALF, miR-144 not detectable. N=3 mice/group. Unpaired ttest **p<0.01 vs. PBS/OVA.

In exosomes isolated from human nasal washes, we were able to detect all three miRNAs by qRT-PCR, although miR-144 only at very low levels (Fig. E.26A). As we did not have access to nasal washes from healthy control children, we could not validate the observed increase in exosomal miRNAs that we found in the mouse model for allergic airway inflammation.

In order to get an insight if the presence of exosomal miRNAs is dependent on clinical parameters of asthma or allergic disease, we stratified our patients in two groups of children with lower IgE levels (still elevated compared to normal levels) and higher IgE levels. miR-17 was significantly higher and miR-21 also trendwise (p=0.08) in patients with high IgE levels compared to patients with lower levels of IgE (Fig. 5.26B). We could not observe such an increase for miR-144. The increased miRNA levels might in part be explained by a higher amount of $CD63^+$ exosomes in human nasal washes from patients with higher IgE levels (Fig. 5.26C).

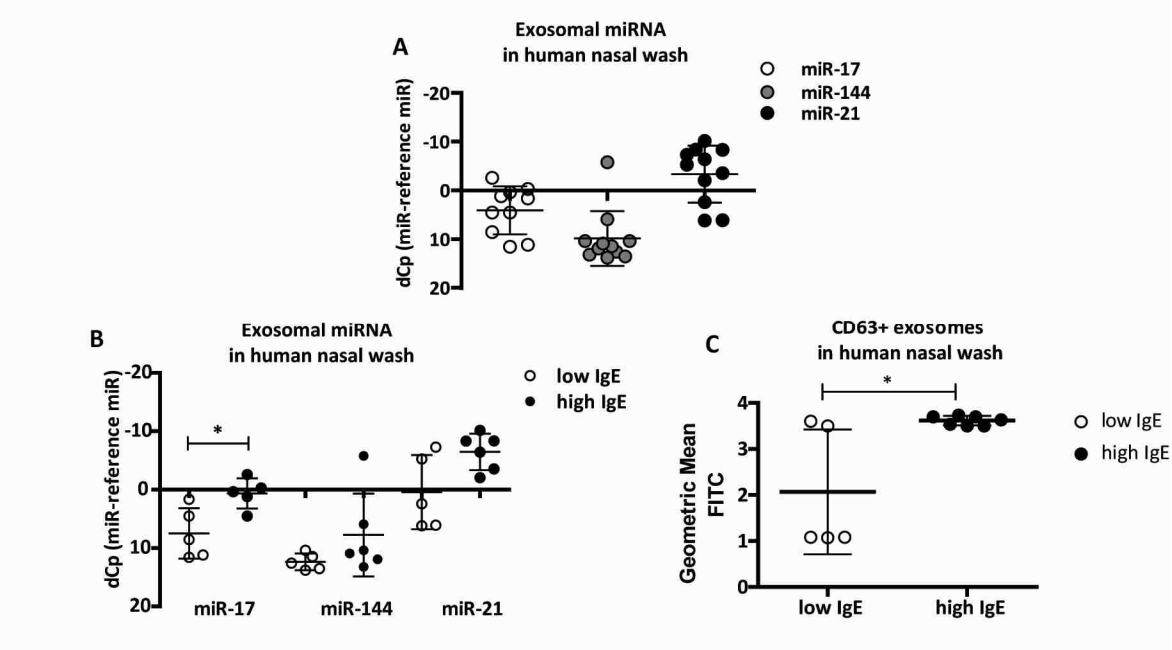

Figure 5.26: miRNAs are present in exosomes in human nasal washes. A, qRT-PCR on isolated exosomes of 1ml of human paediatric nasal washes of 11 children with allergic asthma. **B,** Patients were stratified in 'low' IgE levels in blood (400-900 U/ml) and 'high' IgE levels in blood (900-4500 U/ml). Graph depicts qRT-PCR for miR-17, -21 and -144. **C**, quantification of $CD63^+$ exosomes by flow cytometry, isolated of 1ml of human nasal wash. n=5-6/group.*$p<0.05$ vs. low IgE.

In essence, we could detect miRNA-containing exosomes in murine BALF as well as in human nasal wash. We have first hints that the exosomal levels of miR-17 and -21 might be associated with asthma development as they were shown to be increased in murine BALF of OVA-treated mice, as well as in human nasal washes of patients with higher IgE levels. In humans increased miRNA levels also corrobated with higher total exosome numbers.

5.7. Uptake of exosomes by target cells *in vitro*

5.7.1. Uptake of exosomes by human bronchial epithelial cells

Exosomes are secreted into various biofluids and can be taken up by specific target cells, which are then functionally modified by the exosome content such as miRNAs. By this mechanism, various cell types can communicate with each other and also between different tissues.

In order to investigate if the exosomes, secreted by the primary NHBE cells upon IL-13 stimulus, can be taken up by other airway epithelial cells, we isolated exosomes and labeled them with PKH-67. Those exosomes were then incubated with the 16-HBE14o$^-$ human bronchial cell line. After 24 h many cells containing green fluorescent exosomes could be found. There was no difference in the uptake of exosomes that were secreted by primary NHBE cells upon IL-13 stimuli or control conditions, nor was a difference between exosomes that were secreted to the apical or basal side (Fig. 5.27).

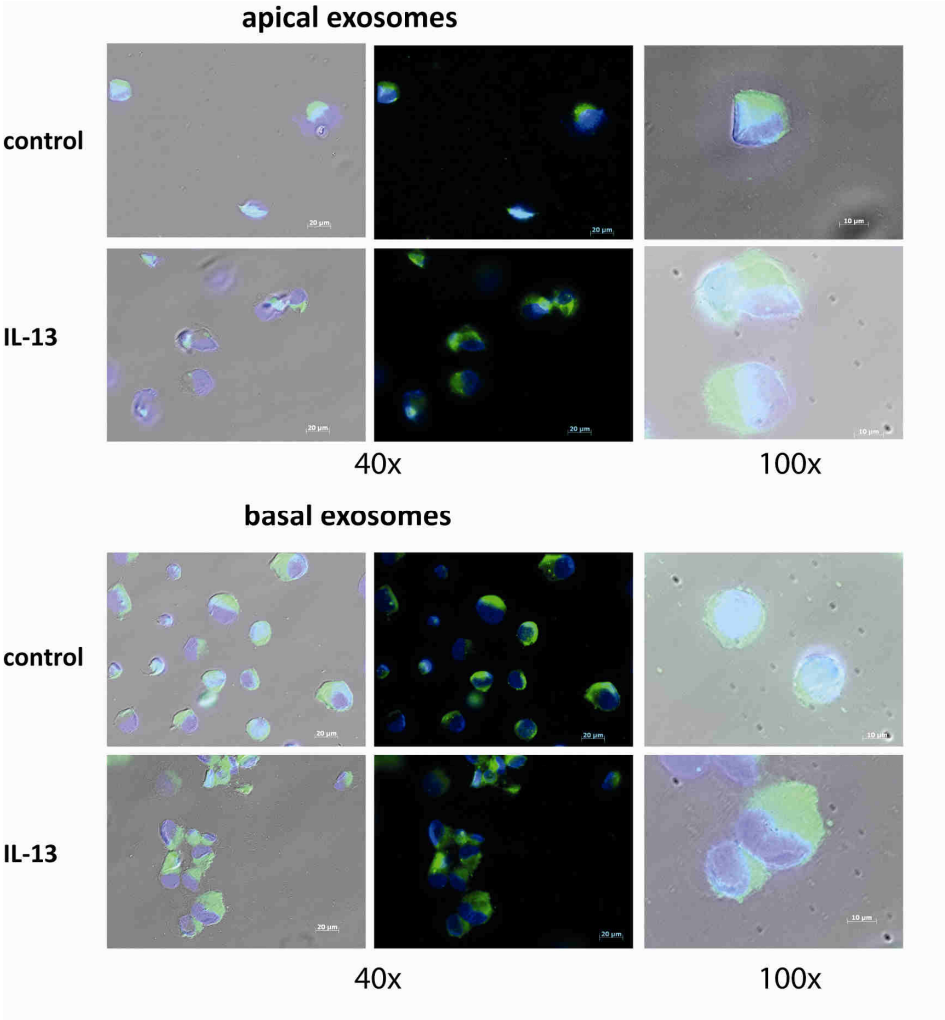

Figure 5.27: NHBE exosomes are taken up by 16-HBE14o$^-$ cells. 16-HBE14o$^-$ cells were cultured for 24 h with isolated NHBE exosomes from either apical (upper two panels) or basal (lower two panels) compartments. Upper panel shows cells with NHBE exosomes derived from control (untreated) cells, lower panel cells with exosomes from IL-13 treated cells. The exosomes were labeled with PKH-67 (green) and the cells with DAPI (blue) for nuclei on glass slides after a cytospin. Outer images were merged with a DIC picture to visualize cell membranes. Representative images of n=3 independent experiments.

5.7.2. Uptake of exosomes by Jurkat cells

As one of the most prominent hallmarks of asthma is a chronic inflammation of the airways, we wanted to investigate if the exosomes are also taken up by immune cells. Figure 5.28 shows cytospin images of Jurkat cells, a human T cell line, with clearly visible exosomes around the nuclei in the cytoplasm.

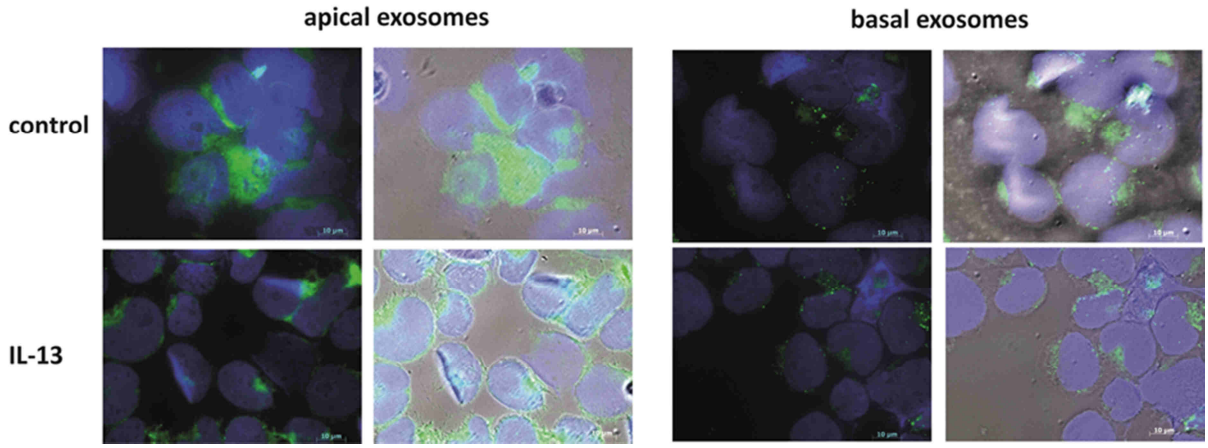

Figure 5.28: NHBE exosomes are taken up by Jurkat cells. Jurkat cells were cultured for 24 h with isolated NHBE exosomes from either apical (left two panels) or basal (right two panels) compartments. Upper panel shows cells with NHBE exosomes derived from control treated cells, lower panel cells with exosomes from IL-13 treated cells. The exosomes were labeled with PKH-67 (green) and the cells with DAPI for nuclei on glass slides after a cytospin. Right images were merged with a DIC picture to visualize cell membranes. Representative images of n=3 independent experiments.

In summary, human bronchial epithelial cells as well as T lymphocytes can take up NHBE derived exosomes. In both cell lines we could not observe a difference in the uptake between exosomes derived from either control or IL-13 treatments or basal vs. apical exosomes.

6. DISCUSSION

The incidence and prevalence of allergies and asthma has been markedly increasing over the last few decades. Despite intensive research, the underlying causes are not yet identified. Several studies in murine models for allergic airway inflammation (AAI) have been already performed. In one of these studies miR-21 was shown to target IL-12p35 and by this influence the Th1/Th2 balance. An ablation of this miRNA also ameliorated OVA-induced AAI (87). In another study, miR-126 was antagonized in an HDM-induced AAI mouse model which reduced the asthmatic phenotype and increased the putative target POU domain class 2 activating factor, which is important for Th2 functions (83). The same group also found miR-145 to play a role in asthma development, as an inhibition had a similar anti-inflammatory action as glucocorticoid treatment (82). Sharma and colleagues attenuated allergic airway disease in mice by inhibiting miR-106a which targets IL-10 (84). One study proposed let-7 to be anti-inflammatory due to targeting of IL-13 and showed that administration of let-7 mimics to mice attenuated the development of AAI (120). Hence several studies have found altered miRNA levels associated with development of allergic airway disease and showed that an antagonism or also an overexpression of single miRNAs can ameliorate the asthmatic phenotype (82–84,87,120). However, in all these studies the miRNAs were modulated during or before the induction of the allergic airway inflammation but not therapeutically in established disease, which would correspond to the situation of human patients. Additionally, a therapeutic use of miRNAs in humans seems highly unlikely as their ability to bind to numerous targets bears the risk to induce massive side effects.

We therefore exploited whole miRNA profiles to identify so far non-characterized pathways where several components are targeted by the dysregulated miRNAs, and investigated the relevance for asthma. By this approach we identified a possible down-regulation of Creb1/Crtc-mediated transcription by miR-17, -144 and -21, associated with a down-regulation of the putative target Sec14l3, in two different mouse models for AAI, human primary bronchial epithelial cell cultures and human nasal epithelial cells from asthmatic children.

6.1. The relevance of mouse models to study asthma

In this study, we used female Balb/c mice and induced allergic airway inflammation by two different allergens: ovalbumin (OVA) and house dust mite (HDM). Those models are widely used in asthma research, however many therapeutic targets identified in the mouse show no, or only limited clinical efficacy in human patients with asthma such as anti-IgE (30), anti-IL-5 (31,32), anti-IL-4 receptor (33) and anti-IL-13 (34). This can be partly explained by fundamental differences between human and mice regarding anatomy, physiology and also immune function. Of note, there is no laboratory animal that develops spontaneously a disease that can be characterized as asthma. Some larger animals, such as cats, horses, dogs and sheep are able to develop bronchial diseases in response to allergens that share some hallmarks with asthma (reviewed in (121)). Thus, every laboratory asthma model will be artificially induced and might entail different responses depending on the method of sensitization, the used antigen and anatomical, immunological properties of the respective animal (reviewed in (121)). Big advantages of mice are that they are genetically very well characterized, easy to handle, breed and manipulate and also many genetically modified strains are commercially available. In contrast to cell culture studies, one can study the complex interplay between different cell types and tissues. After sensitization and challenge with allergen, mice exhibit a clearly defined Th2-type response in their lungs, accompanied by eosinophilia, airway hyperreactivity (AHR) and antigen-specific IgE (reviewed in (122)), characteristics that we could also observe in our mouse models. However, there are three major differences to the human disease: first humans with asthma always show AHR in response to metacholine while mice only do so after allergen challenge; second repeated allergen exposure in sensitized mice leads to tolerance rather than a chronic allergic asthma as in humans; third IgE and mast cells are not very important for the development of AAI in mice, while they play a pivotal role in human asthma (reviewed in (122)).

Therefore, it is of utmost importance to not only rely on data that are generated in mouse models for AAI. In this work, we validated our findings in primary normal human bronchial epithelial cells. Cultured at the air-liquid interface, those cells form a pseudo-stratified epithelium similar to the *in vivo* situation (116). They still represent an isolated system without interaction of different cell types or extracellular matrix. However, this model could be an elegant connection between *in vitro* and *in vivo* experiments, being superior to immortalized cell lines but easier to handle and to test interventions or treatments than an *in vivo* model. Additionally, we validated our findings in nasal epithelial cells from children with allergic asthma and healthy controls.

6.2. Joint regulation of Creb1 and Crtcs by miR-17, -144 and -21

Our group previously found an up-regulation of miR-17 and miR-144, among others, in OVA-induced allergic airway inflammation. This study identified dysregulated miRNAs in lung homogenate of mice with OVA-induced AAI via quantitative and qualitative microarrays. A subsequent *in silico* target gene research with the 100 top-dysregulated miRNAs revealed a miR-17 and -144 up-regulation and a binding to the transcription factor Creb1, which was then functionally validated (104). miRNAs tend to simultaneously address several key regulatory molecules along one signaling pathway (64) and we identified binding sites for both miRNAs and the newly included miR-21 in the 3'UTR of Creb1 co-activators Crtc1, -2 & -3. miRNA-21 was newly included as it was the second highest "hit" in our initial array (adj. p-value 6.18×10^{-13}), was predicted to target Crtc1 and Creb1, and has been already brought into context with allergic airway inflammation (86,87). The putative binding sites were validated in *in vitro* overexpression experiments, validating the previous *in silico* target prediction. Of note, not all three miRNAs did target all factors and sometimes the effects were more prominent on protein than on mRNA level and vice versa. To this end, an over-expression of miR-144 led to a significant decrease in the mRNA levels of all three Crtcs which did not affect the protein level. This might be explained by the fact that depending on the complementarity of the miRNA sequence to the mRNA, the targets are either degraded, deadenylated or the protein translation is inhibited (55). We did observe a small trend for Crtc1 and -3 protein down-regulation after miR-17 overexpression although this did not reach statistical significance. It might be that, due to the half-life of the proteins a down-regulation due to decreased mRNA levels would be only visible at later timepoints.

The transcription of Creb1 downstream targets has lately been proposed to be regulated in a two-hit model (reviewed in (90)): First, Creb is phosphorylated upon stimulation with cAMP and binds to CRE sites in promoters and, second, Crtc1, -2 or -3 are dephosphorylated, translocated to the nucleus and binds to the bZIP domain of Creb to further enhance gene transcription (103). Therefore, a joint miRNA-mediated down-regulation of both factors by miRNAs could have an additive effect on the transcription of Creb1 downstream targets, which might be relevant for asthma. Along with an up-regulation of miR-17, -144 and -21 in lung homogenate of OVA-induced AAI, we detected a slight down-regulation of Creb1 and Crtc1 and -3. This was also observed in HDM-induced allergic airway inflammation, suggesting it to be independent of the type of allergen. The down-regulation was more profound in the HDM-model, which showed a more severe airway inflammation, suggesting it to be associated with disease severity. There was no significant change of CREB1 or

CRTCs in the nasal cells of children with allergic asthma compared to healthy controls. However, the changes in the murine models were investigated 24 hours after the last allergen challenge which does not correspond to the long-lasting chronic disease situation present in the studied children. In mice, the artificially induced allergic airway inflammation is reversible, thus a chronic disease progression could not be studied in our mouse models. However, an association of the CREB1 pathway with asthma development and the disappearance of CREB1 dysregulation later-on is supported by findings in the primary NHBE cells where we saw a down-regulation of both CREB1 and the three CRTCs within 24 hours of IL-13 treatment which then resolved after 4-7 days on mRNA level. Therefore, we speculate that an early down-regulation of the CREB/CRTC pathway in the airway epithelium due to asthmatic stimuli affects the transcription of downstream targets such as SEC14L3. The dysregulation of the central transcription factors might be reversible, but the putative target SEC14L3 might not be. Another reason for the apparent discrepancy of CREB1 expression in the nasal epithelial cells of patients and the mouse model/cell lines could be that we did not stratify patients for medication. Commonly used β_2-agonist act via CREB (123) and could thus regenerate the expression levels in patients with asthma. To address this possibility, future studies in a larger number of children are necessary. Another difference between the human and mouse studies was, that in children the expression was investigated in nasal epithelial cells as opposed to lung tissue in the murine models.

The role for CREB signaling in lung diseases and especially asthma is controversial. On the one hand, CREB is important for the regulation of immune responses, e.g. by regulating the transcription of IL-2, Il-6 and IL-10 (reviewed in (124)). CREB has been shown to be decreased after stimulation with “Th2-derived thymus and activation regulated chemokine” (TARC) in isolated human T cells (123). Additionally, CREB1 binding activity was shown to be negatively correlated with recurrent airway obstruction in horses, a disease that shares many similarities with human asthma (125). Similar to these reports, we observed a down-regulation of Creb1 in two murine models for AAI and also in primary NHBE cells upon induction of goblet cell metaplasia by treatment with the Th2 cytokine IL-13. On the other hand, two reports show an increase of pulmonary phosphorylated (p)CREB in adult steroid-resistant or untreated asthma (126) and of total CREB levels in peripheral blood of patients with recurrent wheeze (127). These reports, however, are not necessarily controversial to our findings of decreased total CREB in bronchial epithelium as total CREB is analyzed in different compartments (blood vs lung). Within the pulmonary compartment pCREB and, respectively, total CREB levels could be regulated differently.

CRTCs have so far mainly been investigated in metabolic processes such as insulin sensitivity and energy balance (90,103,128,129), and their involvement in lung diseases or asthma has to our knowledge not been investigated so far. Crtc3, together with Creb, has been proposed to be essential for transcription of the anti-inflammatory cytokine IL-10 by regulatory macrophages (130). In our study, Crtc3 has shown the strongest down-regulation compared to Crtc1 and -2 in the HDM-induced murine AAI model and also in the primary NHBE cell cultures. Thus, we speculate that the Crtcs might play an important role in chronic inflammatory diseases like asthma. In this context, next to macrophages, regulatory T cells might be interesting to study as they are impaired in function and number in human asthma (131) and they were shown to ameliorate murine AAI after *in vivo* transfer in an IL-10 dependent manner (132).

6.3. Identification of Sec14l3 as relevant Creb1 downstream target gene

We speculate that a miRNA-mediated down-regulation of the very central and ubiquitously expressed transcription factor Creb1 could affect different downstream target genes in different cell types, which could then lead to different hallmarks of asthma pathogenesis. Among the 35 genes which were found to be down-regulated in OVA-induced AAI and contain a CRE site in their promoter region, thus being putative Creb1 targets, was Sec14l3. It seemed an intriguing molecule to investigate further in the development of asthma as it has been proposed to be specifically expressed in the airway epithelium (115) and was found decreased in rat allergic airway inflammation (134). By this “cherry picking” approach, other Creb1 target genes of relevance for asthma pathogenesis might have been ignored. This will be addressed in future studies. For example, the list contains several interesting candidates for allergic airway inflammation such as latent TGF-β binding protein 4 (Ltbp4), which is involved in TGF-β signaling and thereby might play a role in airway remodeling (133). Fatty acid binding protein 5 (Fabp5) has been proposed to play a role in skin barrier function and atopic dermatitis (134).

More than 20 Sec14 family members exist in mammalians and currently they are assumed to act as transporters for hydrophobic ligands like α-tocopherol (135). In particular, Sec14l3 has been proposed to be a sensor of liposomal lipid-packing defects in the lung (136). The assignment of Sec14l3 as Creb target was based on *in silico* mapping of several CRE sites in the promoter region. These CRE sites are highly evolutionary conserved, suggesting that they might be biologically relevant. Still, a formal proof that Sec14l3 expression is controlled by

Creb1/Crtc-mediated transcription is lacking, as only a very small proportion of palindromic CRE sites in promoter regions are truly functional (88). Studies with siRNAs were not possible as Sec14l3/SEC14L3 is not expressed in commonly used murine or human lung cell lines like MLE-12 or 16-HBE14o$^-$. This might be explained by the fact that these cell lines do not contain ciliated cells. SEC14L3 is present in primary NHBE cells after differentiation into a pseudo-stratified epithelium at the air-liquid interface but at that stage those are confluent and non-transfectable.

We observed an association of Sec14l3 expression with ciliated cells in immunofluorescent stainings of mouse lungs, as well as in the highly significant correlation of *SEC14L3* and *FOXJ1* mRNA levels in differentiating primary NHBE cells. In line with our own findings, Shan and colleagues have observed the specific expression of *Sec14l3* mRNA in ciliated airway cells in murine lungs by in situ hybridization (115). In a previous study, this group has shown an inverse correlation of *Sec14l3* mRNA expression and allergic airway inflammation in a rat model (114), which corroborates our findings in two different models of AAI in mice, independent of the type of allergen, and in human paediatric asthma. However to date, it is unknown if Sec14l3 has a functional role in ciliated cells or if the observed loss is due to trans-differentiation into goblet cells upon asthma development. *SEC14L3* has been found to be decreased in nasal epithelium of smokers (137) and during human rhinovirus infection (138). Taken all these observation into consideration, we propose that the association of Sec14l3 loss and goblet metaplasia, which we discovered in this study, might be exploited as a biomarker for judging the integrity of the ciliated epithelium. The detection in nasal brushings makes it extremely valuable as these cells are easily accessible and can be obtained in a non-invasive manner. Thus, the method might even be suitable for infants and children.

6.4. Selection and demographics of paediatric asthma samples

For our human studies we used brushings of the nasal epithelium of children with allergic asthma and healthy controls since the nasal epithelium is in many aspects very similar to the bronchial epithelium and has been proposed to be utilized as an easily-accessible surrogate for bronchial cells (137,139). In a pilot approach, we investigated changes in miRNA and gene expression in seven children with allergic asthma compared to ten healthy controls. We decided to study asthma development in children as it is of utmost importance to identify new treatment targets that are effective in preventing non-reversible airway remodeling. This can

already occur in preschool children, then persist into adulthood (5) and is generally not reversible by common asthma medication.

The 8-12 year old allergic asthma patients were enrolled to the AsthMap study in Washington DC (USA) (107,108) and selected based on physician-diagnosed asthma, present at least for one year, elevated eosinophil counts (>4%) and IgE levels (>150 U/ml) in blood. These patients thus showed features which corresponded to the phenotype of allergic asthma that we observed in our OVA-and HDM-induced AAI models. The ten healthy control children were age-matched and enrolled at the Princess Margaret Hospital for Children in Subiaco (Australia). The fact that the samples were collected at two different centers on two different continents and are, therefore, different in ethnicity (black for the allergic asthma patients vs. caucasian controls) represents the major limitation of this study. There was access to healthy control samples in Washington DC, although they were not age-matched and also not of the same ethnicity. We assumed that age and puberty might have a bigger influence on the expression of our miRNAs and target genes than race or location, so we rather chose the age-matched Australian controls for our analyses. Despite these limitations, we found a significant up-regulation of the three candidate miRNA miR-17, -144 and -21 accompanied by a highly significant down-regulation of *SEC14L3*. However, these findings need further conformation especially also in larger patient cohorts.

6.5. Up-regulation of miR-17, -144 and -21 in human paediatric asthma

In this study, the miRNA regulations in the human paediatric asthma samples were clearly stronger than those observed in the murine AAI models. Especially miR-144 had very low baseline expression levels in healthy children, but was strongly increased in children with allergic asthma.

We observed a similar low expression of miR-144 in untreated primary NHBE cell cultures which increased upon IL-13 stimulus 2-4-fold. This increase was not as high as observed in the nasal epithelial cells, which might be due to the relatively short IL-13 exposure of 7 days. The expression of miR-144 might be further amplified and perpetuated by a continuous stimulus of Th2 cytokines like IL-13 during the development of chronic asthma leading to the high expression we detected in the nasal epithelial cells of children with allergic asthma. It has been already proposed that the majority of pulmonary miRNAs is physiologically present, whereas only a small proportion is generated *de novo* after induction of disease (140). It is

intriguing to speculate that those *de novo* induced miRNAs have a higher importance for disease development or pathogenesis. To our knowledge, miR-144 has not been studied in the context of asthma so far, but has been shown to be abundantly expressed in red blood cells, together with miR-451 (141). A contamination with red blood cells or a different blood content in healthy versus asthmatic samples in our study is unlikely, as the nasal epithelial cells were isolated and purified from brushings in an overnight culture step after which any red blood cells were washed away.

MiR-17 and miR-21 were also significantly increased in the nasal epithelial cells of children with allergic asthma, although to a lesser extent than miR-144. Up-regulation of miR-21 and targeting of IL-12p35 has already been shown in three different models for AAI in mice (86) and it has been implicated to play a role in rodent heart failure, lung fibrosis and cancer (49,142). The miR-17/92 family is involved in lung development (143) but also in the regulation of IL-10 by regulatory T-cells (144). IL-10 transcription has been shown to be regulated by Creb1 and Crtc3 (130). Thus, miR-17 might act on IL-10 via targeting Creb1 and also Crtc3 and could, therefore, play an important role for the function of regulatory T cells. A miR-17 up-regulation, during asthma development might impair IL-10 expression and thereby impair the function of regulatory T cells and benefit chronic inflammation.

6.6. Secretion of miRNAs into exosomes

The initial miRNA profile of dysregulated miRNAs in experimental AAI was performed using whole lung homogenate. Thus, it is unknown which cells express and produce the miRNAs. One research focus in asthma has been recently turned towards the airway epithelium, which is assumed to play an important role in the initiation and perpetuation of the disease (reviewed in (38)). Therefore, we studied the expression changes of our three candidate miRNAs in primary NHBE cells, cultured at the air-liquid interface.

To our surprise, we did not observe a major difference in the miRNAs levels after exposure to early asthmatic stimuli, namely IL-13 treatment, in the primary NHBE cells compared to untreated controls. The expression of miR-17, -144 and -21 increased trendwise after 7 days, but this did not reach statistical significance due to high variability. Thus, we asked if the primary NHBE cells actively secrete the miRNAs into exosomes to communicate with other cell types such as immune cells. If so, after IL-13 treatment an increased amount of miRNAs compared to control cells might be ‘packaged’ into exosomes and secreted. In consequence,

cellular levels would appear unchanged. When we isolated exosomes from the apical as well as the basal side of the cell culture they indeed contained the three candidate miRNAs. The exosomal miRNA levels were significantly increased in the basal medium after 24 hours and four days and on the apical side after seven days which might suggest a change in secretion pattern. It has to be mentioned that it is remains to be clarified if the primary NHBE cells actively secrete the exosomes to the apical side, or if the exosomes diffuse through opened tight junctions from the basal side since the epithelium might get leaky after IL-13 treatment (46,47). Thereby, the apical washes of the cells to obtain exosomes would mimic the BALF obtained from patients or mice.

In line with our study of the NHBE cell line, exosomes isolated from BALF of patients with asthma have a different miRNA content compared to healthy controls (74). Kulshreshtha *et al*. showed lately that epithelial cell-derived exosomes are increased during AAI in mice. We did not observe this in BALF of our OVA model, although the group sizes were rather small (3 animals per group) and exosome numbers should be evaluated in more animals. The authors further reported, that secretion was induced after IL-13 stimulus *in vitro* in BEAS-2B cells and those exosomes had a pro-inflammatory effect on monocyte and macrophages (145). However, this study did not investigate the functional exosome content. We speculate that some of the biological effects of the epithelial-cell derived exosomes might be due to miRNAs inside exosomes, including miR-17, -144 and –21. Along this line, miR-17, and -21 levels were increased in exosomes isolated from BALF of OVA-treated mice. In contrast to the named study, our data do not point to an enhanced secretion of exosomes after IL-13 treatment in primary NHBE cells or in murine BALF in the OVA-model. However, we only investigated CD63 as an exosomal marker and other markers like CD9 or MHCII might give different results. We found all three miRNAs in exosomes isolated from nasal washes of children with allergic asthma but also from primary NHBE cultures with and without IL-13 treatment, suggesting them to be relevant in human asthmatic disease. Unfortunately, we were not able to obtain nasal washes from healthy, age-matched controls for comparison. However, we found a correlation of a higher exosome amount, exosomal miR-17 and miR-21 in nasal washes and IgE levels in serum. This is a first hint that miRNA-containing exosomes in the nasal washes are dependent on allergic disease parameters. However, we are aware that increased IgE levels may not be the perfect marker to judge asthma severity. Future studies will be needed to verify this.

6.7. Uptake of exosomes by target cells *in vitro*

As we found miRNA-containing exosomes at the apical as well as the basal side of the primary NHBE cultures we hypothesized that different cell types might be targeted by apical vs. basal exosomes. Apical exosomes could be taken up by e.g. macrophages or epithelial cells. The basal exosomes might be accessed by cells present in the submucosa like e.g. fibroblasts, smooth muscle cells, but also immune cells like dendritic cells or T cells.

In cell culture, PKH-67-labeled NHBE-derived exosomes were taken up by a human epithelial cell line (16HBE14o$^-$) as well as a human T lymphocyte cell line (Jurkat) within 24 h. There was no obvious difference between the uptake of apical or basal exosomes or between control and IL-13 treated NHBE cells. The regulation and concrete mechanism of exosomal uptake by target cells is currently not clear. The nanovesicles often carry receptor molecules specific for their target cell on the surface or they can directly fuse with the plasma membrane or are phagocytosed (reviewed in (71)).

After uptake of exosomes by the target cells their content needs to be released and localized to different cell compartments to exert its function, another mechanism that is not fully understood yet (reviewed in 58). In this study, we did not confirm a functional uptake of the exosomal miRNAs to other cells. There are, however, studies in the literature showing that miRNAs that are delivered via exosomes are functional in the target cells (72,146,147).

Hence the precise cargo of exosomes and its functions for allergic airway disease needs to be be specified and further investigated in future studies.

6.8. Proposed mechanism

In this work, we identified a molecular axis that potentially contributes to the development of allergic asthma in mice and possibly in humans. We propose that miR-17, -144 and -21 not only regulate the transcription factor CREB1 but also its co-activators CRTC1, -2 and -3. This joint down-regulation might affect the expression of the putative downstream target SEC14L3 in ciliated airway epithelial cells upon goblet cell metaplasia or other relevant target in other cell types such as maybe IL-10 in regulatory T cells or macrophages.

Summarizing the obtained results, the following model can be proposed: epithelial cells secrete exosomes that contain, among others, miR-17, -144 and -21 after IL-13 stimulus e.g. during early development of asthma. The exosomes can fuse with other epithelial cells and thus transfer included miRNA. This mechanism could distribute early 'danger' signals from one epithelial cell to many others, and thereby perpetuate and accelerate the disease progression in a feed-forward loop manner (Fig. 6.1). The exosomes might also be taken up by other cells, such as immune cells including DCs or T cells. A functional miRNA transfer and subsequent CREB1/CRTC down-regulation in the recipient cells could affect other targets and accelerate the development of a chronic inflammatory allergic airway disease.

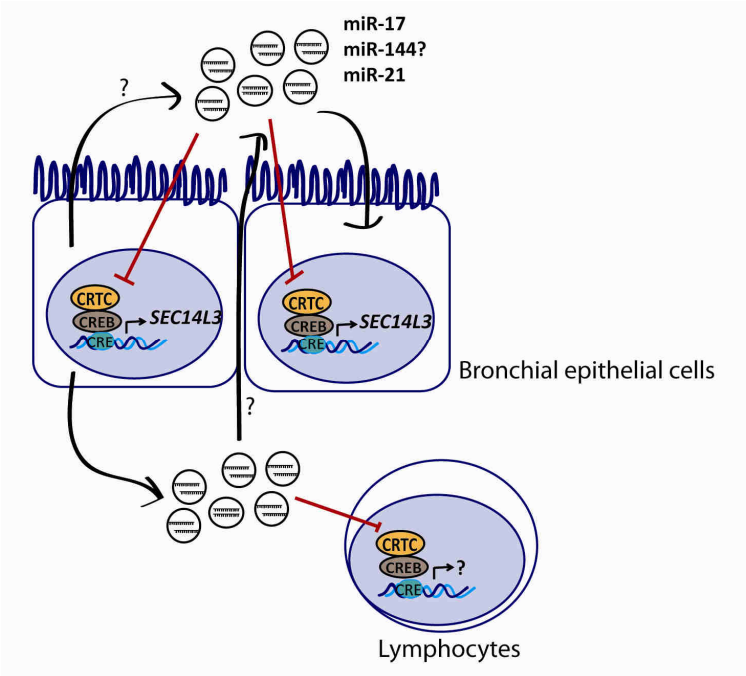

Figure 6.1: Proposed model. miR-17, -21 and maybe -144 (human) are secreted by bronchial epithelial cells into the basal compartment and also into the apical lumen. In asthma, basal exosomes could also diffuse through the opened tight junctions to the apical cell side. Upon uptake by e.g. T-lymphocytes or also in a feed-forward loop manner by other epithelial cells they can cause a global down-regulation of the targeted CREB/CRTC pathway in various cell types with different consequences for the development of allergic airway inflammation.

6.9. Future perspectives

6.9.1. SEC14L3 as biomarker for epithelial integrity

The expression of SEC14L3 is lost during changes of the normal airway epithelium, either induced by smoking (137), virus infection (115) or - as our data suggest - goblet cell metaplasia during asthma development. As SEC14L3 is detectable in the nasal epithelium, it may be used as easily-accessible biomarker for the integrity of the respiratory epithelium. Especially in preschool children, asthma is often hard to differentiate from transient wheeze, hence a marker that enables an evaluation of early changes of the lung epithelium would be very useful. Therefore, in order to establish SEC14L3 as a biomarker for changes in airway epithelium the SEC14L3 down-regulation in asthma has to be validated in larger patient cohorts. Further investigations regarding its function are also warranted.

6.9.2. Epithelial cell-derived exosomes in allergic airway inflammation

In this study we investigated three candidate miRNAs in murine and human allergic airway inflammation. We identified miRNA-17, -21 and -144 as promising candidates to be associated with the development of airway inflammation. Finally, we found them to be secreted into exosomes by airway epithelial cells thus making the miRNAs accessible to other cell types. The target cells of the epithelial secreted exosomes need to be identified and validated. They could include other epithelial cells or immune cells such as T cells. The miR-17, -144 and -21, and others, might be transferred functionally and thereby might regulate the CREB1/CRTC-signaling pathway or other signaling pathways in these target cells.

In future studies the following points should be addressed:

1) Additional downstream targets of the CREB1/CRTC pathway might give more insights into the early development of allergic airway inflammation. One important target to study might be IL-10, which was shown to be regulated by Creb1 and Crtc3 in regulatory macrophages (130). A decrease in this anti-inflammatory cytokine might benefit chronic inflammation in asthma. It has been already shown that regulatory T cells can ameliorate a murine AAI after *in vivo* transfer which was dependent on IL-10 (132). Therefore, Creb1 and the Crtcs should be investigated in regulatory T cells and macrophages in murine AAI models and human patients with asthma.

2) Further studies should address if epithelial cells are the only cells secreting those miRNAs upon asthmatic stimuli. Furthermore, it should be evaluated if the exosomes, secreted after IL-13 treatment, can themselves induce an asthmatic phenotype in epithelial cells in terms of goblet cell metaplasia and mediator release. This would prove that the miRNA are transferred functionally and that secretion into exosomes is crucial for the pathogenesis of asthma, especially for the perpetuation of early asthmatic responses.

3) In addition, exosomes derived from asthmatic patients should be thoroughly analyzed for their cargo, meaning not only miRNA profiles but also mRNA or protein components by high-throughput techniques to decipher the contribution of individual components to the airway inflammatory process. Along this line, it should be further investigated wether exosomes that are secreted from NHBE cells to the apical side are different in cargo and/or surface molecules than those that are secreted to the basal side and if they are differentially taken up by other cells.

.

7. BIBLIOGRAPHY

1. European Respiratory Society. Adult asthma. European Lung White Book. 2014. p. 138–47.

2. Devereux G. asthma and allergy□: food for thought. Nature. 2006;6(November):869–74.

3. Global Initiative for Asthma. BOA Report - GINABurdenReport.pdf [Internet]. [cited 2014 Apr 3]. Available from: http://www.ginasthma.org/local/uploads/files/GINABurdenReport.pdf

4. Postma DS. Gender differences in asthma development and progression. Gend Med. 2007 Jan;4 Suppl B:S133–46.

5. Saglani S, Payne DN, Zhu J, Wang Z, Nicholson AG, Bush A, et al. Early detection of airway wall remodeling and eosinophilic inflammation in preschool wheezers. Am J Respir Crit Care Med. 2007 Nov 1;176(9):858–64.

6. Xu B, Pekkanen J, Hartikainen AL, Järvelin MR. Caesarean section and risk of asthma and allergy in adulthood. J Allergy Clin Immunol. 2001 Apr;107(4):732–3.

7. Barnes KC, Grant A V, Hansel NN, Gao P, Dunston GM. African Americans with asthma: genetic insights. Proc Am Thorac Soc. 2007 Jan;4(1):58–68.

8. Ober C, Loisel DA, Gilad Y. Sex-specific genetic architecture of human disease. Nat Rev Genet. 2008 Dec;9(12):911–22.

9. Goldberg S, Israeli E, Schwartz S, Shochat T, Izbicki G, Toker-Maimon O, et al. Asthma prevalence, family size, and birth order. Chest. 2007 Jun;131(6):1747–52.

10. Kull I, Almqvist C, Lilja G, Pershagen G, Wickman M. Breast-feeding reduces the risk of asthma during the first 4 years of life. J Allergy Clin Immunol. 2004 Oct;114(4):755–60.

11. Bufford JD, Reardon CL, Li Z, Roberg KA, DaSilva D, Eggleston PA, et al. Effects of dog ownership in early childhood on immune development and atopic diseases. Clin Exp Allergy. 2008 Oct;38(10):1635–43.

12. Almqvist C, Egmar A-C, Hedlin G, Lundqvist M, Nordvall SL, Pershagen G, et al. Direct and indirect exposure to pets - risk of sensitization and asthma at 4 years in a birth cohort. Clin Exp Allergy. 2003 Sep;33(9):1190–7.

13. Lemanske RF, Jackson DJ, Gangnon RE, Evans MD, Li Z, Shult PA, et al. Rhinovirus illnesses during infancy predict subsequent childhood wheezing. J Allergy Clin Immunol. 2005 Sep;116(3):571–7.

14. Stein RT, Sherrill D, Morgan WJ, Holberg CJ, Halonen M, Taussig LM, et al. Respiratory syncytial virus in early life and risk of wheeze and allergy by age 13 years. Lancet. 1999 Aug 14;354(9178):541–5.

15. Bisgaard H, Hermansen MN, Buchvald F, Loland L, Halkjaer LB, Bønnelykke K, et al. Childhood asthma after bacterial colonization of the airway in neonates. N Engl J Med. 2007 Oct 11;357(15):1487–95.

16. Tariq SM, Hakim EA, Matthews SM, Arshad SH. Influence of smoking on asthmatic symptoms and allergen sensitisation in early childhood. Postgrad Med J. 2000 Nov;76(901):694–9.

17. Gergen PJ, Fowler JA, Maurer KR, Davis WW, Overpeck MD. The burden of environmental tobacco smoke exposure on the respiratory health of children 2 months through 5 years of age in the United States: Third National Health and Nutrition Examination Survey, 1988 to 1994. Pediatrics. 1998 Feb;101(2):E8.

18. Islam T, Gauderman WJ, Berhane K, McConnell R, Avol E, Peters JM, et al. Relationship between air pollution, lung function and asthma in adolescents. Thorax. 2007 Nov;62(11):957–63.

19. Ege MJ, Mayer M, Normand A-C, Genuneit J, Cookson WOCM, Braun-Fahrländer C, et al. Exposure to environmental microorganisms and childhood asthma. N Engl J Med. 2011 Feb 24;364(8):701–9.

20. Douwes J, Cheng S, Travier N, Cohet C, Niesink A, McKenzie J, et al. Farm exposure in utero may protect against asthma, hay fever and eczema. Eur Respir J. 2008 Sep;32(3):603–11.

21. Peters JL, Boynton-Jarrett R, Sandel M. Prenatal environmental factors influencing IgE levels, atopy and early asthma. Curr Opin Allergy Clin Immunol. 2013 Apr;13(2):187–92.

22. Peters JL, Suglia SF, Platts-Mills TAE, Hosen J, Gold DR, Wright RJ. Relationships among prenatal aeroallergen exposure and maternal and cord blood IgE: project ACCESS. J Allergy Clin Immunol. 2009 May;123(5):1041–6.

23. Mund M, Louwen F, Klingelhoefer D, Gerber A. Smoking and pregnancy--a review on the first major environmental risk factor of the unborn. Int J Environ Res Public Health. 2013 Dec;10(12):6485–99.

24. Li Y-F, Langholz B, Salam MT, Gilliland FD. Maternal and grandmaternal smoking patterns are associated with early childhood asthma. Chest. 2005 Apr;127(4):1232–41.

25. Lim RH, Kobzik L. Maternal transmission of asthma risk. Am J Reprod Immunol. 2009 Jan;61(1):1–10.

26. Kang JY, Kim JW, Kim JS, Kim SJ, Lee SH, Kwon SS, et al. Inhibitory effects of anti-immunoglobulin E antibodies on airway remodeling in a murine model of chronic asthma. J Asthma. 2010 May;47(4):374–80.

27. Mauser PJ, Pitman AM, Fernandez X, Foran SK, Adams GK, Kreutner W, et al. Effects of an antibody to interleukin-5 in a monkey model of asthma. Am J Respir Crit Care Med. 1995 Aug;152(2):467–72.

28. Garlisi CG, Kung TT, Wang P, Minnicozzi M, Umland SP, Chapman RW, et al. Effects of chronic anti-interleukin-5 monoclonal antibody treatment in a murine model of pulmonary inflammation. Am J Respir Cell Mol Biol. 1999 Feb;20(2):248–55.

29. Oh CK, Geba GP, Molfino N. Investigational therapeutics targeting the IL-4/IL-13/STAT-6 pathway for the treatment of asthma. Eur Respir Rev. 2010 Mar;19(115):46–54.

30. Bousquet J, Rabe K, Humbert M, Chung KF, Berger W, Fox H, et al. Predicting and evaluating response to omalizumab in patients with severe allergic asthma. Respir Med. 2007 Jul;101(7):1483–92.

31. Kips JC, O'Connor BJ, Langley SJ, Woodcock A, Kerstjens HAM, Postma DS, et al. Effect of SCH55700, a humanized anti-human interleukin-5 antibody, in severe persistent asthma: a pilot study. Am J Respir Crit Care Med. 2003 Jun 15;167(12):1655–9.

32. Leckie MJ, ten Brinke A, Khan J, Diamant Z, O'Connor BJ, Walls CM, et al. Effects of an interleukin-5 blocking monoclonal antibody on eosinophils, airway hyper-responsiveness, and the late asthmatic response. Lancet. 356(9248):2144–8.

33. Corren J, Busse W, Meltzer EO, Mansfield L, Bensch G, Fahrenholz J, et al. A randomized, controlled, phase 2 study of AMG 317, an IL-4Ralpha antagonist, in patients with asthma. Am J Respir Crit Care Med. 2010 Apr 15;181(8):788–96.

34. Piper E, Brightling C, Niven R, Oh C, Faggioni R, Poon K, et al. A phase II placebo-controlled study of tralokinumab in moderate-to-severe asthma. Eur Respir J. 2013 Feb;41(2):330–8.

35. Holgate ST. Innate and adaptive immune responses in asthma. Nat Med. Nature Publishing Group; 2012 May;18(5):673–83.

36. Georas SN, Guo J, De Fanis U, Casolaro V. T-helper cell type-2 regulation in allergic disease. Eur Respir J. 2005 Dec;26(6):1119–37.

37. Cosmi L, Liotta F, Maggi E, Romagnani S, Annunziato F. Th17 cells: new players in asthma pathogenesis. Allergy. 2011 Aug;66(8):989–98.

38. Lambrecht BN, Hammad H. Allergens and the airway epithelium response: Gateway to allergic sensitization. J Allergy Clin Immunol. Elsevier; 2014 Sep 9;134(3):499–507.

39. Xiao C, Puddicombe SM, Field S, Haywood J, Broughton-Head V, Puxeddu I, et al. Defective epithelial barrier function in asthma. J Allergy Clin Immunol. 2011 Sep;128(3):549–56.e1–12.

40. Lambrecht BN, Peleman RA, Bullock GR, Pauwels RA. Sensitization to inhaled antigen by intratracheal instillation of dendritic cells. Clin Exp Allergy. 2000 Feb;30(2):214–24.

41. Sallmann E, Reininger B, Brandt S, Duschek N, Hoflehner E, Garner-Spitzer E, et al. High-affinity IgE receptors on dendritic cells exacerbate Th2-dependent inflammation. J Immunol. 2011 Jul 1;187(1):164–71.

42. Lambrecht BN, Hammad H. Taking our breath away: dendritic cells in the pathogenesis of asthma. Nat Rev Immunol. 2003 Dec;3(12):994–1003.

43. Kuperman DA, Huang X, Koth LL, Chang GH, Dolganov GM, Zhu Z, et al. Direct effects of interleukin-13 on epithelial cells cause airway hyperreactivity and mucus overproduction in asthma. Nat Med. 2002 Aug;8(8):885–9.

44. Barnes PJ. Immunology of asthma and chronic obstructive pulmonary disease. Nat Rev Immunol. 2008 Mar;8(3):183–92.

45. Lambrecht BN, Hammad H. The airway epithelium in asthma. Nat Med. 2012 May;18(5):684–92.

46. Soyka MB, Wawrzyniak P, Eiwegger T, Holzmann D, Treis A, Wanke K, et al. Defective epithelial barrier in chronic rhinosinusitis: the regulation of tight junctions by IFN-γ and IL-4. J Allergy Clin Immunol. Elsevier; 2012 Nov 11;130(5):1087–96.e10.

47. Fujita H, Chalubinski M, Rhyner C, Indermitte P, Meyer N, Ferstl R, et al. Claudin-1 expression in airway smooth muscle exacerbates airway remodeling in asthmatic subjects. J Allergy Clin Immunol. 2011 Jun;127(6):1612–21.e8.

48. Uehara A, Fujimoto Y, Fukase K, Takada H. Various human epithelial cells express functional Toll-like receptors, NOD1 and NOD2 to produce anti-microbial peptides, but not proinflammatory cytokines. Mol Immunol. 2007 May;44(12):3100–11.

49. O'Connell RM, Rao DS, Chaudhuri A a, Baltimore D. Physiological and pathological roles for microRNAs in the immune system. Nat Rev Immunol. Nature Publishing Group; 2010 Feb;10(2):111–22.

50. Cushing L, Jiang Z, Kuang P, Lü DJ. The Roles of miRNAs and Protein Components of the miRNA Pathway in Lung Development and Diseases. 2014 Sep 11;

51. Lee RC, Feinbaum RL, Ambros V. The C. elegans heterochronic gene lin-4 encodes small RNAs with antisense complementarity to lin-14. Cell. 1993 Dec 3;75(5):843–54.

52. Lee Y, Kim M, Han J, Yeom K-H, Lee S, Baek SH, et al. MicroRNA genes are transcribed by RNA polymerase II. EMBO J. 2004 Oct 13;23(20):4051–60.

53. Borchert GM, Lanier W, Davidson BL. RNA polymerase III transcribes human microRNAs. Nat Struct Mol Biol. 2006 Dec;13(12):1097–101.

54. Cai X, Hagedorn CH, Cullen BR. Human microRNAs are processed from capped, polyadenylated transcripts that can also function as mRNAs. RNA. 2004 Dec;10(12):1957–66.

55. Winter J, Jung S, Keller S, Gregory RI, Diederichs S. Many roads to maturity: microRNA biogenesis pathways and their regulation. Nat Cell Biol. 2009 Mar;11(3):228–34.

56. Song G, Wang L. MiR-433 and miR-127 arise from independent overlapping primary transcripts encoded by the miR-433-127 locus. PLoS One. 2008 Jan;3(10):e3574.

57. Han J, Lee Y, Yeom K-H, Nam J-W, Heo I, Rhee J-K, et al. Molecular basis for the recognition of primary microRNAs by the Drosha-DGCR8 complex. Cell. 2006 Jun 2;125(5):887–901.

58. Hutvágner G, McLachlan J, Pasquinelli AE, Bálint E, Tuschl T, Zamore PD. A cellular function for the RNA-interference enzyme Dicer in the maturation of the let-7 small temporal RNA. Science. 2001 Aug 3;293(5531):834–8.

59. Khvorova A, Reynolds A, Jayasena SD. Functional siRNAs and miRNAs exhibit strand bias. Cell. 2003 Oct 17;115(2):209–16.

60. Filipowicz W, Bhattacharyya SN, Sonenberg N. Mechanisms of post-transcriptional regulation by microRNAs: are the answers in sight? Nat Rev Genet. 2008 Feb;9(2):102–14.

61. Carthew RW, Sontheimer EJ. Origins and Mechanisms of miRNAs and siRNAs. Cell. 2009 Feb 20;136(4):642–55.

62. Shalgi R, Lieber D, Oren M, Pilpel Y. Global and local architecture of the mammalian microRNA-transcription factor regulatory network. PLoS Comput Biol. 2007 Jul;3(7):e131.

63. Chen C-Y, Chen S-T, Fuh C-S, Juan H-F, Huang H-C. Coregulation of transcription factors and microRNAs in human transcriptional regulatory network. BMC Bioinformatics. BioMed Central Ltd; 2011 Jan;12 Suppl 1(Suppl 1):S41.

64. Zhou Y, Ferguson J, Chang JT, Kluger Y. Inter- and intra-combinatorial regulation by transcription factors and microRNAs. BMC Genomics. 2007 Jan;8:396.

65. Gupta SK, Bang C, Thum T. Circulating microRNAs as biomarkers and potential paracrine mediators of cardiovascular disease. Circ Cardiovasc Genet. 2010 Oct;3(5):484–8.

66. Raposo G, Nijman HW, Stoorvogel W, Liejendekker R, Harding C V, Melief CJ, et al. B lymphocytes secrete antigen-presenting vesicles. J Exp Med. 1996 Mar 1;183(3):1161–72.

67. Blanchard N, Lankar D, Faure F, Regnault A, Dumont C, Raposo G, et al. TCR activation of human T cells induces the production of exosomes bearing the TCR/CD3/zeta complex. J Immunol. 2002 Apr 1;168(7):3235–41.

68. Esser J, Gehrmann U, D'Alexandri FL, Hidalgo-Estévez AM, Wheelock CE, Scheynius A, et al. Exosomes from human macrophages and dendritic cells contain enzymes for leukotriene biosynthesis and promote granulocyte migration. J Allergy Clin Immunol. 2010 Nov;126(5):1032–40, 1040.e1–4.

69. Kesimer M, Scull M, Brighton B, DeMaria G, Burns K, O'Neal W, et al. Characterization of exosome-like vesicles released from human tracheobronchial ciliated epithelium: a possible role in innate defense. FASEB J. 2009 Jun;23(6):1858–68.

70. Lee Y, El Andaloussi S, Wood MJ a. Exosomes and microvesicles: extracellular vesicles for genetic information transfer and gene therapy. Hum Mol Genet. 2012 Oct 15;21(R1):R125–34.

71. Ramachandran S, Palanisamy V. Horizontal transfer of RNAs: exosomes as mediators of intercellular communication. Wiley Interdiscip Rev RNA. 3(2):286–93.

72. Valadi H, Ekström K, Bossios A, Sjöstrand M, Lee JJ, Lötvall JO. Exosome-mediated transfer of mRNAs and microRNAs is a novel mechanism of genetic exchange between cells. Nat Cell Biol. 2007 Jun;9(6):654–9.

73. Lässer C, Alikhani VS, Ekström K, Eldh M, Paredes PT, Bossios A, et al. Human saliva, plasma and breast milk exosomes contain RNA: uptake by macrophages. J Transl Med. 2011 Jan;9:9.

74. Levänen B, Bhakta NR, Paredes PT, Barbeau R, Hiltbrunner S, Pollack JL, et al. Altered microRNA profiles in bronchoalveolar lavage fluid exosomes in asthmatic patients. J Allergy Clin Immunol. 2013 Jan 16;18–23.

75. Chen C-Z, Li L, Lodish HF, Bartel DP. MicroRNAs modulate hematopoietic lineage differentiation. Science. 2004 Jan 2;303(5654):83–6.

76. Brosh R, Shalgi R, Liran A, Landan G, Korotayev K, Nguyen GH, et al. p53-Repressed miRNAs are involved with E2F in a feed-forward loop promoting proliferation. Mol Syst Biol. 2008 Jan;4(229):229.

77. Marson A, Levine SS, Cole MF, Frampton GM, Brambrink T, Johnstone S, et al. Connecting microRNA genes to the core transcriptional regulatory circuitry of embryonic stem cells. Cell. 2008 Aug 8;134(3):521–33.

78. Poy MN, Eliasson L, Krutzfeldt J, Kuwajima S, Ma X, Macdonald PE, et al. A pancreatic islet-specific microRNA regulates insulin secretion. Nature. 2004 Nov 11;432(7014):226–30.

79. Jasinski-Bergner S, Mandelboim O, Seliger B. The Role of MicroRNAs in the Control of Innate Immune Response in Cancer. J Natl Cancer Inst. 2014 Oct;106(10).

80. Williams AE, Larner-Svensson H, Perry MM, Campbell G a, Herrick SE, Adcock IM, et al. MicroRNA expression profiling in mild asthmatic human airways and effect of corticosteroid therapy. PLoS One. 2009 Jan;4(6):e5889.

81. Solberg OD, Ostrin EJ, Love MI, Peng JC, Bhakta NR, Hou L, et al. Airway Epithelial miRNA Expression is Altered in Asthma. Am J Respir Crit Care Med. 2012 Sep 6;(C):1–91.

82. Collison A, Mattes J, Plank M, Foster PS. Inhibition of house dust mite-induced allergic airways disease by antagonism of microRNA-145 is comparable to glucocorticoid treatment. J Allergy Clin Immunol. Elsevier Ltd; 2011 Jul;128(1):160–7.e4.

83. Mattes J, Collison A, Plank M, Phipps S, Foster PS. Antagonism of microRNA-126 suppresses the effector function of TH2 cells and the development of allergic airways disease. Proc Natl Acad Sci U S A. 2009 Nov 3;106(44):18704–9.

84. Sharma A, Kumar M, Ahmad T, Mabalirajan U, Aich J, Agrawal A, et al. Antagonism of mmu-mir-106a attenuates asthma features in allergic murine model. J Appl Physiol. 2012 Aug;113(3):459–64.

85. Polikepahad S, Knight JM, Naghavi AO, Oplt T, Creighton CJ, Shaw C, et al. Proinflammatory role for let-7 microRNAS in experimental asthma. J Biol Chem. 2010 Sep 24;285(39):30139–49.

86. Lu TX, Munitz A, Rothenberg ME. MicroRNA-21 is up-regulated in allergic airway inflammation and regulates IL-12p35 expression. J Immunol. 2009 Apr 15;182(8):4994–5002.

87. Lu TX, Hartner J, Lim E-J, Fabry V, Mingler MK, Cole ET, et al. MicroRNA-21 limits in vivo immune response-mediated activation of the IL-12/IFN-gamma pathway, Th1 polarization, and the severity of delayed-type hypersensitivity. J Immunol. 2011 Sep 15;187(6):3362–73.

88. Mayr B, Montminy M. Transcriptional regulation by the phosphorylation-dependent factor CREB. Nat Rev Mol Cell Biol. 2001 Aug;2(8):599–609.

89. Rudolph D, Tafuri a, Gass P, Hämmerling GJ, Arnold B, Schütz G. Impaired fetal T cell development and perinatal lethality in mice lacking the cAMP response element binding protein. Proc Natl Acad Sci U S A. 1998 Apr 14;95(8):4481–6.

90. Altarejos JY, Montminy M. CREB and the CRTC co-activators: sensors for hormonal and metabolic signals. Nat Rev Mol Cell Biol. Nature Publishing Group; 2011 Mar;12(3):141–51.

91. Gonzalez G a, Montminy MR. Cyclic AMP stimulates somatostatin gene transcription by phosphorylation of CREB at serine 133. Cell. 1989 Nov;59(4):675–80.

92. Gonzalez GA, Yamamoto KK, Fischer WH, Karr D, Menzel P, Biggs W, et al. A cluster of phosphorylation sites on the cyclic AMP-regulated nuclear factor CREB predicted by its sequence. Nature. 1989 Feb 23;337(6209):749–52.

93. Montminy MR, Bilezikjian LM. Binding of a nuclear protein to the cyclic-AMP response element of the somatostatin gene. Nature. 328(6126):175–8.

94. Montminy MR, Sevarino KA, Wagner JA, Mandel G, Goodman RH. Identification of a cyclic-AMP-responsive element within the rat somatostatin gene. Proc Natl Acad Sci U S A. 1986 Sep;83(18):6682–6.

95. Johannessen M, Delghandi MP, Moens U. What turns CREB on? Cell Signal. 2004 Nov;16(11):1211–27.

96. Gonzalez G a, Montminy MR. Cyclic AMP stimulates somatostatin gene transcription by phosphorylation of CREB at serine 133. Cell. 1989 Nov 17;59(4):675–80.

97. Shi Y, Venkataraman SL, Dodson GE, Mabb AM, LeBlanc S, Tibbetts RS. Direct regulation of CREB transcriptional activity by ATM in response to genotoxic stress. Proc Natl Acad Sci U S A. 2004 Apr 20;101(16):5898–903.

98. Sun P, Enslen H, Myung PS, Maurer RA. Differential activation of CREB by Ca2+/calmodulin-dependent protein kinases type II and type IV involves phosphorylation of a site that negatively regulates activity. Genes Dev. 1994 Nov 1;8(21):2527–39.

99. Zhang X, Odom DT, Koo S-H, Conkright MD, Canettieri G, Best J, et al. Genome-wide analysis of cAMP-response element binding protein occupancy, phosphorylation, and target gene activation in human tissues. Proc Natl Acad Sci U S A. 2005 Mar 22;102(12):4459–64.

100. Conkright MD, Guzmán E, Flechner L, Su AI, Hogenesch JB, Montminy M. Genome-wide analysis of CREB target genes reveals a core promoter requirement for cAMP responsiveness. Mol Cell. 2003 Apr;11(4):1101–8.

101. Iourgenko V, Zhang W, Mickanin C, Daly I, Jiang C, Hexham JM, et al. Identification of a family of cAMP response element-binding protein coactivators by genome-scale functional analysis in mammalian cells. Proc Natl Acad Sci U S A. 2003 Oct 14;100(21):12147–52.

102. Conkright MD, Canettieri G, Screaton R, Guzman E, Miraglia L, Hogenesch JB, et al. TORCs: transducers of regulated CREB activity. Mol Cell. 2003 Aug;12(2):413–23.

103. Wang Y, Inoue H, Ravnskjaer K, Viste K, Miller N, Liu Y, et al. Targeted disruption of the CREB coactivator Crtc2 increases insulin sensitivity. Proc Natl Acad Sci U S A. 2010 Feb 16;107(7):3087–92.

104. Schulz N. microRNA profiling and target identification in a mouse model for allergic asthma. Ludwig-Maximilians-Universität München; 2012.

105. Alessandrini F, Beck-Speier I, Krappmann D, Weichenmeier I, Takenaka S, Karg E, et al. Role of oxidative stress in ultrafine particle-induced exacerbation of allergic lung inflammation. Am J Respir Crit Care Med. 2009 Jun;179(11):984–91.

106. Cozens AL, Yezzi MJ, Kunzelmann K, Ohrui T, Chin L, Eng K, et al. CFTR expression and chloride secretion in polarized immortal human bronchial epithelial cells. Am J Respir Cell Mol Biol. 1994 Jan;10(1):38–47.

107. Freishtat R, Iqbal S, Pillai D. High prevalence of vitamin D deficiency among inner-city African American youth with asthma in Washington, DC. J Pediatr. 2010;156(6):948–52.

108. Stemmy EJ, Benton AS, Lerner J, Alcala S, Constant SL, Freishtat RJ. Extracellular cyclophilin levels associate with parameters of asthma in phenotypic clusters. J Asthma. 2011 Dec;48(10):986–93.

109. Benton A, Kumar N, Lerner J. Airway platelet activation is associated with airway eosinophilic inflammation in asthma. J Investig Med. 2010;58(8):987–90.

110. Benton A, Wang Z, Lerner J. Overcoming heterogeneity in pediatric asthma: tobacco smoke and asthma characteristics within phenotypic clusters in an African American cohort. J Asthma. 2010;47(7):728–34.

111. Watson A. MUC7 polymorphisms are associated with a decreased risk of being diagnosed with asthma in an African-American population. J Investig Med. 2009;57(8):882–6.

112. Chen C, Ridzon DA, Broomer AJ, Zhou Z, Lee DH, Nguyen JT, et al. Real-time quantification of microRNAs by stem-loop RT-PCR. Nucleic Acids Res. 2005 Jan;33(20):e179.

113. Maier KL, Alessandrini F, Beck-Speier I, Hofer TPJ, Diabaté S, Bitterle E, et al. Health effects of ambient particulate matter--biological mechanisms and inflammatory responses to in vitro and in vivo particle exposures. Inhal Toxicol. 2008 Feb;20(3):319–37.

114. Shan L, Kawakami T, Asano S, Noritake S, Yoshimoto D, Yamashita K, et al. Inverse relationship between Sec14l3 mRNA/protein expression and allergic airway inflammation. Eur J Pharmacol. Elsevier B.V.; 2009 Aug 15;616(1-3):293–300.

115. Shan L, Noritake S, Fujiwara M, Asano S, Yoshida-Noro C, Noro N, et al. Sec14l3 is specifically expressed in mouse airway ciliated cells. Inflammation. 2012 Apr;35(2):702–12.

116. Schamberger AC, Mise N, Jia J, Genoyer E, Yildirim AÖ, Meiners S, et al. Cigarette smoke-induced disruption of bronchial epithelial tight junctions is prevented by transforming growth factor-β. Am J Respir Cell Mol Biol. American Thoracic Society; 2014 Jun 1;50(6):1040–52.

117. Choksi SP, Lauter G, Swoboda P, Roy S. Switching on cilia: transcriptional networks regulating ciliogenesis. Development. 2014 Apr 1;141(7):1427–41.

118. Tanabe T, Kanoh S, Tsushima K, Yamazaki Y, Kubo K, Rubin BK. Clarithromycin inhibits interleukin-13-induced goblet cell hyperplasia in human airway cells. Am J Respir Cell Mol Biol. American Thoracic Society; 2011 Nov 14;45(5):1075–83.

119. Temann U a, Prasad B, Gallup MW, Basbaum C, Ho SB, Flavell R a, et al. A novel role for murine IL-4 in vivo: induction of MUC5AC gene expression and mucin hypersecretion. Am J Respir Cell Mol Biol. 1997 Apr;16(4):471–8.

120. Kumar M, Ahmad T, Sharma A, Mabalirajan U, Kulshreshtha A, Agrawal A, et al. Let-7 microRNA-mediated regulation of IL-13 and allergic airway inflammation. J Allergy Clin Immunol. Elsevier Ltd; 2011 Nov;128(5):1077–85.e1–10.

121. Zosky GR, Sly PD. Animal models of asthma. Clin Exp Allergy. 2007 Jul;37(7):973–88.

122. Epstein MM. Do mouse models of allergic asthma mimic clinical disease? Int Arch Allergy Immunol. 2004 Jan;133(1):84–100.

123. Heijink IH, Vellenga E, Oostendorp J, de Monchy JGR, Postma DS, Kauffman HF. Exposure to TARC alters beta2-adrenergic receptor signaling in human peripheral blood T lymphocytes. Am J Physiol Lung Cell Mol Physiol. 2005 Jul;289(1):L53–9.

124. Wen AY, Sakamoto KM, Miller LS. The role of the transcription factor CREB in immune function. J Immunol. 2010 Dec 1;185(11):6413–9.

125. Couëtil LL, Art T, De Moffarts B, Becker M, Mélotte D, Jaspar F, et al. DNA binding activity of transcription factors in bronchial cells of horses with recurrent airway obstruction. Vet Immunol Immunopathol. 2006;113(1-2):11–20.

126. Chiappara G, Chanez P, Bruno a, Pace E, Pompeo F, Bousquet J, et al. Variable p-CREB expression depicts different asthma phenotypes. Allergy. 2007 Jul;62(7):787–94.

127. Jin R, Xu H-G, Yuan W-X, Zhuang L-L, Liu L-F, Jiang L, et al. Mechanisms elevating ORMDL3 expression in recurrent wheeze patients: role of Ets-1, p300 and CREB. Int J Biochem Cell Biol. 2012 Jul;44(7):1174–83.

128. Song Y, Altarejos J, Goodarzi MO, Inoue H, Guo X, Berdeaux R, et al. CRTC3 links catecholamine signalling to energy balance. Nature. Nature Publishing Group; 2010 Dec 16;468(7326):933–9.

129. Canettieri G, Coni S, Della Guardia M, Nocerino V, Antonucci L, Di Magno L, et al. The coactivator CRTC1 promotes cell proliferation and transformation via AP-1. Proc Natl Acad Sci U S A. 2009 Feb 3;106(5):1445–50.

130. Clark K, MacKenzie KF, Petkevicius K, Kristariyanto Y, Zhang J, Choi HG, et al. Phosphorylation of CRTC3 by the salt-inducible kinases controls the interconversion of classically activated and regulatory macrophages. Proc Natl Acad Sci. 2012 Oct 2;1–6.

131. Hartl D, Koller B, Mehlhorn AT, Reinhardt D, Nicolai T, Schendel DJ, et al. Quantitative and functional impairment of pulmonary CD4+CD25hi regulatory T cells in pediatric asthma. J Allergy Clin Immunol. 2007 May;119(5):1258–66.

132. Kearley J, Barker JE, Robinson DS, Lloyd CM. Resolution of airway inflammation and hyperreactivity after in vivo transfer of CD4+CD25+ regulatory T cells is interleukin 10 dependent. J Exp Med. 2005 Dec 5;202(11):1539–47.

133. Koli K, Wempe F, Sterner-Kock A, Kantola A, Komor M, Hofmann W-K, et al. Disruption of LTBP-4 function reduces TGF-beta activation and enhances BMP-4 signaling in the lung. J Cell Biol. 2004 Oct 11;167(1):123–33.

134. Yamane Y, Moriyama K, Yasuda C, Miyata S, Aihara M, Ikezawa Z, et al. New horny layer marker proteins for evaluating skin condition in atopic dermatitis. Int Arch Allergy Immunol. 2009 Jan;150(1):89–101.

135. Zimmer S, Stocker A, Sarbolouki MN, Spycher SE, Sassoon J, Azzi A. A novel human tocopherol-associated protein: cloning, in vitro expression, and characterization. J Biol Chem. 2000 Aug;275(33):25672–80.

136. Hishikawa D, Shindou H, Harayama T, Ogasawara R, Suwabe A, Shimizu T. Identification of Sec14-like 3 as a novel lipid-packing sensor in the lung. FASEB J. 2013 Dec;27(12):5131–40.

137. Zhang X, Sebastiani P, Liu G, Schembri F, Zhang X, Dumas YM, et al. Similarities and differences between smoking-related gene expression in nasal and bronchial epithelium. Physiol Genomics. 2010 Mar 3;41(1):1–8.

138. Proud D, Turner RB, Winther B, Wiehler S, Tiesman JP, Reichling TD, et al. Gene expression profiles during in vivo human rhinovirus infection: insights into the host response. Am J Respir Crit Care Med. 2008 Nov;178(9):962–8.

139. McDougall CM, Blaylock MG, Douglas JG, Brooker RJ, Helms PJ, Walsh GM. Nasal epithelial cells as surrogates for bronchial epithelial cells in airway inflammation studies. Am J Respir Cell Mol Biol. 2008 Nov;39(5):560–8.

140. Moschos S a, Williams AE, Perry MM, Birrell M a, Belvisi MG, Lindsay M a. Expression profiling in vivo demonstrates rapid changes in lung microRNA levels following lipopolysaccharide-induced inflammation but not in the anti-inflammatory action of glucocorticoids. BMC Genomics. 2007 Jan;8:240.

141. Rasmussen KD, Simmini S, Abreu-Goodger C, Bartonicek N, Di Giacomo M, Bilbao-Cortes D, et al. The miR-144/451 locus is required for erythroid homeostasis. J Exp Med. 2010 Jul 5;207(7):1351–8.

142. Morrisey EE. The magic and mystery of miR-21. J Clin Invest. American Society for Clinical Investigation; 2010 Nov 1;120(11):3817–9.

143. Lu Y, Thomson JM, Wong HYF, Hammond SM, Hogan BLM. Transgenic over-expression of the microRNA miR-17-92 cluster promotes proliferation and inhibits differentiation of lung epithelial progenitor cells. Dev Biol. 2007 Oct;310(2):442–53.

144. De Kouchkovsky D, Esensten JH, Rosenthal WL, Morar MM, Bluestone JA, Jeker LT. microRNA-17-92 regulates IL-10 production by regulatory T cells and control of experimental autoimmune encephalomyelitis. J Immunol. 2013 Aug;191(4):1594–605.

145. Kulshreshtha A, Ahmad T, Agrawal A, Ghosh B. Proinflammatory role of epithelial cell-derived exosomes in allergic airway inflammation. J Allergy Clin Immunol. Elsevier Ltd; 2013 Feb 13;131(4):1194–203.e14.

146. Mittelbrunn M, Gutiérrez-Vázquez C, Villarroya-Beltri C, González S, Sánchez-Cabo F, González MÁ, et al. Unidirectional transfer of microRNA-loaded exosomes from T cells to antigen-presenting cells. Nat Commun. Nature Publishing Group, a division of Macmillan Publishers Limited. All Rights Reserved.; 2011 Jan 19;2:282.

147. Montecalvo A, Larregina AT, Shufesky WJ, Stolz DB, Sullivan MLG, Karlsson JM, et al. Mechanism of transfer of functional microRNAs between mouse dendritic cells via exosomes. Blood. 2012 Jan 19;119(3):756–66.

8. Appendix

8.1. Abbreviations

A

AAI: allergic airway inflammation

Ago: argonaute

AHR: airway hyperreactivity

Alum: aluminium hydroxid/magnesium hydroxid

AMPK: AMP-activated kinase

APC: antigen presenting cell

AsthMaP: asthma severity modifying polymorphisms project

ATF1: activating transcription factor 1

B

BALF: broncho-alveolar lavage fluid

bp: basepairs

BSA: bovine serum albumin

bZIP: basic leucine zipper

C

cAMP: cyclic adenosine monophosphate

C. elegans: Caenorhabditis elegans

CN: calcineurin

CRE: cAMP-responsive element

CREB: cAMP responsive element binding protein

CREM: cAMP response element modulator

CRTC: cAMP-regulated transcriptional co-activator

D

DAPI: 4',6-diamidino-2-phenylindole

DC: dendritic cell

DGCR8: DiGeorge critical region 8 protein

DMSO: Dimethyl Sulfoxide

DNA: Deoxyribonucleic acid

E

EDTA: ethylenediaminetetraacetic acid

ELISA: enzyme-linked immuno sorbent assay

F

FABP5: fatty acid binding protein 5

FCS: fetal calf serum

FEV1: forced expiratory volume in 1 s

FOXJ1: forkheadbox protein J1

G

GAPDH: glycerinaldehyde-3-phosphate dehydrogenase

GM-CSF: granulocyte-macrophage colony-stimulating factor

H

HBSS: hank's buffered saline solution

HDM: house-dust mite

HPRT: hypoxanthine guanine phosphoribosyltransferase

Hsa: homo sapiens

I

Ig: Immunoglobulin

IL: interleukin

ILC: innate lymphoid cell

J

K

KID: kinase-inducible domain

L

LTBP4: latent TGF-ß binding protein 4

M

MAPK: mitogen-activated protein kinase

MHC: major histocompability complex

miRNA/miR: microRNA

mmu: mus musculus

MUC5AC: mucin 5AC

MVB: multivesicular bodies

N

n.d.: not detectable

NHBE: normal bronchial epithelial cells

nm: nanometer

NOD: nucleotide oligomerization domain

Nt: nucleotides

O

OVA: ovalbumin

P

PAS: periodic acid schiff

PBS: phosphate buffered saline

PP: phophatase

PRR: pattern recognition receptor

P/S: penicillin/streptavidin

Q

qRT-PCR: quantitative real-time PCR

R

RISC: RNA-induced silencing complex

RNA: ribonucleic acid

S

Sec14l3: sec14-like3

Ser: serine

SEM: standard error of the mean

SD: splicing domain

SIK: salt-inducible kinase

siRNA: small interfering RNA

T

TAD: transactivation domain

TARC: th2-derived thymus and activation regulated chemokine

TGF-ß: transforming growth factor-ß

Th: T helper

TLR: toll-like receptor

TRBP: TAR binding protein

TSLP: thymic stromal lymphopoetin

U

UTR: untranslated region

V

W

X

Y

Z

8.2. Acknowledgements

The least I can do at the end is to say **T H A N K Y O U** to all that participated to this work and supported me throughout the last four years. I could not have done it without you.

First of all, I want to thank Prof. Dr. Elfriede Noessner for the excellent supervision, the technical advice and very helpful discussions. Thank you also to Prof. Dr. Susanne Krauss-Etschmann for the possibility to perform this very interesting project in her lab, for the good working atmosphere, the trust in me, and the kind support at all times. I am sure the following years in Borstel together will be just as inspirational and exciting.

Next, I want to acknowledge all present and former members of the SKE lab at the CPC in Munich, in particular Petra Nathan, Stefan Dehmel, Rabea Imker, Marc Kästle, Katrin Milger, Theresa Käuferle, YingYan Yu, Jeremias Götschke, Franziska Vocht, Eva Brudy, Birte Konrad, Katharina Singer, Katharina Jeltsch, Nikola Schulz and Inge Kepert. I think I can speak for all if I say that we had a great time, always a good working atmosphere, teamspirit and lots of fun at national and international meetings around the world.

Thanks a lot to Prof. Dr. Oliver Eickelberg and Dr. Antje Brand for giving me the opportunity to work at such an inspiring, international and fast-paced workplace that is the CPC. I have to say a big thank you also to Dr. Dr. Melanie Königshoff, Camille Beunèche and Dr. Doreen Franke for the great organization of the CPC research school. Not only did I receive great training in different aspects of research and soft skills, but also they made it possible for me to meet various very important people in the lung field. I would also like to thank the Helmholtz Graduate program HELENA for additional education and also the funding of my short-term research stay in USA.

This brings me to my colleagues from the CPC: I want to thank all PhD students that started with me four years ago, especially the inhabitants of the 2nd floor PhD office and in particular Andrea Schamberger, Bettina Oehrle, Juliane Bartmann, Nunja Habel-Ungewitter, Franzi Uhl and Nora Semren. We had lots of fun together and supported each other during difficult times with consoling coffee breaks or wine evenings. I hope this friendship will continue for a long time ☺.

An important Thank You goes to all collaborators, who contributed to this work: First, I want to thank Dr. Francesca Alessandrini for all her help with the mouse models, the paper writing and the fruitful technical discussions!! Thanks also to Andreas Kowarsch and Steffen Sass from the MIPS in Munich for the support and very valuable bioinformatics help, as well as

Dieter C. Gruenert for providing the 16HBE14o$^-$ cell line. I want to acknowledge Prof. Dr. Andrew Kicic and Prof. Dr. Stephen M. Stick for providing additional human nasal cells and the great collaboration.

In April 2013 I had the great opportunity to work for 6 weeks in the laboratory of Prof. Dr. Rob Freishtat at the Children's National Medical Center in Washington DC. I want to sincerely thank you Rob, Sarah Ferrante, Sarah Alcala, Claire Hoptay, Lisa Maltz and Drew Wiles for welcoming me and for these amazing six weeks and the resulting collaborations!! I really would love to come back some day and see you all again.

Last but not least, I want to thank my family, especially my parents, and my friends. You have supported me so much throughout this entire journey and managed to keep me going even if everything was falling apart.

8.3. Eidesstattliche Versicherung

Ich, Sabine Bartel, erkläre hiermit an Eides statt, dass ich die vorliegende Dissertation mit dem Thema

microRNA-based identification of pulmonary signaling pathways in experimental asthma -
The role of the cAMP responsive element binding protein (Creb1)

selbständig verfasst, mich außer der angegebenen keiner weiteren Hilfsmittel bedient und alle Erkenntnisse, die aus dem Schrifttum ganz oder annähernd übernommen sind, als solche kenntlich gemacht und nach ihrer Herkunft unter Bezeichnung der Fundstelle einzeln nachgewiesen habe. Ich erkläre des Weiteren, dass die hier vorgelegte Dissertation nicht in gleicher oder in ähnlicher Form bei einer anderen Stelle zur Erlangung eines akademischen Grades eingereicht wurde.

Ort, Datum Unterschrift